

**DESIGN OF A
SEMI-AUTOMATIC
ALGORITHM FOR
SHORELINE EXTRACTION
USING SYNTHETIC
APERTURE RADAR (SAR)
IMAGES**

JOHN N. FLEMING

June 2005



**TECHNICAL REPORT
NO. 231**

**DESIGN OF A SEMI-AUTOMATIC
ALGORITHM FOR SHORELINE
EXTRACTION USING SYNTHETIC
APERTURE RADAR (SAR) IMAGES**

John N. Fleming

Department of Geodesy and Geomatics Engineering
University of New Brunswick
P.O. Box 4400
Fredericton, N.B.
Canada
E3B 5A3

June 2005

© John Fleming 2004

PREFACE

This technical report is an unedited reproduction of a thesis submitted in partial fulfillment of the requirements for the degree of Master of Science in Engineering in the Department of Geodesy and Geomatics Engineering, September 2004. The research was supervised by Dr. Yun Zhang and Dr. David E. Wells.

As with any copyrighted material, permission to reprint or quote extensively from this report must be received from the author. The citation to this work should appear as follows:

Fleming, John N. (2005). *Design of a Semi-Automatic Algorithm for Shoreline Extraction using Synthetic Aperture Radar (SAR) Images*. M.Sc.E. thesis, Department of Geodesy and Geomatics Engineering Technical Report No. 231, University of New Brunswick, Fredericton, New Brunswick, Canada, 149 pp.

ABSTRACT

The coastal zones are one of the most rapidly changing environments in the world. The coast takes up a big portion of the Chilean territory, which results in one of the highest ratios of coastal kilometres to territory per km² in the world.

The capability for all-weather, day/night-imaging acquisition, short revisit periods and global coverage of Synthetic Aperture Radar (SAR) makes them a powerful remote sensing tool for mapping or maps updating.

Over coastal areas, the nautical chart is one of the most usable sources of information for navigational, military, planning and coastal management purposes. One of the most important features in nautical charts is the coastline, which constitutes the physical boundaries of oceans, seas, straits and canals, etc.

Digitizing a feature such as the coastline is a very tedious and time-consuming operation. The development of a semi-automatic algorithm to detect shoreline is a required task that has to be implemented in the process of nautical chart production in the Chilean Hydrographic and Oceanographic Service. Doing so would save a large amount of time in the process of coastline digitizing, which currently is achieved manually.

Previous works have achieved good results in shoreline extraction. But, these works are less appropriate when applied to areas with high local environmental noise caused by the rough sea surface.

After identifying the general steps governing the detection of shorelines in SAR images, this thesis develops a new technique to enhance land-water boundaries called the Multitemporal Segmentation Method. Also, the iterative application of windows to get rid of the noise over the sea surface is developed to achieve land-water separation.

After detecting the coastline, the bias in the delineation is acceptable, reducing the offsets towards the sea that can result from the application of common filters.

Depending on the application and the scale of the final product, analysis by the operator is still very important in this semiautomatic method. The extracted coastline requires a final examination. Also, the extracted coastline is referred to the in-situ water line; consequently it must be referred to the desired tidal datum.

ABSTRACTO

Las zonas costeras constituyen unos de los ambientes más cambiantes en el mundo. La franja costera corresponde a una gran porción del territorio chileno, el cual posee una las más altas proporciones costa por kilómetros cuadrados de territorio en el mundo.

La capacidad de adquisición en cualquier condición día-noche o clima, cortos periodos de visita y cubierta global hacen de las imágenes SAR una poderosa herramienta de sensorio remoto para producir o actualizar existentes mapas.

En zonas costeras, la carta náutica es la fuente de información mas usada para propósitos como navegación, actividades militares, planificación y manejo costero. Uno de los elementos más importantes en la carta náutica es la línea de costa, que constituye la frontera física de océanos, mares, estrechos y canales.

La digitalización es un proceso que consume gran parte del tiempo. El desarrollo de un algoritmo semiautomático para la detección de línea de costa ahorrara una gran cantidad de tiempo en el proceso cartografico, actividad que actualmente es realizada en forma manual en el Servicio Hidrográfico y Oceanográfico de la Armada de Chile.

Trabajos anteriores han logrado muy buenos resultados en extracción de línea de costa. Pero, estos pueden fallar en áreas con gran ruido ambiental causado por la rugosidad de la superficie marina.

Luego de identificar los pasos que gobiernan la detección de línea de costa en imágenes SAR, esta tesis propone una nueva técnica llamada Método de Segmentación Multitemporal para resaltar la franja tierra-agua. Además, la aplicación iterativa de ventanas para remover el ruido en la superficie del mar es propuesta para obtener una separación entre agua y tierra.

Una vez que la línea de costa es detectada y vectorizada, el error en su delineación es aceptable, reduciendo su desplazamiento hacia el mar si se usan filtros tradicionales.

Dependiendo de la aplicación y la escala final del producto, el análisis del operador es aun muy importante en este método semiautomático. La nueva línea de costa requiere una revisión final. Además, la línea de costa detectada corresponde a la línea de costa al momento de la adquisición de la imagen, por lo que debe ser referenciada al datum de marea deseado.

ACKNOWLEDGEMENTS

This work couldn't be achieved without the support of people and institutions I really want to thank.

First of all, I wish to thank the Chilean Navy, especially the Hydrographic and Oceanographic Service for having given me this opportunity for this academic and personal growth. More than an academic experience it really was an experience of life, which carried out my family to live for two years in this wonderful country.

More than two years after arriving to Fredericton, I can see my growth and how was my academic improvement during this program. Because that I would like to thank my supervisor Dr. Yun Zhang and Dr. Dave Wells for giving me all their support and guiding me in the accomplishment of this project as well as the entire support during my Master's program.

I would also like to express my gratitude to the Geodesy and Geomatics Faculty at the University of New Brunswick for giving me the opportunity to share with great and wonderful people and for opening my eyes in this wonderful world of science. Especially thanks to my friend David Mayunga for his support when I really needed and for those nice conversations while drinking coffee.

Thanks my wife Ingrid for her comprehension and love, my lovely daughter Christine and my gorgeous two weeks old son Patrick for giving me the most amazing gift and making me the happiest father in the world.

Especially I also want to give my thanks and love to my parents for their continuous support and affection that they always have given to me.

TABLE OF CONTENTS

ABSTRACT	ii
ABSTRACTO	iii
ACKNOWLEDGEMENTS	iv
TABLE OF CONTENTS	v
LIST OF TABLES	ix
LIST OF FIGURES	ix
1. INTRODUCTION	01
1.1 Background	01
1.1.1 The Necessity of Maintaining and Updating Satellite Images Databases in Chile.....	02
1.1.2 Remote Sensing in the Chilean Navy Hydrographic and Oceanographic Service.....	04
1.1.3 The aim of Coastline Extraction for Nautical Cartography.....	06
1.1.4 Semi-Automatic Extraction of Coastline.....	06
1.1.5 Opportunities and Advantages using Radar Images.....	08
1.2 Problem Addressed	11
1.3 Objectives of this Thesis	12
1.4 Methodology used in this Thesis	13
1.5 Contribution of this Thesis	15
1.6 Thesis Outline	16
2. EXISTING WORK ON COASTLINE DETECTION WITH RADAR IMAGES	17
2.1 Background	17
2.2 Different Representation of Data in SAR Images	18
2.2.1 SAR Interferometry.....	18
2.2.2 Single Amplitude Images.....	19
2.2.3 Polarimetric Images.....	19
2.3 Shoreline Detection in the Spatial Domain	20
2.3.1 Single Channel SAR Images.....	20
2.3.1.1 The use of Spatial Filters.....	21
2.3.1.2 Texture Analysis in Edge Detection.....	24

2.3.2	Shoreline Extraction using Polarimetric SAR Images.....	27
2.3.3	Shoreline Detection in the Frequency domain.....	28
2.4	Summary.....	30
3.	INHERENT PROBLEMS ENCOUNTERED USING AMPLITUDE IMAGES.....	32
3.1	Background.....	32
3.2	Radar Geometry.....	32
3.2.1	Radar Distortions in Amplitude Images.....	36
3.2.1.1	Foreshortening.....	37
3.2.1.2	Layover.....	37
3.2.1.3	Shadowing.....	38
3.3	Geographic Characteristics and the Incidence Angle.....	39
3.4	Spatial Resolution.....	39
3.5	Summary.....	40
4.	TESTING BASIC OPERATIONS FOR LAND-WATER SEPARATION IN SAR IMAGES..	42
4.1	Introduction.....	42
4.2	Existing Filters usable for Land-Water Separation.....	42
4.2.1	Noise Reduction in SAR Images.....	44
4.2.2	Enhancement of Land-Water Boundary.....	46
4.2.2.1	Most used Edge Detection and Enhancement Techniques.....	47
4.2.2.1.1	Edge Detection.....	47
4.2.2.1.1.1	Derivative Operators.....	48
4.2.2.1.1.2	The Roberts Edge Detector.....	49
4.2.2.1.1.3	The Sobel Operator.....	50
4.2.2.1.1.4	Edge Detecting Templates.....	50
4.2.2.1.1.5	Linear Edge Detecting Templates.....	51
4.2.2.1.1.6	Sobel Template.....	52
4.2.2.1.2	Edge Enhancement.....	53
4.2.3	Testing Existing Techniques for Shoreline Enhancement.....	53
4.2.3.1	Edge Detection Focusing on the Shoreline.....	54
4.2.3.2	Texture Analysis Focusing on the Shoreline.....	56
4.2.3.2.1	Texture.....	57

4.2.3.2.1.1	Statistics.....	57
4.2.3.2.1.1.1	Mean Windows.....	57
4.2.3.2.1.1.2	Standard Deviation Windows.....	58
4.2.3.2.1.2	Gray-level Cooccurrence Matrices (GLCM).....	59
4.2.3.2.1.2.1	Edge Detection using GLCM	
Variance windows.....		59
4.2.4	Existing Techniques used to Reduce the Unnecessary Edges.....	62
4.2.4.1	The use of Smoothing Filters.....	62
4.2.4.2	The use of Digital Morphology.....	62
4.2.4.2.1	Binary Dilation.....	63
4.2.4.2.2	Binary Erosion.....	64
4.2.4.2.3	Opening and Closing.....	65
4.2.4.2.4	Application of Opening Filter to Reduce the	
Undesirable Edges.....		65
4.2.5	Land-Water Separation.....	66
4.2.5.1	Gray-level Segmentation or Threshold.....	67
4.2.5.2	Application of Land-Water Segmentation.....	68
4.3	Summary.....	70
5.	DEVELOPMENT OF A NEW METHOD FOR LAND-WATER SEPARATION.....	71
5.1	Introduction.....	71
5.2	Data Used and Methodology Selected in this Research.....	72
5.3	The Multitemporal Analysis for Noise Reduction.....	72
5.3.1	Averaging the Images.....	73
5.3.2	Principal Components Analysis (PCA).....	75
5.3.3	Multiplying the Images.....	78
5.3.4	The Modified Algorithm using Multitemporal Images.....	79
5.4	Results in Coastline Detection after the Multitemporal Analysis.....	80
5.5	Multitemporal Segmentation for Island-Noise Discrimination.....	82
5.5.1	Removing Noise and Refining the Coastline Detection.....	83
5.5.1.1	Analyzing and Removing Noise.....	86
5.5.1.1.1	Island-Noise Discrimination.....	86

5.6	A Window-based Algorithm to Eliminate the Noise.....	94
5.6.1	An Iterative Method to Delete Noise and to Fill Gaps.....	96
5.7	Results in Coastline Detection After the Multitemporal Segmentation Method.....	100
5.7.1	Testing the Refined Algorithm in Different Areas.....	102
5.8	Summary.....	105
6.	RESULTS AND DISCUSSION.....	106
6.1	Introduction.....	106
6.2	Quantitative Analysis in Coastline Detection.....	107
6.3	Qualitative Analysis in Coastline Detection.....	109
6.4	Summary.....	115
7.	APPLICATION OF THE DETECTED COASTLINE FOR GIS.....	116
7.1	Introduction.....	116
7.2	Vectorization of the Detected Coastline using CARIS SAMI.....	116
7.2.1	Procedure to Export the Image as CARIS SAMI File.....	117
7.3	The Needs to Adjust the Shoreline with a Tidal Model.....	125
7.4	Summary.....	128
8.	CONCLUSIONS AND RECOMMENDATIONS.....	129
8.1	Conclusions.....	129
8.1.1	Regarding the Algorithm.....	129
8.1.2	Regarding the Data Used.....	131
8.1.3	Identification of Main Concepts the Proposed Method.....	131
8.2	Recommendations.....	133
8.3	Further Work and Development.....	133
8.	REFERENCES.....	136
	APPENDIX I.....	139
	APPENDIX II.....	143

LIST OF TABLES

Table	Page
6.1 Comparison Between the use of Most Common Filters After Multitemporal Analysis and the M.S.M.....	109

LIST OF FIGURES

Figure	Page
2.1 Erteza Method for Coastline Extraction.....	22
2.2 Lee and Jurkevich Method for Coastline Extraction.....	24
2.3 Mason and Davenport Method for Coastline Extraction.....	26
2.4 Yu and Acton Method for Coastline Extraction.....	28
2.5 Niedermeier Method for Coastline Extraction.....	29
3.1 Geometric Configuration of SAR Images.....	34
3.2 Slant and Ground Range Geometry during the Image Acquisition.....	35
3.3 Radar Distortions caused by the Slant Range Geometry and the Terrain Elevation..	38
4.1 Coastline Detection Methodology using Most Common Filters.....	43
4.2 Different Filters used for Speckle Reduction.....	46
4.3 Linear Edge Detecting Templates.....	51
4.4 Sobel Templates.....	53
4.5 Histograms of the Original Image and its Respective Sobel Image.....	55
4.6 Enhanced Image and its Respective Histogram.....	56
4.7 Sobel and Texture (Variance) Images.....	61
4.8 Effects of Dilation over the Original Image using a 3x3 Structuring Element.....	64
4.9 Application of a 5x5 Mean Filter followed by Gray Level Opening.....	66
4.10 Thresholding Operation used to Separate Object from Background.....	67

4.11 Application of a Single Threshold Operation to the Radar Image.....	68
4.12 Results on Segmentation using Single SAR Images.....	70
5.1 Multitemporal Images.....	74
5.2 Result in Averaging two Images.....	75
5.3 Results on Principal Components Analysis.....	78
5.4 Multitemporal Analysis in the use of Most Common Filters to Detect Edges.....	80
5.5 Final Edge Detection over the Averaged Image.....	82
5.6 Visual Analysis of the Remaining Noise after the Multitemporal Analysis.....	83
5.7 Final Proposed Method to Detect the Coastline using the Multitemporal Segmentation Method.....	85
5.8 Effect of Multitemporal Analysis between two 16-bits Images.....	87
5.9 Island and Noise Discrimination after the Multitemporal Analysis between two 16-bits Images.....	88
5.10 The Resulting Image after Applying Multi-image Segmentation.....	90
5.11 The Effect after Enhancing the Land Pixels.....	91
5.12 Numeric Values of Pixels over Land and Noise.....	92
5.13 The Enhanced Image after the Multitemporal Segmentation Method.....	93
5.14 The Window used to Remove the Noise and to Fill the Gaps.....	94
5.15 Application of Basic Star-shape Window.....	95
5.16 Application of a Small 3x3 Window.....	95
5.17 A 5x5 Dilation Operation.....	96
5.18 A 3x3 Closing Operation.....	96
5.19 Iterative use of Windows to Delete the Noise and to Fill the Gaps.....	98
5.20 The Image after Most of the Gaps are Closed.....	99
5.21 The Image after Closing Operation using Digital Morphology.....	99
5.22 The Resulting Image after Contrasting with the Original Image.....	100
5.23 The Detected Coastline after using the M.S.M. Developed in this research.....	101
5.24 Four Different Areas where the Algorithm was Tested.....	104
6.1 Nautical Chart of the Analyzed Area used to Analyze the Coastline.....	107
6.2 The Effect of Shadow Caused by Step Relieves Such as Hills or Trenches.....	110
6.3 The Effect of Low Backscatter of Flood Areas or Wetlands.....	111

6.4 Information used to Visually Analyze the Coastline in Areas with Problems.....	111
6.5 The Effect of Shoreline Delineation in Cases where the Islands are Close to the Main Shoreline.....	112
6.6 The Effect of Shoreline Delineation in Cases of Narrow and Indented Canals.....	113
6.7 The Effect of False Edges in Water and How the Algorithm can Discriminate False from Real Edges.....	114
7.1 Shoreline Vectorization of Area 1 after using the Contour Following Algorithm with CARIS SAMI.....	120
7.2 Shoreline Vectorization of Area 2 after using the Contour Following Algorithm with CARIS SAMI.....	121
7.3 Shoreline Vectorization of Area 3 after using the Contour Following Algorithm with CARIS SAMI.....	122
7.4 Shoreline Vectorization of Area 4 after using the Contour Following Algorithm with CARIS SAMI.....	123
7.5 Shoreline Vectorization of Area 5 after Using the Contour Following Algorithm with CARIS SAMI.....	124
7.6 Geometric Model to Reference the Extracted Shoreline into a Tidal Datum.....	127

Chapter 1

INTRODUCTION

This thesis is focused on the development of a semi-automatic coastline extraction method using radar images over areas subject to notable environmental parameters such as wind, which produce large amounts of textural noise over the sea surface. The reduction of that noise and an adequate technique to discriminate land from that noise is developed in this project, solving one of the most important problems in feature detection using radar images over coastal areas.

The extracted coastline has a wide range of application, especially in areas of fjords and channels such as the south of Chile.

1.1. Background

A large percentage of the global population lives in coastal regions. Consequently, these areas are under intense pressure from urban growth, industry and tourism. A prerequisite for sustainable management of these environmentally sensitive areas is the availability of accurate and up-to-date information on their extent, state, and rate of change.

For those countries with large coastal extensions, the nautical chart product is one of the most usable sources of information either for navigational, military, planning and coastal management purposes.

1.1.1. The Necessity of Maintaining and Updating Satellite Image Databases in Chile

Chile is a long and narrow country with more than 83,850 km. of linear coast including continental coast and southern islands, fjords and channels. The Chilean coastal zone is a long strip, above 38° latitude, with great geomorphologic, climatic and oceanographic diversity. The coast takes up a big portion of the Chilean territory, given the narrow and long shape of the country, which results in one of the highest ratios of coastal kilometres to territory per km² in the world [Alvial and Recule, 1999].

The northern zone's exposed and rugged coast becomes less craggy farther south and then turns rugged again in the higher latitudes, ending in a zone of about 10,000 islands, islets and channels that form a complex system, of glacial origin [Alvial and Recule, 1999]. In this southern part of Chile, the heavy continental influence on the channel zones inland waters generates different situations that also break the homogeneity of the water masses.

Together with these basic environmental characteristics, various natural phenomena frequently occur in the coastal zone, which presents risks that must be evaluated when considering a coastal development. These include earthquakes, tidal waves, floods and irregular oceanographic events, such as El Niño. A set of processes associated with

environmental changes also occur, which cannot be predicted now but which must be taken into account, such as the processes of deforestation, especially in hydrologic basins, desertification, the thinning ozone layer, and the increasing intensity and frequency of harmful phytoplankton proliferations [Alvial and Recule, 1999].

As can be seen this is not only a very diverse coastal zone, but also a tremendously variable one, with hard to predict phenomena, which demand great flexibility from the management models to be implemented.

Besides its natural and geographical aspects, the fast growth of economic activities in the south of Chile is demanding an urgent and adequate management of coastal zones that requires the use of current technology to obtain information over this large territory.

Chile has experienced remarkable growth in salmon farming. In a few short years, Chile has become the second largest exporter of farmed salmon in the world [APSTC, 2000; Barret et al., 2002]. Because of the fast growth of this zone in commercial, tourism and transportation activities, the creation and maintenance of databases using remote sensing techniques such as aerial photography or satellite images is highly necessary. However, the maintenance and updating of a photographic database in the Chilean territory is a difficult task. This is due to the difficulties in some remote and very sparsely populated areas in the far south of Chile, where detailed surveying and photogrammetric flights are difficult because of the weather conditions and the lack of aircraft facilities.

1.1.2. Remote Sensing in the Chilean Navy Hydrographic and Oceanographic Service

Remote sensing information is becoming widely important for the Hydrographic and Oceanographic Service of the Chilean Navy (S.H.O.A. in spanish). S.H.O.A. has a photogrammetric section to process aerial photographs focusing on the extraction of information for the nautical chart.

As stated before, the wild geography of the south of Chile makes the use of this technology indispensable for the extraction of information and their corresponding use for management, monitoring and creation of digital mapping of a given area.

These areas are mostly used as navigational routes and they are quickly becoming important due to the development of aquaculture and tourism activities. Therefore, both paper nautical charts and electronic navigational charts have great importance and increasing demand in the mentioned area.

Aerial photography is the current remote sensing information used in SHOA to extract the coastline and height contours for further use as the main layer in the nautical chart.

To extract the information from the aerial photography, the actual procedures used in SHOA are:

Digital Analogue Procedure: Using aerial photography and ground control points to perform triangulation. The cartographic base is constructed using optical-digital equipment.

Digital Procedure: Using aerial photography and ground control points to perform the triangulation. The cartographic base is performed using digital equipment after the photography has been scanned.

After the photographs have been processed and corrected, both procedures use manual digitizing of the features to get the restitution.

However there is a lack of information regarding aerial photographs along the Chilean coast, especially in those remote areas where high-cloud conditions persist. Also, some remote areas are difficult to cover by flight plans because of weather conditions and the lack of airports or land installations for logistical purposes. For these reasons, many remote areas should be more effectively analyzed using space borne images.

Furthermore, in the case of remote areas, analysis of satellite images is a powerful tool to provide information for mapping purposes. Satellite images play an important role, because the images are available without logistic operations, except to obtain the corresponding ground information used to correct the image geometrically. Therefore, and considering its advances regarding spatial resolution, satellite images have an increasing value for cartographic purposes.

However, optical satellite images still have a problem regarding the presence of clouds in the study area, which is the principal limitation in the south of Chile. This problem can be solved using radar images, because of their inherent property of acquiring the information at all times and weather conditions.

1.1.3. The Aim of Coastline Extraction for Nautical Cartography

One of the most important features in nautical charts is the coastline. Coastline areas constitute the physical boundaries of oceans, seas, straits and channels. Also, it is the principal point of reference to be used by all the navigational methods for safely sailing near to coast.

Nautical charts provide detailed and reliable information to sailors about the real configuration of the coast where they are sailing. The principal preoccupation of sailors is to avoid shoals, which implies keeping a safe distance from the shoreline while sailing. Of course, it also depends of bathymetric information and coast configuration. Then, it is possible to infer that coastline and soundings are the primary physical features present in the nautical chart.

1.1.4. Semi-Automatic Extraction of Coastline

Digitizing is a very tedious and time-consuming operation still present in most of the cartographic and hydrographic agencies in the world. Also, the human element is still required in the process of image interpretation [Zelek, 1990]. Photo interpretation is the process of extracting enough information from an image to create meaningful map representations. The following factors determine the amount of information that can be extracted from an image:

- a) The degree of detail available in an image, which depends on the following factors:

- The scale or resolution of the image.
 - The contrast amongst distinct features in the image.
 - The spectral range of the imagery.
- b) The data extraction method.
 - c) The skill of the operator.
 - d) The characteristics of the features of interest. Those characteristics can either be *spatial* such as pattern texture, size, and shape, *spectral* such as intensity (single image) or color (multiple channels image).
 - e) Also in radar images, the reduction of noise due to environmental parameters is important to achieve a successful features extraction [Zelek, 1990].

Coastline information is usually the strongest edge present in an image, either in optical or radar images. Edge information provides clues for the locations of boundary features such as shorelines. An edge is a point that indicates the presence of an intensity change in certain conditions. A boundary is a collection of connected edge points [Zelek, 1990].

Currently, many edge detectors have been developed and used depending on whether edges are obtained from optical images or radar images.

Because optical images receive energy coming from the sun reflected from the earth in various channels of the electromagnetic spectrum, the procedures to extract shapes and edges is more straightforward than using a single channel active remote sensing image (radar images).

1.1.5. Opportunities and Advantages using Radar Images

Optical images have better spectral and spatial resolution than radar images, which is a big advantage. However, as stated before, optical images have problems when acquiring the information over cloudy areas. Those problems can be solved using radar images.

The real opportunities that radar images offer to mapping are:

- Coastline mapping for unmapped areas.

Radar images are well suited for coastline mapping for unmapped areas, allowing the use of shoreline information, which is widely used and is one of the most important features in the nautical chart.

- Coastline map updating.

Because the coastline is frequently highly sensitive to erosion and sea level rises resulting from climate warming, the updating of coastline using radar images is widely used to update old surveys and monitor change due to erosion or accretion.

- Digital coastline generation and update for Electronic Chart Display and Information Systems (ECDIS).

The system displays in real time the location of the ship in relative or absolute orientation, giving the sailor a reference parameter about the location of the ship with respect to the coastline.

- National sovereignty to map the offshore extent of the Exclusive Economic Zone (EEZ) as defined by the United Nations Convention on the Law of the Sea (UNCLOS).

- Coastal physical characteristics (depending on the image resolution and the feature size).
 - Anthropogenic shoreline features (e.g. piers, breakwaters).
 - Offshore features (e.g. breakers, reef areas).
 - Terrestrial features (e.g. roads, land use).

The above opportunities for radar images are important keys to design and develop marine and coastal information systems for coastal management, improving coastline maps and features for GIS applications, especially when this information is used for mapping the intertidal zone.

The advantages of using radar images to extract coastline are the following:

- Reliable, rapid access to current, usable images at any time of the year. Its capability for all weather, day/night-imaging acquisition gives excellent time resolution.
- Frequent global coverage expedites single image and stereo data collection for large national or regional mapping projects.
- Short revisit periods permit frequent observation of cultural features for change detection activities.
- Topographic information provides new perspective on structure, landforms, drainage patterns and water bodies.
- Because it is sensitive to surface roughness, soil moisture and terrain, it can get clear and concise delineation of land/water boundaries. It facilitates coastal mapping and map updating.
- Radar images can complement and enhance data from other sensors.
- Synoptic spatial coverage:

- Image acquisition faster than tidal-wave phase speed.
- HH polarization is optimal for land-water discrimination.
- Variable incidence angle:
 - Flexible image acquisition times correlated with high tides.
 - Image acquisition at large incidence angle, which is optimal for land water discrimination.
- Variable resolution.
- Absolute geometric accuracy (nominal): +/- 200 metre (sea level with no Ground Control Points).

Specifically for coastline mapping, large incidence angles provide a larger radar backscatter contrast, which improves the discrimination of the water-land boundary. The smooth surface of a water body acts as a specular reflector in contrast to the diffuse scattering, which occurs over land. Open water surfaces will appear dark in comparison to the brighter returns from land. However, this is only true when acceptable environmental conditions occur at the time of image acquisition. If the water surface is too rough due to the effect of the wind, a large incidence angle will act as a detrimental factor in discriminating the coastline.

Also, shoreline detection and the identification of areas of erosion or sedimentation can be improved by acquiring multi-temporal data with different look directions (e.g., ascending or descending).

Even though the resolution of radar imagery is gradually getting better, it is still poor for producing a cartographic product at large scales. Currently, radar images can be used for mapping at maximum 1:50.000 if using RADARSAT-1 with 8-metre resolution.

Scheduled for launch in 2005, RADARSAT-2 will be the most advanced commercial Synthetic Aperture Radar (SAR) satellite in the world. With RADARSAT2 improved object detection and recognition, it will enable a variety of new applications including mapping at scales of 1:20,000 [Radarsat International, 2004].

1.2. Problem Addressed

The extraction of coastline is not so straightforward using radar images because of the inherent noise called “speckle noise” and the environmental conditions at the time of the image acquisition. Besides noise reduction, the main goal is to solve the problem of the strong backscatter caused by the effect of strong wind over the sea surface. That “wind forced noise” is a very common problem in the extraction of coastlines over fiords and channel areas; especially when the water surface is rough close to the shoreline.

Hence, the use of an adequate algorithm to eliminate speckle and to detect the shoreline is fundamental in achieving a semi-automatic extraction of reliable and consistent coastline over indented and navigationally hazardous areas.

Even when previous works in coastline detection have achieved good results, the application of those existing algorithms is often not appropriate for noisy areas, especially when the noise and islands have similar gray-level value.

Regarding the resolution, in this thesis, the use of satellite radar images ERS-1 precision georeferenced image (PRI) will be used to extract the coastline. Considering

that the resolution of these images is 12.5 metres, the aim of coastline detection is the further use in nautical cartography with a scale of 1:70,000 or smaller.

1.3. Objectives of this Thesis

The implementation and the use of radar images to extract features of interest over the coastal areas (i.e. coastline) is a real challenge for S.H.O.A, and is currently part of a recent project destined to elaborate nautical cartography of some areas in Antarctica using radar images.

The main objective of this thesis is to develop a semi-automatic method to detect planimetric features (coastlines) using single radar images containing a high backscatter coming from the sea surface, which is a very common problem in coastal images.

First, the establishment of a general procedure to roughly achieve land-water separation using the most common methodology is tested. Because using essential filters does not solve the noise problem, this thesis is focused on the procedure to minimize the backscatter coming from rough sea surfaces to achieve better results in the separation between land and water.

This procedure is based in the multitemporal analysis between two images. Hence, performing image-image operations to smooth the roughness over sea surface, the land-water boundary is better enhanced.

A novel procedure called the Multitemporal Segmentation Method (M.S.M.) is proposed to achieve land-noise discrimination. After improving the input image using

the M.S.M., an iterative application of windows designed to delete the noise on the sea surface and to fill some of the gaps in land caused by shadows, is applied to enhance the land-water boundary for later coastline detection.

The extracted and vectorized coastline can be used to upgrade existing electronic or paper charts or for being used as the base of new nautical charts over remote areas.

1.4. Methodology used in this Thesis

Different procedures used to extract the shoreline in the spatial domain roughly include [Chen and Shyu, 1998]:

- Obtaining a rough separation between the land and water, and
- Refinement the rough land-water boundaries by edge detection and edge tracing algorithms to extract the accurate shoreline position.

In this research, a rough land-water separation is achieved using basic operations with some modifications to avoid large offset in coastline delineation, ensuring better results.

After testing those filters, the first consideration of coastline extraction is to solve the problem of random noise coming from the sea surface due the wind conditions. As stated before, that roughness is random because it depends on environmental conditions. Then, the location of the strong sea backscatter should change between two different images, providing an efficient key to eliminate that wind-forced noise.

To solve this problem, this thesis proposes a segmentation method based in the use of two previously registered images acquired at different times.

The methodology used to achieve the goal of coastline extraction consists of two steps. First, a rough land–water separation using essential filters is obtained. This step is based in a series of operations in the spatial domain to reduce noise while smoothing the image preserving the main edge, which in this case is the shoreline. This process consists in getting rid of all the edges except the shoreline. After successive operations, the land-water segmentation is achieved, giving acceptable results.

After that rough land-water separation, a novel procedure focused in the reduction of environmental noise is developed with the proposed Multitemporal Segmentation Method. The output image after the M.S.M. is used to achieve the final land-water separation using windows designed to eliminate the noise over the sea surface without deleting the islands.

This research is based in the use of neighborhood operations to enhance the image in the boundary zones between land and sea, using ENVI software from Research System to apply the basic filters and Microsoft Visual C++ to run the designed functions in C language to apply the M.S.M. and the applications of windows.

The extracted coastline is vectorized using CARIS SAMI, a module of CARIS GIS. The desired shoreline vector product for this thesis does not represent tidal information, because it is referred to the in-situ water line. Consequently, tidal models must be applied after the shoreline detection. Therefore, with sufficient tide and shore topography information, an image extracted waterline estimate can be improved to any tidal references. Tidal models are not covered in this thesis.

The proposed methodology is a semi-automated method, and of course it considers that the operator's experience is essential to achieve good results.

1.5. Contribution of this Thesis

This thesis reviews existing procedures for coastline detection in the spatial domain and proposes a method to enhance and to achieve the semi-automatic extraction of planimetric features such as the coastline.

Previous work has achieved very good results in the shoreline extraction using different data sets of SAR images. However those analyses have been done in areas relatively noise-free (which is not the usual case in radar images).

The real contribution of this thesis is the shoreline extraction in images that contains a high amount of noise caused by wind over the sea surface.

Because noise is an important problem in radar images, a new technique to get rid of the noise coming from the sea surface is proposed, giving very good results for further shoreline extraction.

Because this technique avoids the use of filters that dilate the object boundaries, the offset achieved in the detected coastline is better if compared with the application of the most common filters tested in this thesis. Also, the detected coastline doesn't have to be refined using thinning techniques or another accurate algorithm.

This semi-automatic algorithm can be applied to larger areas, saving a large amount of time compared with the traditional methods of digitalization of the coastline.

1.6. Thesis Outline

Chapter two outlines some previous work achieved in coastline extraction.

Chapter three describes the inherent problems encountered in SAR amplitude images to successfully detect the shoreline.

Chapter four describes the procedure used for land-water separation following the most common procedure using existing filters in image processing.

Chapter five describes the proposed method to enhance the image in the way that land-noise discrimination is achieved, and the further detection of the shoreline after the noise was eliminated.

Chapter six analyzes the detected coastline and the uncertainties present in the results.

Chapter seven describes the extraction and vectorization of the shoreline using CARIS SAMI and how this information could be used for GIS purposes.

Finally, the conclusions and recommendations are presented in chapter eight.

Chapter 2

EXISTING WORK ON COASTLINE DETECTION WITH RADAR IMAGES

2.1 Background

Synthetic Aperture Radar (SAR) is an active system. It sends energy in the microwave range to the Earth's surface and measures the reflected signal. Therefore, images can be acquired during the day and night, completely independent of solar illumination, which is particularly important in high latitudes (polar night) and is the main reason for choosing these kinds of images.

The microwaves emitted and received by ERS SAR are at much longer wavelengths (5.6 cm) than optical or infrared waves. Microwaves easily penetrate clouds, and images can be acquired independently of weather conditions.

The basic principle of radar is the transmission and reception of pulses. Short time duration (microsecond) high-energy pulses are emitted and the returning echoes recorded, providing information on magnitude, phase, time interval between pulse emission and return from the object, polarization and Doppler frequency. The same antenna is often used for transmission and reception.

Because radar imaging is an active system, the properties of the transmitted and received electromagnetic radiation (power, frequency, polarization) can be optimized according to mission specification goals.

2.2 Different Representation of Data in SAR Images

2.2.1 SAR Interferometry

In general from radar images it is possible to extract two kinds of information depending of the application required. These informations are referred to phase and amplitude.

SAR interferometry makes use of the phase information by subtracting the phase value in one image from that of the other, for the same point on the ground. This is, in effect, generating the interference between the two-phase signals and is the basis of interferometry.

SAR Interferometry (INSAR) is currently a hot topic, which is rapidly evolving thanks to the spectacular results achieved in various fields such as the monitoring of earthquakes, volcanoes, land subsidence and glacier dynamics. It is also used in the construction of Digital Elevation Models (DEM's) of the Earth's surface and the classification of different land types.

Coastline detection using InSAR images usually has some limitations, especially regarding the temporal correlation, if data of larger ERS repeat cycles (e.g. 35 days) are used [Schwäbisch et al, 2004].

Commonly, coastline detection using InSAR techniques are used just to support the interpretation of the amplitude information [Schwäbisch et al, 2004].

This thesis is focused on the extraction of shoreline using single amplitude images, which are currently available for this research.

2.2.2 Single Amplitude Images

The electromagnetic radiation involved can be imagined as a sine wave. Conventional SAR images are made up (as a raster) of the amplitude or ‘strength’ of the sine wave - shown in images as grey level intensity values, represented in one channel.

The strength or amplitude on the backscatter of the signal is directly proportional to the surface roughness and the dielectric constant of the material. Depending on the incidence angle and the surface roughness, the backscatter may occur in different ways (specular, diffuse, corner reflection).

2.2.3 Polarimetric Images

Polarimetric radar measures the complex scattering matrix of a target with quad polarizations. The scattering matrix measured in the linear {H,V} basis consists of E_{hh} , E_{hv} , E_{vh} and E_{vv} complex signals, where H and V represent horizontal and vertical polarization, respectively. E_{hv} indicates the signal of horizontal transmits polarization and vertical receive polarization, and the other three signals are defined similarly [Yu and Acton, 2004].

In the reciprocal backscatter case, since $E_{hv} = E_{vh}$, the complex scattering matrix can be represented by a complex scattering vector:

$$\mathbf{u} = [E_{hh} \ E_{hv} \ E_{vv}]^T \quad \text{Equation 2.1}$$

Where the superscript T denotes the transpose of the matrix.

One-look polarimetric SAR data for each image pixel can be represented using equation 2.2, or equivalently, as the covariance matrix (CM):

$$C = u(u)^+ \quad \text{Equation 2.2}$$

Where (+) denotes the Hermitian (transpose and complex conjugate) of the matrix. SAR data are often multilook processed for speckle reduction and data compression by averaging neighboring single-look data:

$$Z = \frac{1}{n} \sum_{k=1}^n u(k)[u(k)]^+ \quad \text{Equation 2.3}$$

Where n is the number of looks, and $u(k)$ is the k th 1-look sample.

Using polarimetric data classification algorithms it is possible to classify it into three classes of dominant scattering mechanism: odd bounce, even bounce and diffusive scattering, and a class that cannot be grouped into any of the three [Yu and Acton, 2004].

2.3 Shoreline Detection in the Spatial Domain

2.3.1 Single Channel SAR Images

Shorelines are usually well defined in most image types as an edge between two contrasting regions, near the land-water interface [Jeremy et al., 2001].

In general, the different procedures used to extract the shoreline in the spatial domain include [Chen and Shyu, 1998]:

- Obtaining a rough separation between the land and water, and;
- Refinement of the rough land-water boundaries by edge detection and edge tracing algorithms to extract a more accurate shoreline position.

In the spatial domain the automatic extraction of coastlines includes the following steps:

- Filtering the image to eliminate noise.
- Enhancement of land-water boundary.
- Detection of shoreline using edge detection techniques.
- Use of an algorithm to trace the coastline.
- Refinement of coastline.

Most of the research in coastline extraction has been done in the spatial domain using amplitude images. This chapter briefly describes the previous work done in the extraction of this important feature.

2.3.1.1 The use of Spatial Filters

Using amplitude SAR images and processing the image to get rid of all the undesirable edges, while keeping the coastline, is the most widely used concept to successfully extract non-linear edges such as the shoreline.

Erteza [1998] begins by 1) using speckle reduction by median filter and 2) histogram equalization to accentuate the land-water boundary. Immediately after, 3) thresholding is applied and the final processing step for the land-water boundary enhancement consists

in 4) two passes of a maximum filter. In this case, a window is scanned over the entire image and the center pixel of the window is replaced by the maximum value of all the pixels in the window. The maximum filtering is performed using two passes of a 7x7 window. Once the enhancement of land-water boundary step has been performed, the next step is 5) to form and mark a one pixel wide boundary between land and water using a contour tracing algorithm directly over the image.

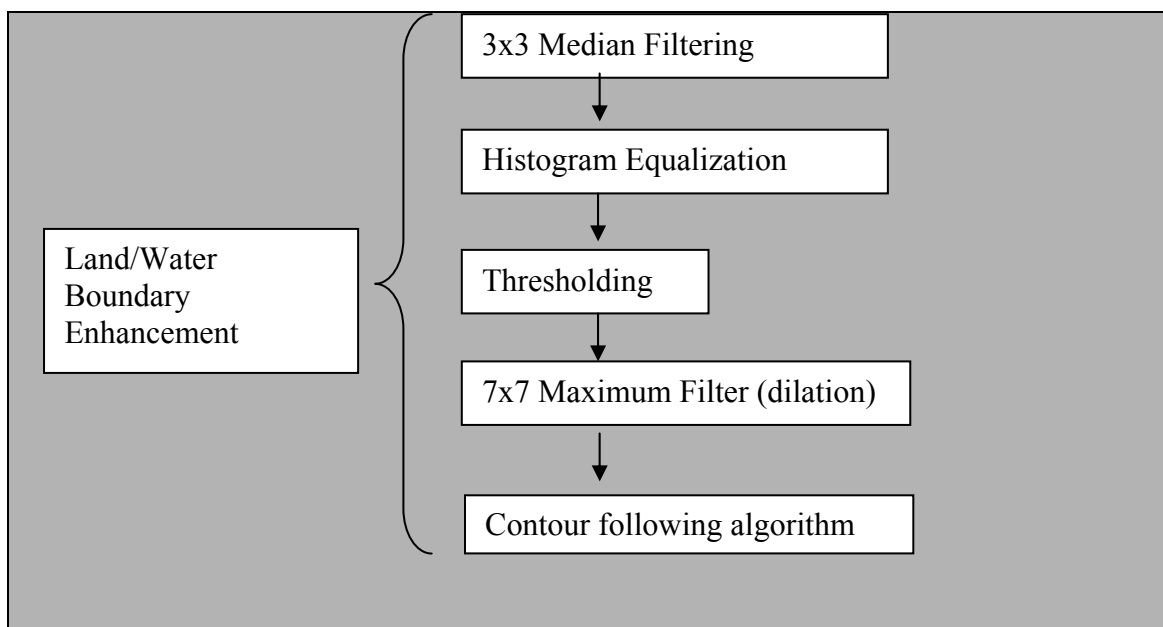


Figure 2.1. Erteza [1998] Method for Coastline Extraction

Due to the size of maximum filter applied twice, before refinement, this procedure will move the coastline far from the original position (about 14 pixels). That situation is not applicable for nautical chart mapping over a navigational route in fiords or channels.

Another approach made by Lee and Jurkevich [1990], presents a coastline detection method based in a series of operations described in general terms as follows:

After performing 1) the speckle smoothing and filtering using an adaptive Lee filter, 2) Sobel edge detection is applied. Once all the edges present in the image (land, water and coastline) are obtained, 3) a 5x5 mean filter is applied more than one time, dilating the edges to fill the gaps. The smoothed image is then 4) thresholded. Hence, water-land separation is achieved. For this binary image, 5) Roberts edge detection is computed, producing a thinner contour image ready to be traced with a clockwise contour following algorithm.

The reason for applying Robert's operator is that the edges generated are 1-pixel wide, making the edge tracing more precise [Lee and Jurkevich, 1990].

Because the mean filter is applied twice, the detected coastline pixels are, on average, six to eight pixels away from the original image coastline pixels.

To refine the coastline, a (5x5) mean filter is applied twice over the edge, followed by a thresholding operation. Then, the coastline is retraced using the same algorithm, but now only the inside edges are traced. After refinement, the new coastline matches that of the original image to within a pixel or two.

Because the mean filter is applied more than once, before refinement, the land-water boundary is also affected producing an offset of approximately six to eight pixels away from the original image coastline pixels [Lee and Jurkevich, 1990].

They achieved reasonable positional accuracy using their method, but state that refinements are necessary to achieve the accuracy required for geographical mapping. However, this methodology cannot solve the problem regarding environmental noise. So, in the application of the contour-following algorithm, the operator must achieve image interpretation to avoid the delineation of contours over noisy areas.

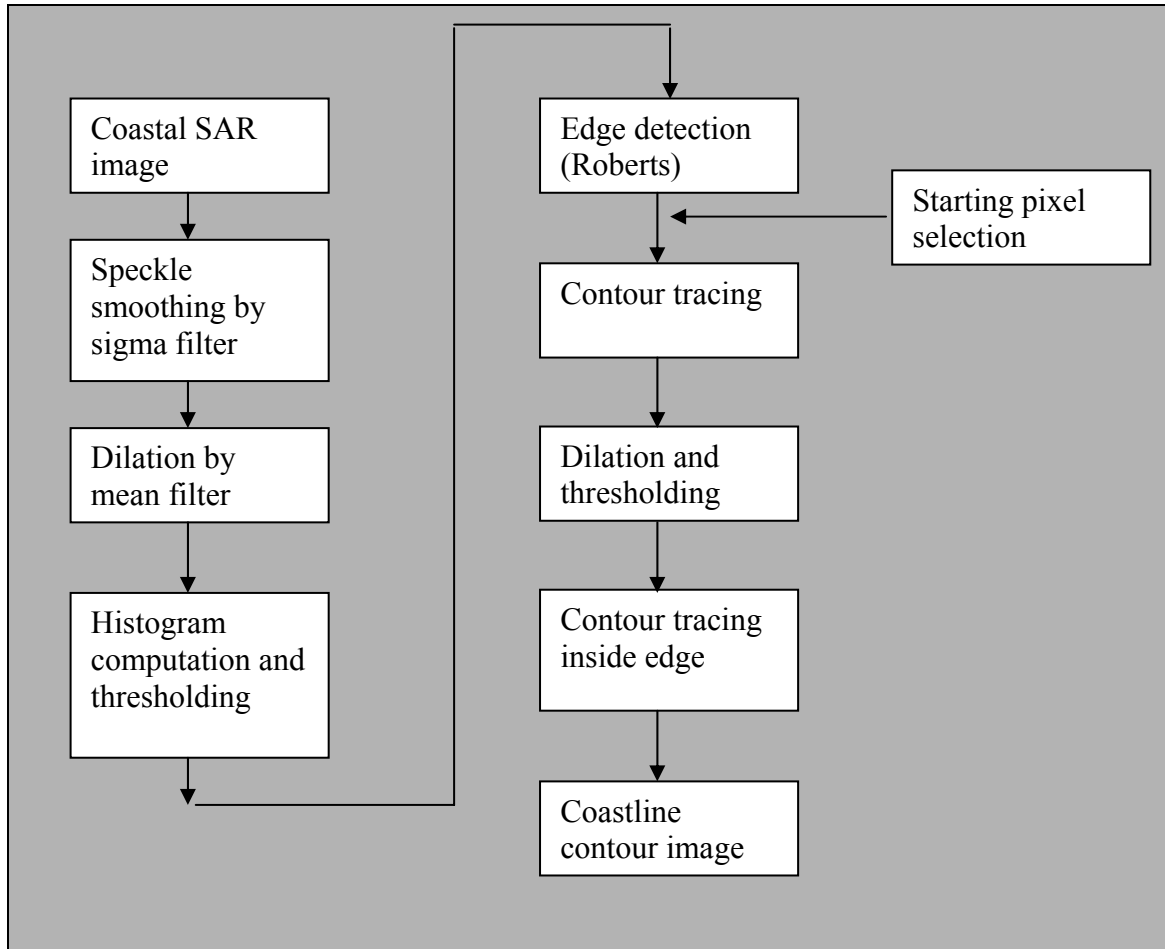


Figure 2.2. Lee and Jurkevich [1990] Method for Coastline Extraction

2.3.1.2 Texture Analysis in Edge Detection

Other efforts include the work of Mason and Davenport [1996], in which a speckle sensitive edge detector, the contrast ratio filter [Touzi et al., 1998] detector, was combined with an active contour model for coastline extraction.

Mason and Davenport describe a semi-automatic method for the determination of the shoreline in ERS-1 SAR images. The methodology used in that paper has been designed

for the use in the construction of a digital elevation model (DEM) of an intertidal zone using a combination of remote sensing and hydrodynamic modeling techniques.

The Mason and Davenport method is a coarse-to fine processing approach, in which sea regions are first detected as regions of low edge density in a low resolution image. They use a sequence of image processing algorithms. The procedure starts by finding a rough division between land and sea (note the concept of land-water enhancement) in a coarse resolution processing stage. This rough sea-land segmentation is shown in the left part of the workflow in Figure 2.4. After that, the SAR sub-image areas near the shoreline are processed at high resolution using an active contour model algorithm. This procedure is shown in the right part of Figure 2.4.

This procedure also achieves good results over areas without excessive noise. More than 90% of the shoreline detected by this methodology appears visually correct [Mason and Davenport, 1996]. However, this method fails when texture in sea backscatter is similar to some portions of land.

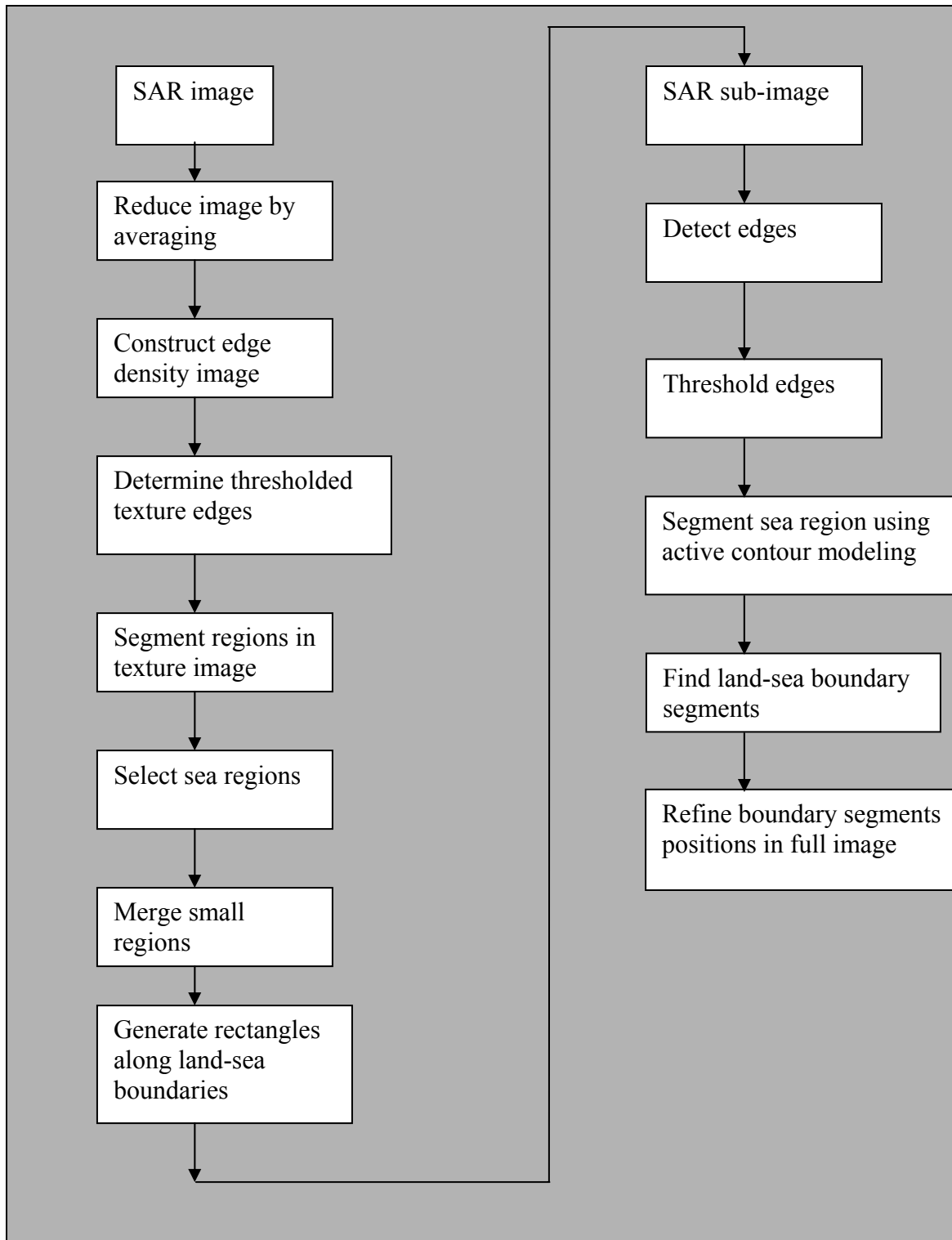


Figure 2.3. Mason and Davenport [1996] Method for Coastline Extraction

2.3.2 Shoreline Extraction using Polarimetric SAR Images

Polarimetric images have been recognized as having stronger power to discriminate between different terrain covers than is possible with a single polarization SAR image.

Besides the shoreline detection in polarimetric SAR images using traditional classification techniques, Yu and Acton [2004] presented another approach (see Figure 2.4).

They apply first a polarimetric filter to yield a single, speckle reduced base image. Primary edge information is then derived by Instantaneous Coefficient of Variation (ICOV) operator from a Speckle Reducing Anisotropic Diffusion (SRAD) processed base image. SRAD is used to enhance edges in the base image and further reduce speckle noise in the image. Next, the resulting edge image is parsed by a watershed segmentation algorithm, which partitions the image scene into a set of disjoint segments. Region merging is performed to eliminate subscale segments. By adopting a region adjacency graph (RAG) representation for segments and calculating a similarity metric from the radar brightness (not texture) for each pair of adjacent regions, the region pairs with high similarity are merged iteratively until a desired result is achieved, eliminating the undesired boundary segments while delineating the coastlines correctly [Yu and Acton, 2004].

This procedure gives better results than Lee and Jurkevich or Mason and Davenport methods [Yu and Acton, 2004]. However, because this procedure is based in segments, it fails in the identification of small islands, especially when noisy images are used.

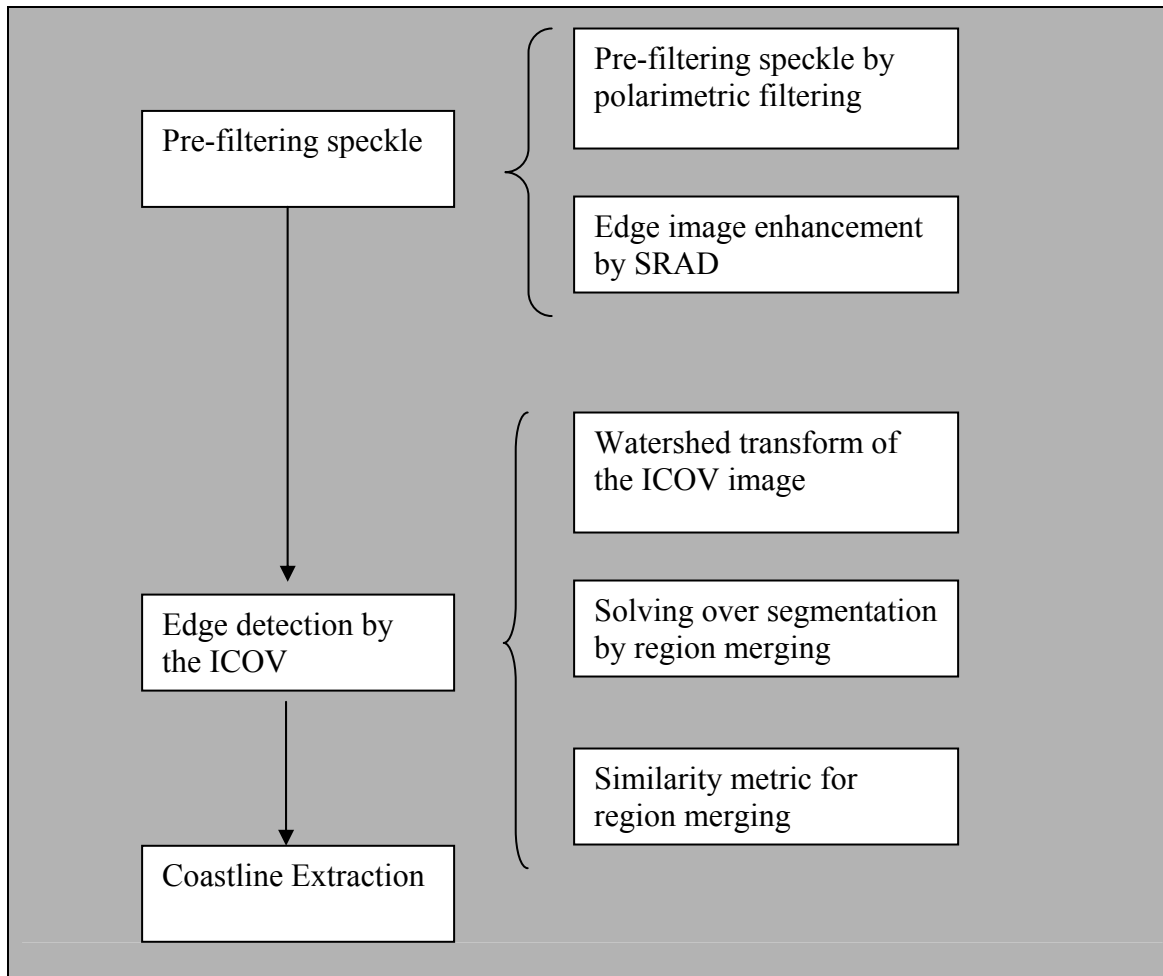


Figure 2.4. Yu and Acton Method [2004] for Coastline Extraction

2.3.3 Shoreline Detection in the Frequency Domain

The edge detector achieved by Niedermeier et al. [1999] consists of three parts. A first guess part leads to a coarse land-water determination, based on the fact that wavelet based edge detector enhances strong edges over land areas and only weak edges over sea. From this, a thresholding and a so-called blocktracing are performed yielding a

rough segmentation into water, land and small coastal area in between. Figure 2.5 outlines the principal steps.

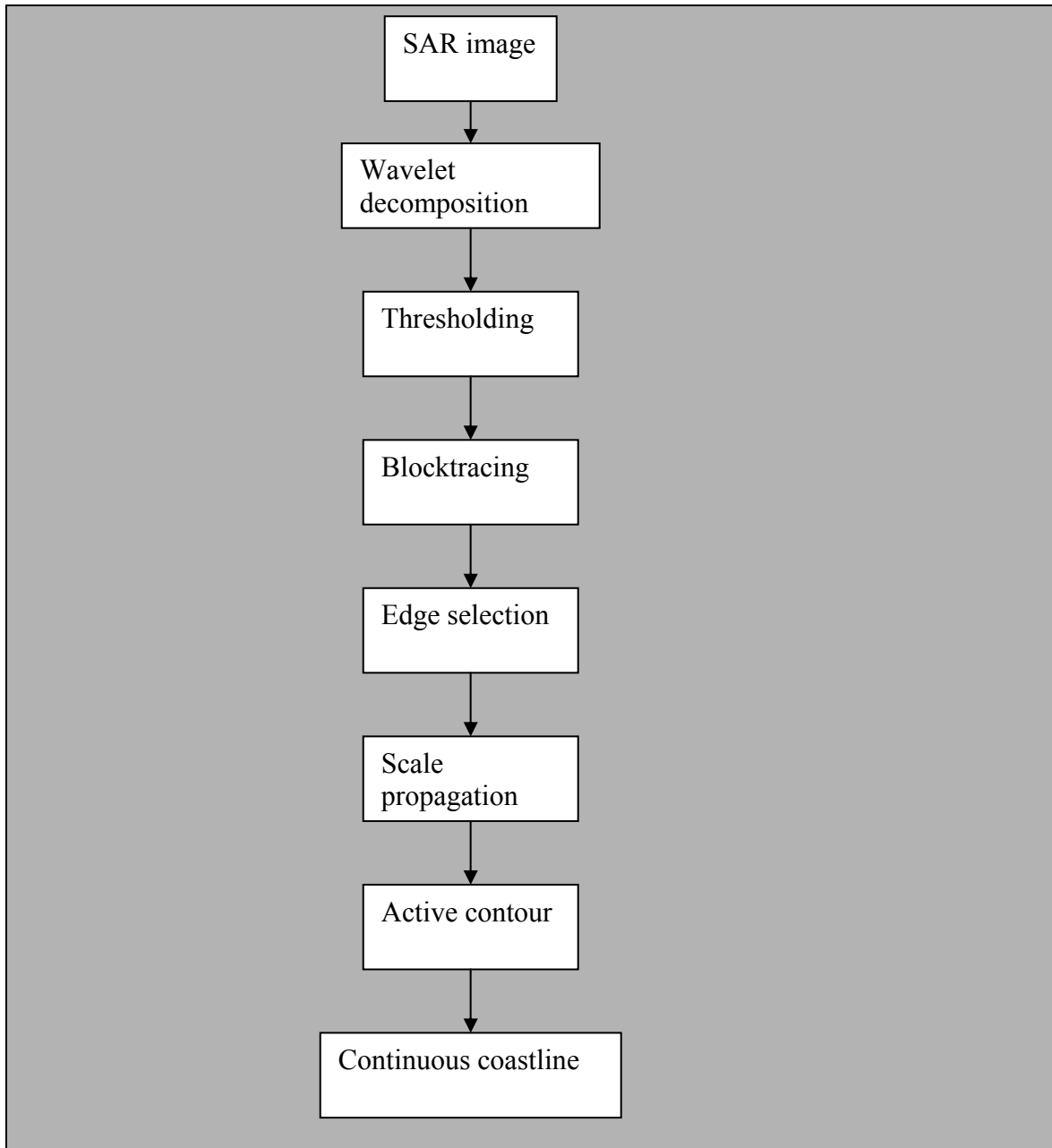


Figure 2.5. Niedermeier [1999] Method for Coastline Extraction

In a refinement step the full resolution edge is detected in the coastal region. Due to wavelet theory its localization gets better using scale propagation. As a final step, individual edge segments are connected to a continuous shoreline using a snake algorithm.

The wavelet-based edge detector algorithm seems to be a suitable choice for extracting coastlines from SAR images. The separation of edges from noise is achieved by thresholding the resulting image after filtered with wavelet. However, this threshold operation fails when it is applied to edges detected over strong and local rough surface areas.

2.4 Summary

After introducing brief concepts regarding the different representations for a SAR image, this chapter described some of the previous works achieved in coastline detection using amplitude images, which generally are based in land-water separation procedures with the further application of a contour following algorithm.

Previous work describes the extraction of coastline using algorithms in the spatial domain. Also, some work has been done in the frequency domain using wavelet transform to detect the edges and the use of active contours method to extract the shoreline. However, the main problem regarding the rough sea surface caused by strong wind cannot be easily solved because “*wind-forced*” noise is local and its gray level value can be easily higher than pixel values in some areas in land.

The techniques described here give good results in the extraction of shorelines over relatively environmental noise-free areas. In that way, most of these previous works have been achieved in areas where the texture of the sea pixels are homogeneous and well differentiated from land pixels. Consequently, they still present some problems if applied in areas with local sea roughness. This problem is solved in this thesis by the use of the Multitemporal Segmentation Method.

Chapter 3

INHERENT PROBLEMS ENCOUNTERED USING AMPLITUDE IMAGES

3.1 Background

Because this research is based in the extraction of coastline using single amplitude SAR images, a brief description regarding SAR images is outlined in this chapter.

Radar concepts differ from optical theory both in geometry and in the kind of information received. Images provided by optical sensors contain information about the surface layer of the imaged objects (i.e., color), while microwave images provide information about the geometric and dielectric properties of the surface or volume studied (i.e., roughness)[European Space Agency, 2004].

When seeking the land-water separation, inherent distortions and noise present in radar images are responsible for most problems in the automatic or semi-automatic features detection. Hence, accurate shoreline position is hard to achieve by extracting land-water boundaries by edge detection and edge-tracing algorithms.

3.2 Radar Geometry

Remote sensing image data in the microwave range of wavelengths is generally gathered using the technique of side-looking radar. A pulse of electrical energy at the microwave frequency (or wavelength) of interest is radiated to the side of the aircraft (or spaceborne) at an incidence angle [Richards and Jia, 1999].

The platform is flying in its orbit and carries a SAR sensor, which points perpendicular to the flight direction. The projection of the orbit down to Earth is known as the *ground track* or *subsattellite track*. The area continuously imaged from the radar beam is called *radar swath*. In the case of ERS, due to the look angle of about 23 degrees, the imaged area is located some 250 km to the right of the *subsattellite track*. The radar swath itself is divided in a *near range* (i.e. the part closer to the ground track) and a *far range* [European Space Agency, 2004]. Figure 3.1 shows the general diagram of the image acquisition in radar geometry.

In SAR images, the direction of the satellite's movement is called azimuth direction, while the imaging direction is called range direction. The SAR measures the power of the reflected signal, which determines the brightness of each picture element (pixel) in the image.

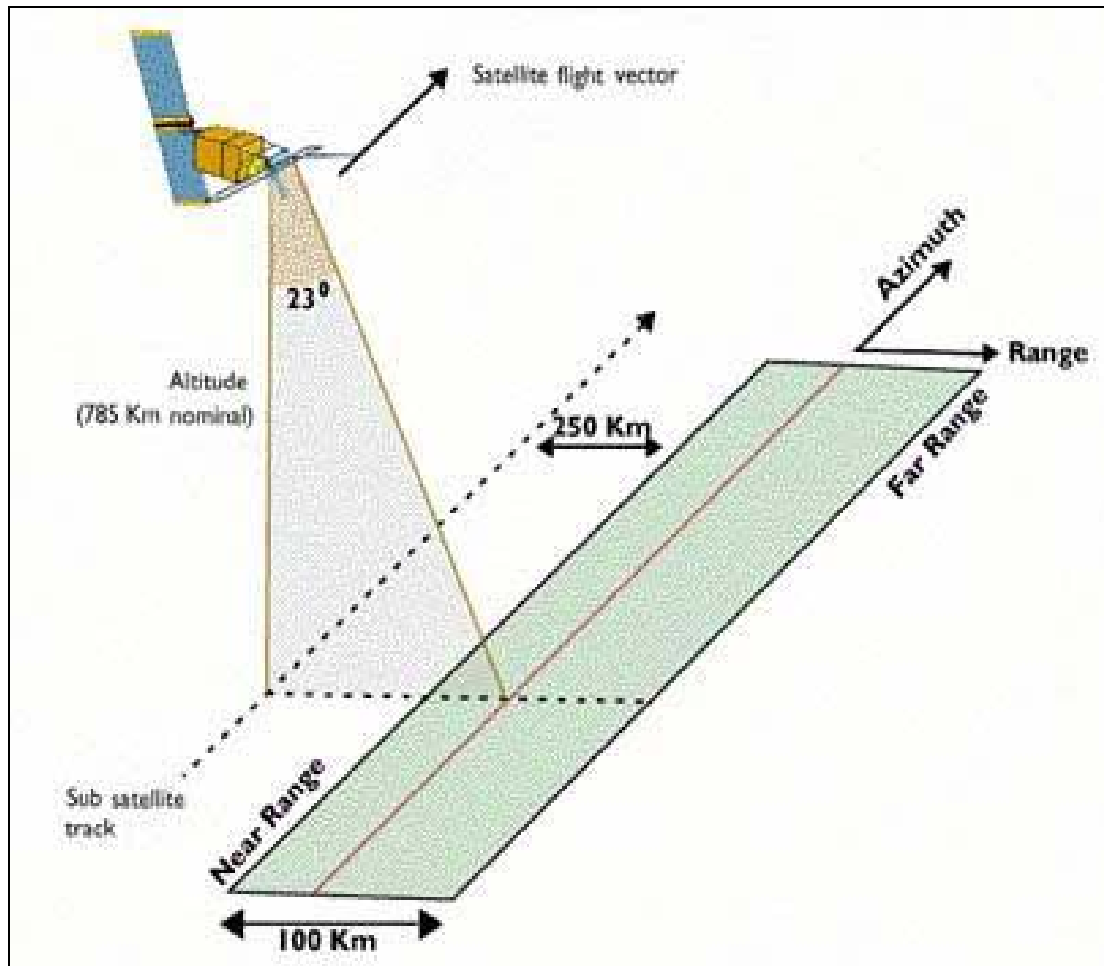


Figure 3.1. Geometric Configuration of SAR Images [European Space Agency, 2004]

The returning signal is based in the backscatter properties of the material where the signal is reflected. Different surface features exhibit different scattering characteristics:

- Urban areas: very strong backscatter.
- Forest: medium backscatter.
- Calm water: smooth surface, low backscatter.
- Rough sea: increased backscatter caused by wind and current effects. This effect is very important for hydrographic applications and coastal mapping. This problem is the main issue in this thesis and it is solved with the method proposed.

Also, there are two kinds of data display, as shown in Figure 3.2:

- Slant range image, in which distances are measured between the antenna and the target.
- Ground range image, in which distances are measured between the platform ground track and the target, and placed in the correct position on the chosen reference plane.

From an image production viewpoint, the slant range resolution is not of interest. Rather it is the projection of this onto the horizontal plane as ground range resolution that is of value for the user. Slant range data is the natural result of radar range measurements.

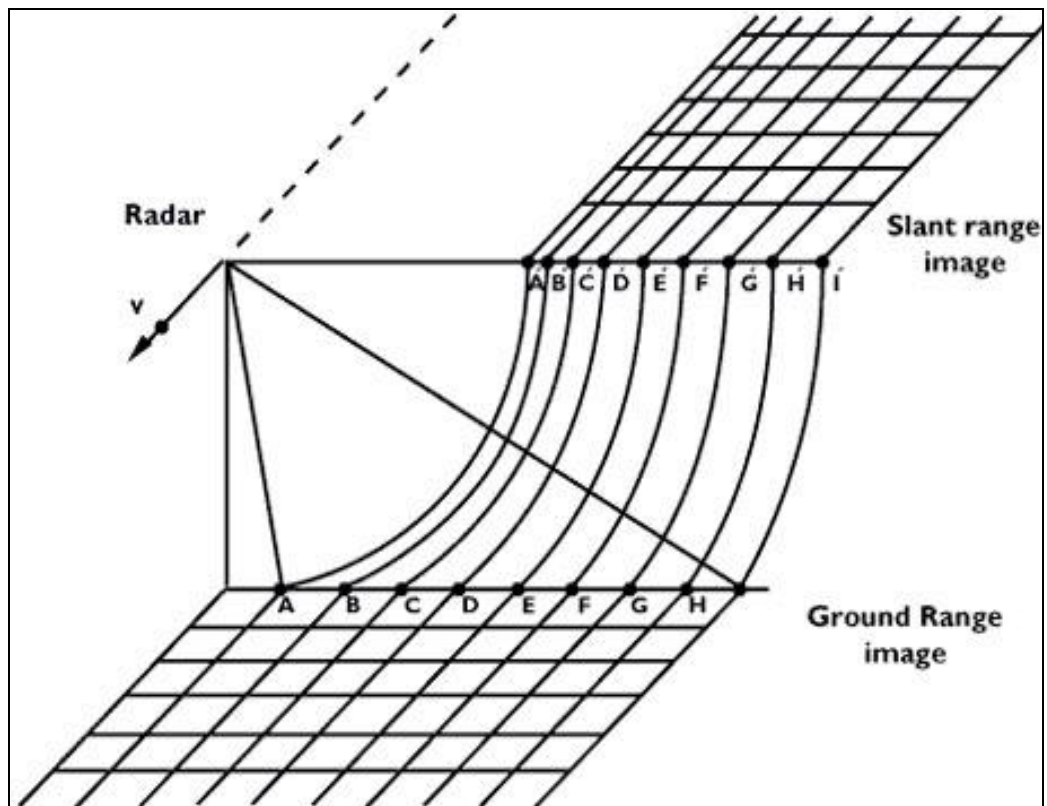


Figure 3.2. Slant and Ground Range Geometry during the Image Acquisition [European Space Agency, 2004]

Transformation to ground range requires correction at each data point for local terrain slope and elevation. Geometric distortions are one of the most important constraints in radar images and they must be corrected to achieve the final product.

3.2.1 Radar Distortions in Amplitude Images

The geometric distortions present on a radar image can be divided into:

- Range distortions: Radar measures slant ranges but, for an image to represent the surface correctly, it must be ground range corrected.
- Elevation distortions: This occurs in those cases where points have an elevation different from the mean terrain elevation.

Both kinds of distortions produce different kinds of effects in the image. These effects are shown in Figure 3.3.

Probably the most striking feature in SAR images is the "strange" geometry in range direction. The SAR imaging principle causes this effect: measuring signal travel time and not angles as optical systems do. The time delay between the radar echoes received from two different points determines their relative distance in the image. Because of this signal travel time measurement, different distortions can happen to the radar images in the range direction, depending also on the terrain elevation.

3.2.1.1 Foreshortening

Foreshortening is a dominant effect in SAR images of mountainous areas. Especially in the case of steep-looking spaceborne sensors, the across-track slant-range differences between two points located on foreslopes of mountains are smaller than they would be in flat areas. This effect results in an across-track compression of the radiometric information backscattered from foreslope areas. To solve this, the image must be compensated during the geocoding process if a terrain model is available.

Foreshortening is obvious in mountainous areas, where the mountains seem to "lean" towards the sensor. It is worth noting that foreshortening effects are still present on ellipsoid corrected data.

3.2.1.2 Layover

If, in the case of a very steep slope, targets in the valley have a larger slant range than related mountaintops, then the foreslope is "reversed" in the slant range image. This phenomenon is called layover: the ordering of surface elements on the radar image is the reverse of the ordering on the ground. Generally, these layover zones, facing radar illumination, appear as bright features on the image due to the low incidence angle.

Ambiguity occurs between targets hidden in the valley and in the foreland of the mountain, in cases where they have the same slant-range distance. For steep incidence angles this might also include targets on the back slope.

Geocoding can not resolve the ambiguities due to the representation of several points on the ground by one single point on the image; these zones also appear bright on the geocoded image.

3.2.1.3 Shadowing

A slope away from the radar illumination with an angle that is steeper than the sensor depression angle provokes radar shadows.

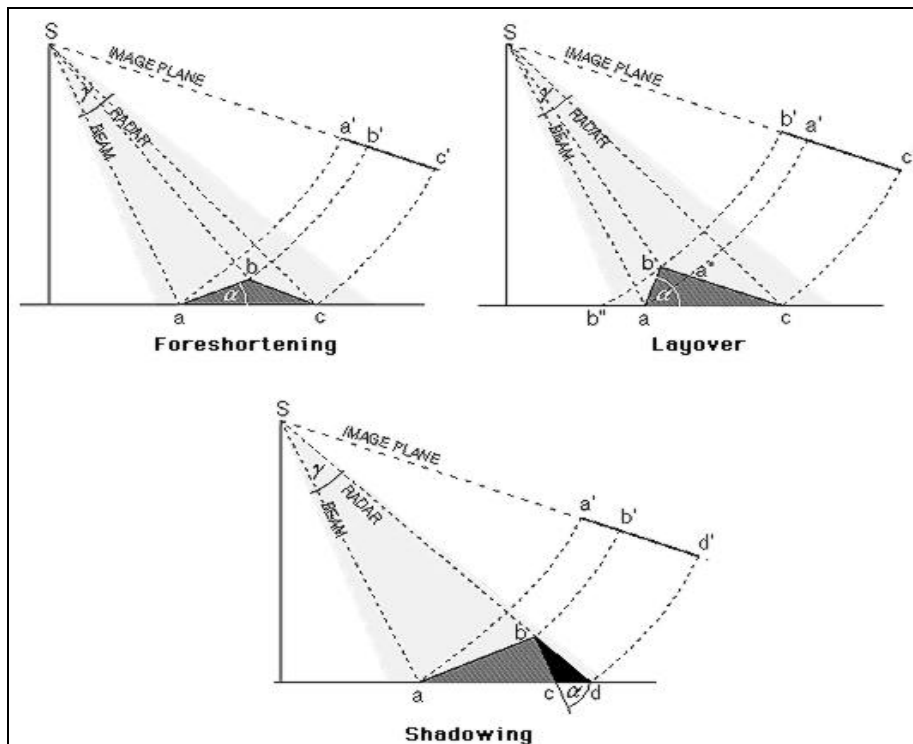


Figure 3.3. Radar Distortions caused by the Slant Range Geometry and the Terrain Elevation [The Alaska Satellite Facility, 2004]

It should be also noted that the radar shadows of two objects of the same height are longer in the far range than in the near range. Shadow regions appear as dark (zero signal or pixel value) with any changes due solely to system noise, sidelobes, and other effects normally of small importance.

3.3 Geographic Characteristics and the Incidence Angle

Based upon the previous considerations on SAR image geometry, the following remarks can be formulated in order to assist the interpreter (from ESA webpage):

- For regions of low relief, larger incidence angles give a slight enhancement to topographic features. So does a very small incidence angle.
- For regions of high relief, layover is minimized and shadowing exaggerated by larger incidence angles. Smaller incidence angles are preferable to avoid shadowing.
- Intermediate incidence angles correspond to low relief distortion and good detection of land (but not water) features.
- Small incidence angles are necessary to give acceptable levels of backscattering from ocean surfaces.
- Planimetric applications need the use of ground range data, which usually requires the use of digital elevation data and image transformation.

3.4 Spatial Resolution

In images, the spatial resolution is described by the pixel size [Richards and Jia, 1999]. Even more fundamental, at least two pixels are required to represent each resolution cell, which is a consequence of spatial sampling rules.

Spatial resolution is the most important parameter to discriminate features like objects or edges. In the case of coastal mapping, the discrimination between land and water in coastal zones is an important problem to solve, and it is directly related to spatial resolution as well as radiometric resolution or intensity levels in the case of radar images.

By convention, pixel size in SAR imagery is chosen to conform to standard map scales hence, it must be a discrete multiple (or divisor) of 100 metres. For example, ERS-1 data, having nominal resolution of 28 metres in range and azimuth, is delivered with 12.5 metre pixel spacing.

This means that rocks smaller than 12.5 metres cannot be detected using these kinds of images. Consequently, this consideration must be taken into account regarding the application of the generated coastline.

2.5 Summary

Radar images have inherent problems due their special configuration, which will cause differences in backscatter or shadowing effects. These detrimental effects will affect the achievement of an efficient procedure to achieve land-water separation. The

low-level pixel value from shadow areas can be usually less than the pixel values from the sea surface.

Chapter 4

TESTING BASIC OPERATIONS FOR LAND-WATER SEPARATION IN SAR IMAGES

4.1 Introduction

This chapter presents a combination of linear filters and morphological operations used to enhance the land-water boundary, getting rid of the edges present over land, while preserving the main edge consisting in the shoreline.

The general procedure most widely used to detect the shoreline is tested to obtain a rough land-water separation in the analyzed areas. The application of morphological operations will help to solve the offset caused by the application of large smoothing filters.

The area analyzed has a high backscatter on the sea surface; therefore, this chapter tests the results after using common filters for land-water separation.

4.2 Existing Filters usable for Land-Water Separation

From previous works done in coastline detection it was possible to identify the main concepts applied that achieved acceptable results. These concepts are: reduction of

noise, land-water enhancement and edge detection. Also, the use of a contour-following algorithm is widely applied in most of them. The same main concepts are applied in this chapter. In general terms, land water enhancement is achieved using basic operations.

As shown in Figure 4.1, to extract information from radar images, first, an adequate process of filtering the image to eliminate speckle must be achieved without losing spatial resolution. Then, the procedure for the enhancement of water-land boundary is very important to roughly determine the shoreline.

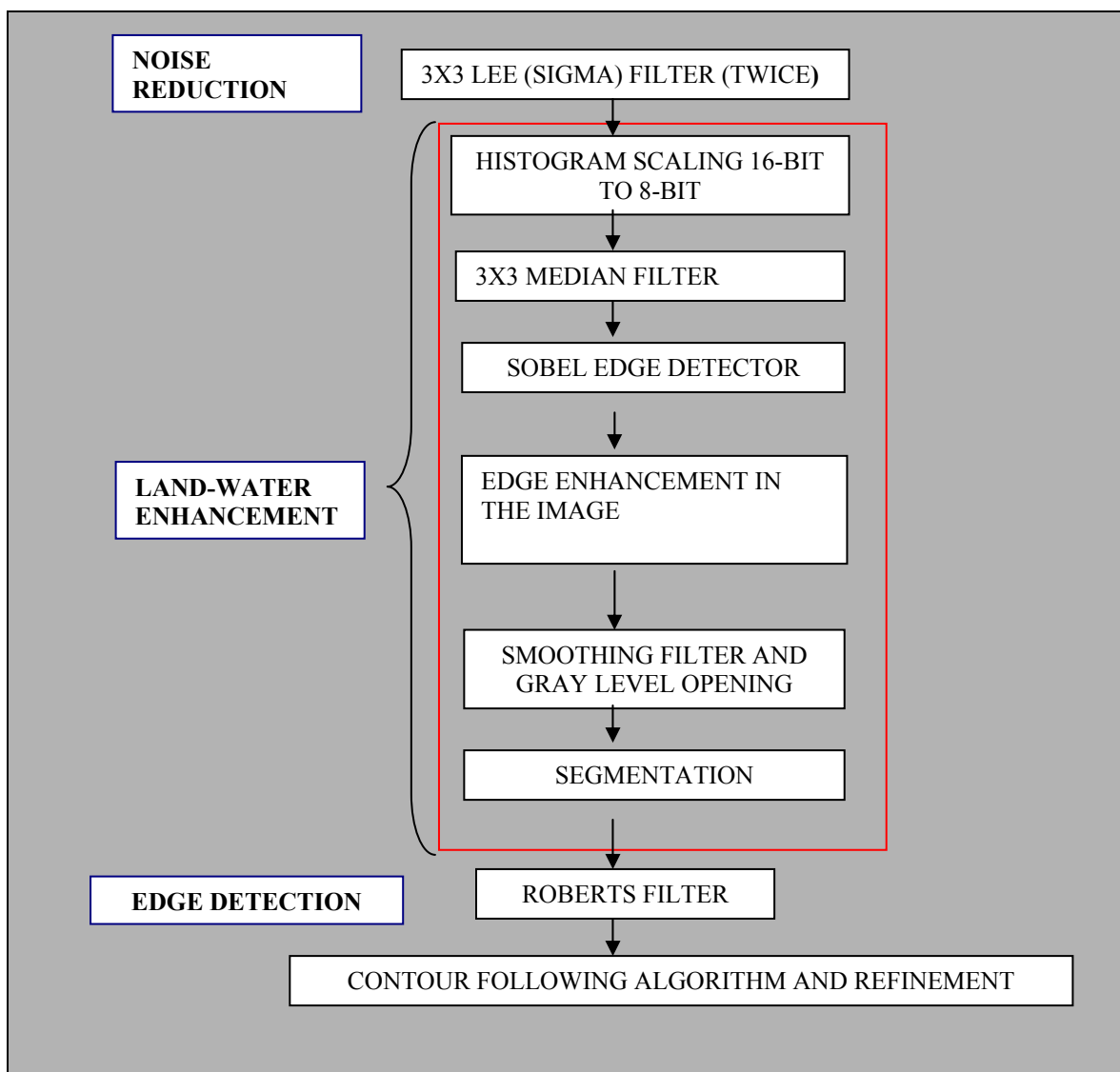


Figure 4.1. Coastline Detection Methodology using Most Common Filters

4.2.1 Noise Reduction in SAR Images

Speckle noise is a multiplicative process that is the primary source of corruption in coherently illuminated imaging modalities including synthetic aperture radar [Schultze and Wu, 1995]. This is caused by the random constructive and destructive interference of the de-phased, but coherent return waves scattered by the elementary scatterers within each resolution cell [Xiao et al, 2003]. A complete description of speckle is in Henderson and Lewis [1998].

Most commonly used speckle filters have good speckle-smoothing capabilities. However, the resulting images are subject to degradation of spatial and radiometric resolution, which can result in the loss of image information. The amount of speckle reduction desired must be balanced with the amount of detail required for the spatial scale and the nature of the particular application [Xiao et al, 2003].

Most of these algorithms are based on smoothing the image while preserving the features present in it. Particularly, SAR images assume a multiplicative noise. Described by Lee and Jurkevich [1990], the basic relation of this model is given by the equation 4.1.

$$z_{i,j} = x_{i,j} v_{i,j} \quad \text{and} \quad v_{i,j} \sim (1, \sigma^2) \quad \text{Equation 4.1}$$

Where $z_{i,j}$ is the gray level of the observed SAR pixel, $x_{i,j}$ is its ideal or noise-free counterpart, and $v_{i,j}$ is the noise characterized by a distribution with mean equal to one and variance σ^2 . This assumed statistical model for noise could vary according to the

different existing approaches to smooth the speckle noise without degrading the sharpness of the major edges in the image.

Much work has been done on speckle filtering of SAR imagery. Filtering techniques can be grouped into multi-look processing and posterior speckle filtering techniques [Xiao et al, 2003].

Multi-look techniques have the disadvantage that the greater the number of views used to filter the image, the smoother the processed image while losing spatial resolution. To avoid that, many posterior techniques have been developed to further reduce speckle. They are based on either the spatial or the frequency domain. Adaptive filters based on the spatial domain are more widely used than frequency domain filters. Most frequently used adaptive filters including Lee and Frost assume a Gaussian distribution for the speckle noise, while the Gamma filter assumes a gamma distribution.

Good results over SAR images can be achieved using the Frost Filter or Lee filter, using a number of looks equal to four and using a 5x5 window.

Others less frequently used filters are the mean filter (to smooth the image) and the median filter. The last one has the advantage that smoothes the image while preserving the edges [Richards and Jia, 1999].

In general, there were no big differences between the set of speckle reduction filters. However, because of the problem of backscatter over sea surface, a good approach was using the selected filter more than once to minimize the speckle associated and the bright return from rough water or other matters in a predominantly dark part of the image [Erteza, 1998]. Using median filter, a 3x3 or 5x5 windows is good enough to remove those single points whose values are out of line with neighboring pixels. Figures

4.2a) to 4.2d) show some results after applying existing SAR speckle filters. From all the tested filters, the Lee filter was selected to smooth the speckle over the analyzed images.

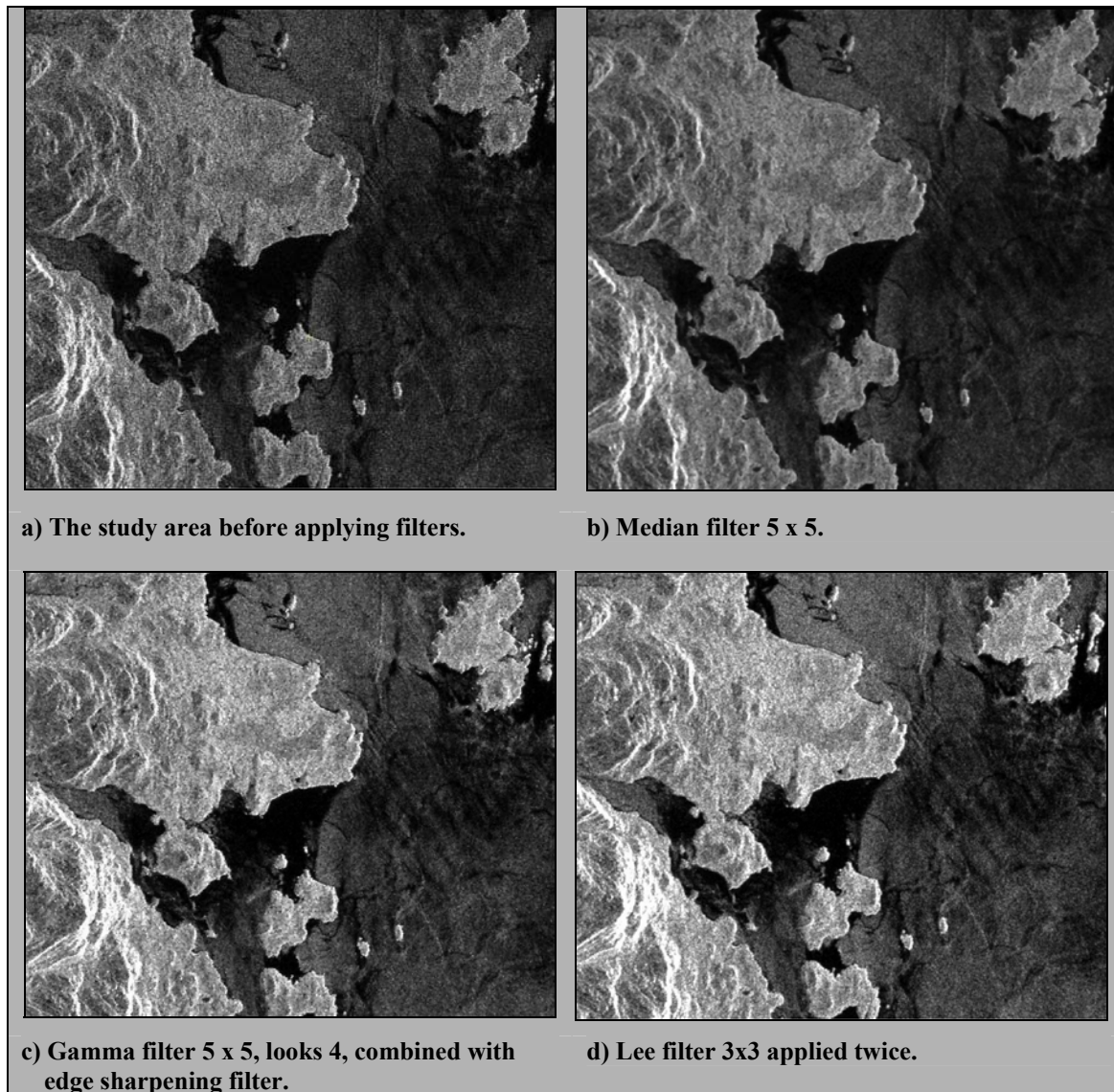


Figure 4.2. Different Filters used for Speckle Reduction

4.2.2 Enhancement of Land-Water Boundary

Separation between land and water is the most important step in the coastline extraction procedure. The first step, reduction of noise, is intended to minimize variation

within pixels of land and within pixels of water, while maintaining the distinct characteristics for each.

Edge enhancement is a way of increasing geometric detail in an image, considering that an edge is the boundary between an object and the background [Parker, 1997]. In this case, land and water are considered objects and background respectively. All lines or edges have a direction such that one side is always brighter than the other [Zelek, 1990].

Because the coastline is the most important feature in this image, enhancement of the land-water boundary is a necessary task. The most commonly used procedure is histogram equalization to increase the contrast throughout the image. Another method to modify and spread the histogram of gray level values is transforming the image from unsigned 16-bit to 8-bit. Then the old 65,536 different gray values image is now transformed to 256 gray levels. Even when this elemental operation changes the digital number of pixels, it is well suited to enhance the contrast between land and water. The histogram scaling produces a lack of radiometric resolution that is detrimental to detect features in land. That effect has no importance because the main purpose is the coastline enhancement and no land analysis is being performed.

4.2.2.1 Most used Edge Detection and Enhancement Techniques

4.2.2.1.1 Edge Detection

Edge detection is the process of locating the edge pixels. An edge enhancement will increase the contrast between the edges and the background in such a way that edges become more visible [Parker, 1997]. In addition, edge tracing is the process of following the edges, usually collecting the edge pixels into a list [Martin and Tosunoglu, n.d.].

Usually an edge can be modeled as a step or as a ramp. In the “real world” edges change gradually over the images, so the ramp is the best one to fit. There are three economically different techniques to detect edges over an image [Richards and Jia, 1999]. The most commonly used algorithms from these techniques are used in this research.

4.2.2.1.1.1 Derivative Operators

The rate of change of a function, and the rate of change of grey levels in an image is large near an edge and small in relatively constant areas [Parker, 1997]. The gradient vector can be applied (partial derivative in x and y direction) in a discrete way, calculating the differences in grey levels over some local region.

$$\Delta_{x1} A(x,y) = A(x+1,y) - A(x-1,y)$$

$$\Delta_{y1} A(x,y) = A(x,y+1) - A(x,y-1)$$

Equation 4.2

Then, the magnitude is calculated, that will give the strength of the edge:

$$Gmag = \sqrt{\left(\left(\frac{\partial A}{\partial x}\right)^2 + \left(\frac{\partial A}{\partial y}\right)^2\right)} = \sqrt{(\nabla^2 x + \nabla^2 y)} \quad \text{Equation 4.3}$$

Direction of the edge:

$$Gdir = \tan^{-1}\left(\frac{\nabla x}{\nabla y}\right) \quad \text{Equation. 4.4}$$

Then, if the resulting gradient exceeds threshold, the edge is detected, otherwise will not be detected.

4.2.2.1.1.2 The Roberts Edge Detector

For digital image data in which x and y are “discretized”, the continuous derivatives are replaced by differences [Richards and Jia, 1999].

$$\Lambda_1 = A(x, y) - A(x + 1, y + 1)$$

$$\Lambda_2 = A(x + 1, y) - A(x, y + 1) \quad \text{Equation 4.5}$$

They constitute the discrete components of the vector derivative at the point $x + \frac{1}{2}, y + \frac{1}{2}$, in the diagonal directions. Hence both horizontal and vertical edges are detected, as will be diagonal edges. Since this procedure computes a local gradient it is necessary to choose a threshold value above which edge gradients are said to occur.

4.2.2.1.1.3 The Sobel Operator

Sobel computes discrete gradient in the horizontal and vertical directions at the pixel location x,y .

It is more costly to evaluate than the Roberts filter. The orthogonal components of the gradient are:

Equation 4.6

$$\Lambda_1 = \{A(x-1, y+1) - 2A(x-1, y) + A(x-1, y-1)\} - \{A(x+1, y+1) - 2A(x+1, y) + A(x+1, y-1)\}$$

$$\Lambda_2 = \{A(x-1, y+1) - 2A(x, y+1) + A(x+1, y+1)\} - \{A(x-1, y-1) - 2A(x, y-1) + A(x+1, y-1)\}$$

Hence, horizontal and vertical as well diagonal edges are detected. As before, a threshold on the responses is generally chosen to allow an edge map to be produced in which small responses, resulting from noise or minor gradients, are suppressed.

4.2.2.1.1.4 Edge Detecting Templates

Template operators are used not only for smoothing and enhancement, but also for line and edge detection. A template is a box or window previously defined and moved over the image row-by-row and column-by-column. In general terms, the product of the pixel brightness values, covered by the template at a particular position and the template entries are summed to give the template response. This response is then used to define a

new brightness value for the pixel currently at the center of the template [Richards and Jia, 1999].

4.2.2.1.1.5 Linear Edge Detecting Templates

Richards and Jia [1999] describes a 3x3 edge-detection template that detects edges in the vertical, horizontal and diagonal directions as it is shown in Figure 4.3.

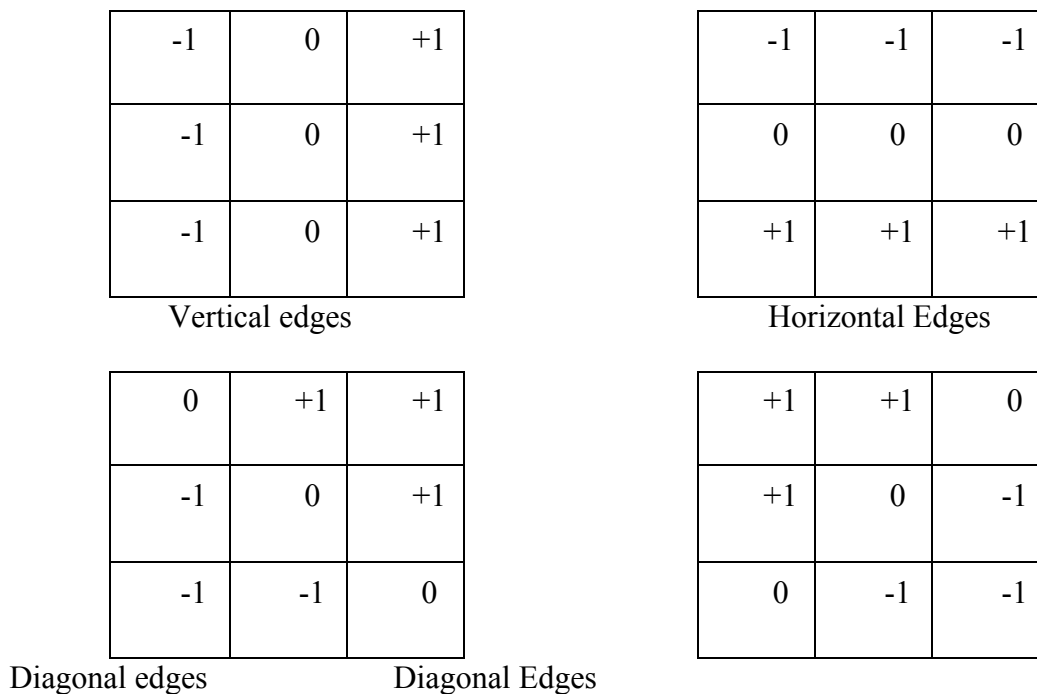


Figure 4.3. Linear Edge Detecting Templates
 These templates can be used to detect edges in the vertical, horizontal and diagonal directions.

In this approach, the edge is defined as a two pixels wide columns or rows depending on whether the vertical or horizontal edges are detected. All four templates

must be applied to obtain edges in all orientations, using a threshold to determine the edge map. If the threshold is too low it will lead to many false edge counts. On the other hand, if the threshold is too high, little discontinuities will appear on the detected edge.

4.2.2.1.1.6 Sobel Template

As specified before, the Sobel edge detector is a derivative-based operator that is used in templates form for computational purposes. The purpose is to use a small discrete template as a model instead of using a derivative operator [Parker, 1997]. In other words, it is a spatial derivative technique but reduced to templates. Here, the following templates are used in the form of convolution mask, locating the resulting pixel value in the center of the template in the output image.

Kernels in Figure 4.4 are designed to respond maximally to edges running vertically and horizontally related to the pixel grid. After calculation, the resulting image is thresholded. All pixels will have some responses to templates but the very large responses will correspond to an edge.

Sx

1	0	1
-2	0	2
-1	0	1

Vertical Edges

Sy

1	2	1
0	0	0
-1	-2	-1

Horizontal Edges

Figure 4.4. Sobel Templates

These templates can be used to detect edges in the vertical and horizontal directions.

4.2.2.1.2 Edge Enhancement

Edge enhancement is a particularly simple and effective means for increasing geometric detail in an image. First edges are detected and then they are either added back into the original image to increase contrast in the vicinity of an edge, or the edges are highlighted using saturated (black, white or colour) overlays on borders [Richards and Jia, 1999]. If the edges are added back into the original image in varying proportions, the boundaries are enhanced.

Land-water enhancement is one of the most important steps to achieve a good segmentation between them, and further coastline delineation.

4.2.3 Testing Existing Techniques for Shoreline Enhancement

After histogram scaling, the next step is to eliminate edges in land, keeping the coastline edge with minimum changes. In the spatial domain, another important step is focused on getting rid of the edges present in land, while preserving the main edge, which consists of the shoreline.

Previous works in coastline detection use similar techniques that focus on the enhancement of land-water boundary.

4.2.3.1 Edge Detection Focusing on the Shoreline

This chapter presents a combination of linear filters and morphological operations used to enhance the land-water boundary, getting rid of the edges present in land, while preserving the main edge consisting in the shoreline.

After scaling the image from 16 bits to 8-bits, some pixels have high gray-level values if compared with its neighbors. Because that, a median filter 3x3 window is applied to smooth the image while enhancing the edges.

Although all the edges present in the image can be detected using any edge detector method, using the Sobel filter to detect all the edges gives good results, because using a 3x3 window the detected edges are strong and consistent.

Because the new pixel values in the Sobel image correspond to the rate of change between neighboring pixel values in the original image, the resulting histogram from Sobel shows low gray level values in the areas with a low rate of change (most of the image data), and high gray level values in the edges, being even higher in those

prominent edges (i.e. shoreline). Figure 4.5 shows the corresponding histograms with gray-level values obtained from the original image (left) and the histogram obtained from the resulting image after Sobel edge detector is applied (right).

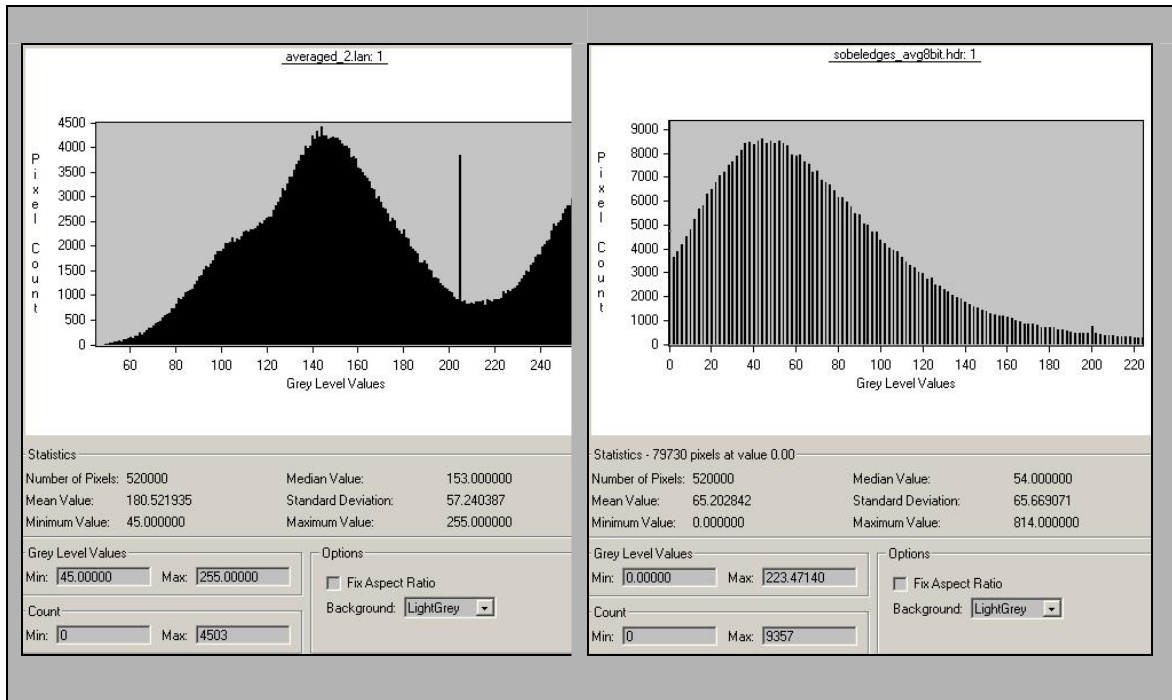


Figure 4.5. Histograms of the Original Image and its Respective Sobel Image

After the edge detection stage, edge enhancement is applied using different proportions. From testing different combinations, it was found that 30% of the pixel value obtained using Sobel added to 70% of the pixel value from the original image produced the best results. Figure 4.6 shows the effect of this operation focusing on the enhancement of the land-water boundary while avoiding the influences of other edges present in land. The resulting image once 30% of the pixel value obtained using Sobel is added to the 70% of the pixel value from the original image. The left image shows the resulting image and the right image shows the corresponding grey-level values histogram.

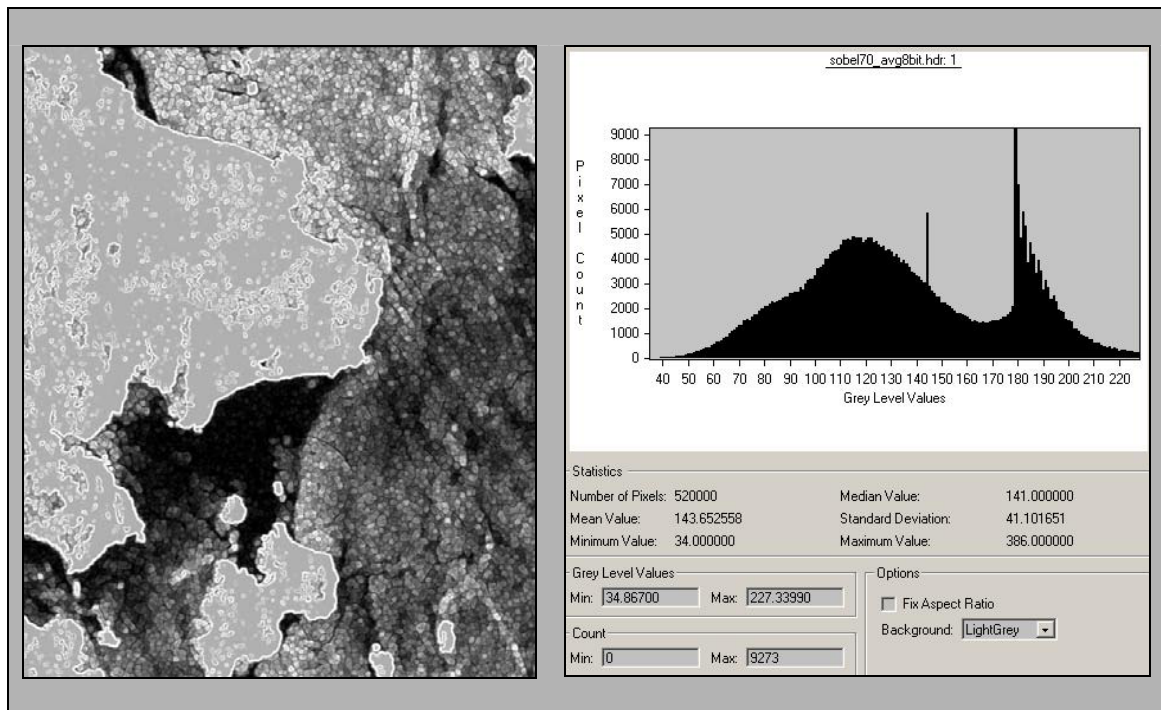


Figure 4.6. Enhanced Image and its Respective Histogram

Using this technique, the grey-level value of the pixels on land is decreased and made more homogeneous. The application of this technique produces a steeper land-water separation.

4.2.3.2 Texture Analysis Focusing on Shoreline

In another approach, the Sobel edge detector applied in the land-water enhancement step was replaced by texture analysis using different parameters. A set of texture measurements is calculated for all pixels in an input image.

4.2.3.2.1 Texture

Texture can be defined as a repetition of a pattern over a region. Texture is an important issue to be analyzed in radar images. Texture is studied to perform segmentation, where the result could be an image in which texture has been replaced by a unique grey level or color. The following sections describe different approaches to measure texture [Parker, 1997].

4.2.3.2.1.1 Statistics

A region can be identified using its particular texture. This method is based in the use of small windows $W \times W$ pixels to capture samples of the particular properties over an area. The window moves over the image calculating the following parameters for each case separately.

4.2.3.2.1.1.1 Mean Windows

The use of average grey level is not recommended to distinguish between textures [Parker, 1997]. Average windows are usually used to blurr the image. As a result of the moving window, the boundary between textured regions can only be determined within

a distance of about W pixels, where W is the width of the window. Each pixel in the image is replaced by the average of the levels seen in a region $W \times W$ pixels in size centered at that pixel. Then, thresholding the image into two regions using the new average levels proceeds. Boundary regions (exact location) depend on the threshold that is applied to the mean-level image.

4.2.3.2.1.1.2 Standard Deviation Windows

Standard Deviation Windows work better than mean windows [Parker, 1997]. It is more consistent in the changes in levels than is in the levels themselves. After calculating the mean of each window, the standard deviation of each pixel is calculated with respect to the mean. The resulting value is displayed in the center of the window. The formula is shown in Equation 4.7.

$$Mn = \frac{\sum (x - \bar{x})^n}{N}$$

Equation 4.7

4.2.3.2.1.2 Gray – Level Co-occurrence Matrices (GLCM)

Statistical windows are easy to calculate but it do not provide any information about the repeating nature of texture. Gray Level Co-occurrence Matrices (GLCM) contains

information about the positions of pixels having similar grey level values. They attempt to capture directionality of patterns. The idea is to scan the image and keep track of how often pixels that differ by a specified amount in value are separated by a fixed distance in “ d ” position.

Directionality is determined by using multiple matrices, each one for each direction of interest. Then, the matrix, associating them to texture, captures distance and direction. Therefore, for every value of “ d ”, we have 4 images (horizontal, vertical and two diagonal) each of which is 256 x 256 for an original image with 256 levels of gray. However, this procedure produces an enormous amount of data. To minimize data, a few simple numerical values called descriptors are calculated to encapsulate the information. In other words, the grey –level difference between pixels in a given direction is recorded in a small window of the original image. Those descriptors could be represented by statistical moments defined before and others descriptors such as maximum probability, contrast, homogeneity and entropy. After the descriptor is calculated, it is placed at current pixel’s position in the output image.

4.2.3.2.1.2.1 Edge Detection using GLCM Variance Windows

The measurements are based on second-order statistics computed from the grey level co-occurrence matrices. Either texture measures for a specific direction or directional invariant measures can be computed. After testing different parameters for texture

analysis, it was found that variance acted better to detect edges. Therefore, this parameter was used to analyze the texture in the image.

Figure 4.7 shows the effects of applying texture analysis during the enhancement of land-water boundary and a comparison between Sobel (left) and texture analysis using variance (right) in the detection of all the edges present in the image. Below each picture, its respective histogram shows the grey level distribution. Grey level pixels in the texture image are too high, causing problems for further operations.

Visually, the resulting image after texture using variance windows acted similar to the images treated with the Sobel edge detector, however the implementation of this procedure implies more computational cost. Therefore, Sobel operator was finally chosen to detect the edges in the land-water enhancement process.

However, after using Sobel and adding the 70% of image back to contrast coastline boundary (Figure 4.6), there are still some undesirable edges in land close to the coastline that should be eliminated without modifying the shoreline.

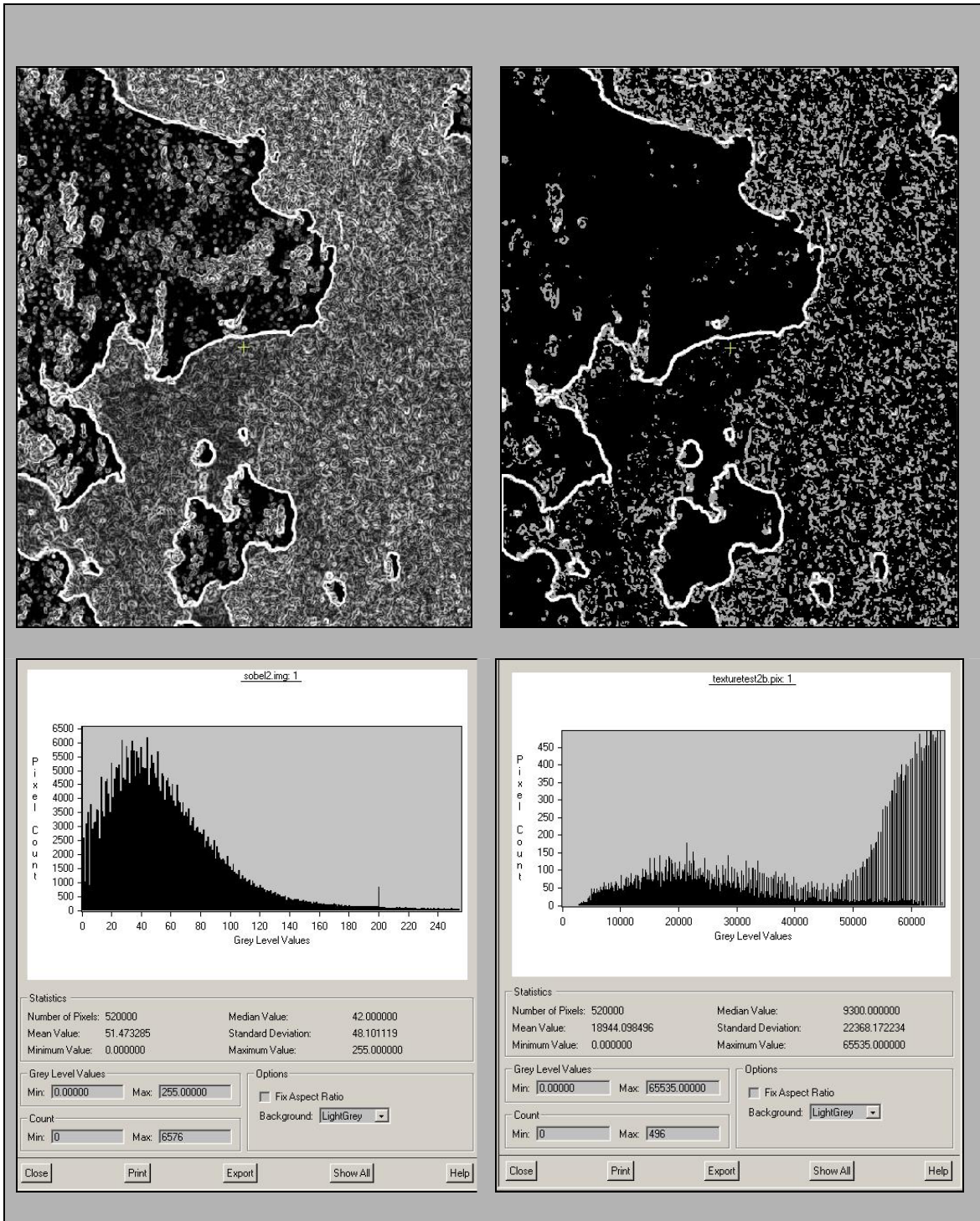


Figure 4.7. Sobel and Texture (Variance) Images

4.2.4 Existing Techniques used to Reduce the Unnecessary Edges

4.2.4.1 The use of Smoothing Filters

To get rid of the undesirable edges, the image is smoothed using a 5x5 mean window. Larger windows will be detrimental, and will produce large offsets in the shorelines. To avoid this effect, this smoothing window is applied just once. After the application of the smoothing window, digital morphology can be used to reduce the unnecessary edges.

4.2.4.2 The use of Digital Morphology

After smoothing the image, a gray level opening operation is performed using a 3x3 window. In gray level images, the opening operation (gray-scale erosion followed by gray-scale dilation) is a smoothing operation that decreases the average pixels value.

Digital morphology is a way to describe or analyze the shape (the form and structure of an object) of a digital (raster) object. In an image, pixels are organized into groups having a two-dimensional structure called shape. A group of mathematical operations can be applied to the set of pixels to enhance or highlight specific aspects of the shape so that they can be counted or recognized [Martin and Tosunoglu, n.d.].

These different properties are inherent to morphological operations:

Being A and B a set of pixels,

- Translation: $(A)_x = \{c \mid c = a + x, a \in A\}$
- Reflection: $\hat{A} = \{c \mid c = -a, a \in A\}$
- Union: $A \cup B = \{c \mid ((c \in A) \text{ or } (c \in B))\}$
- Intersection: $A \cap B = \{c \mid (c \in A) \& (c \in B)\}$
- Complement : $A^c = \{c \mid c \in A\}$
- Difference: $A - B = A \cap B^c$

In this chapter, dilation and erosion, which are basics operations based in these fundamental properties, are described as binary (bi-level) operations. In general, an operator is defined as a set of black pixels with a specific location for each of its pixels given by the pixel row and column indices [Parker, 1997].

4.2.4.2.1 Binary Dilation

Binary dilation can be defined as:

$$A + B = \{c \mid c = a + b, a \in A, b \in B\}$$

Where A represents the image to be transformed and B is a second set of pixels called structure element, with a particular shape that acts on the pixels of A producing an expected result. In Figure 4.8, the pixel marked with an x corresponds to the origin of the image. Then, the structuring element is a template moving over the image, producing the dilation. In general terms, dilation is a morphological operation to make the object wider by adding neighboring pixels at the boundaries in the directions specified by the

structuring element. In binary images, it can be implemented by marking all white pixels having at least one black neighbor, and then setting all of the marked pixels to black [Parker, 1997].

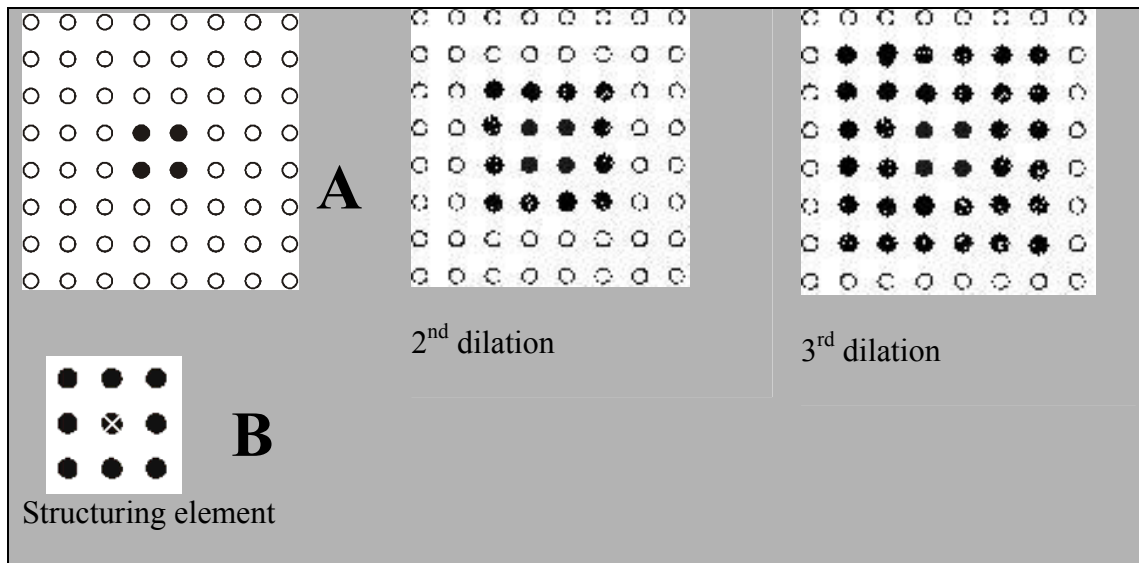


Figure 4.8. Effects of Dilation over the Original Image using a 3x3 Structuring Element

4.2.4.2.2 Binary Erosion

Binary erosion produces the inverse results obtained by the dilation operation, but the procedure is slightly different from the inverse procedure of dilation. Erosion corresponds to the set of pixels “ c ” such that the structuring element B translated by “ c ” corresponds to a set of black pixels in A . As the result, any pixel that does not match the pattern defined by the black pixel in the structuring element will not belong to the result.

Hence, erosion makes the object image smaller by removing the outer layer of pixels from an object. This can be implemented by marking all black pixels having at least one

white neighbor, and then setting to white all of the marked pixels. Mathematical operations differ between dilation and erosion, and those concepts can be applied either to binary or gray level images.

4.2.4.2.3 Opening and Closing

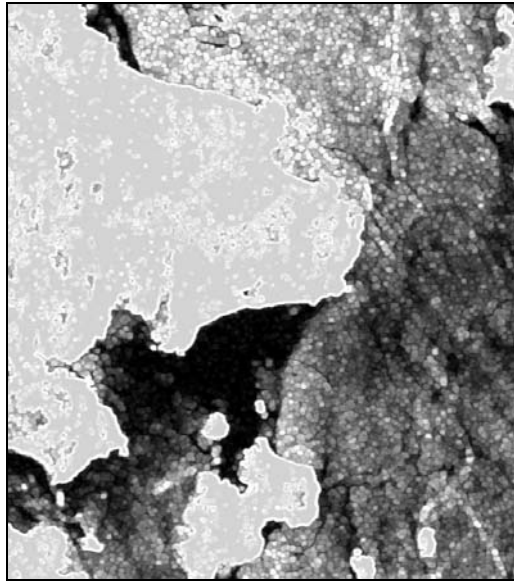
The application of erosion followed immediately by dilation using the same structuring elements is called *opening*. This binary operation attempts to open small gaps between touching objects in an image [Martin and Tosunoglu, n.d.]. Also, it can be explained as a process that destroys edges. This concept is directly applied to the analyzed coastal image to get rid of the edges present in land while preserving the coastline.

Also, the application of a dilation procedure immediately followed by erosion using the same structuring element is called closing. As its name indicates, it closes or fills the gaps between objects. Practically, closing is a process that joins edges. More information regarding morphological operations can be found in Parker, 1997.

4.2.4.2.4 Application of Opening Filter to Reduce the Undesirable Edges

Opening will act over neighboring pixels, destroying the edges in the touching objects of the image. Then the image is smoothed while the strongest edges remain (coastline).

Another tested technique to get rid of the edges in land was achieved by applying the Fourier transformation and applying a low-pass filter to smooth the image.



However, the result did not improve too much the final result. Hence, the use of low pass filters and opening operation was the best approach to locally reduce the gray-pixel values over the unnecessary edges. The results are shown in Figure 4.9.

Figure 4.9. Application of a 5x5 Mean Filter followed by Gray Level Opening

4.2.5 Land-Water Separation

Because at this stage, the land-water boundary has been very well enhanced without an excessive loss of spatial features, a threshold is applied to segment the image for further coastline extraction.

4.2.5.1 Grey-Level Segmentation or Threshold

Gray Level Segmentation is a conversion between a gray-level image and a bi-level image. Bi-level image is a monochrome image only composed of black and white pixels. It should contain the most essential information of the image (i.e. number, position and shape of objects), but is not comparable with the information offered by the grey-level image [Martin and Tosunoglu, n.d.]. Pixels with similar gray levels in a nearby region usually belong to the same object. By gray level segmentation we simplify many recognition and classification procedures [Parker, 1997]. The most common procedure is done by thresholding.

Thresholding is the procedure where all gray-level below this value will be classified as black (0), and those above will be white (1).

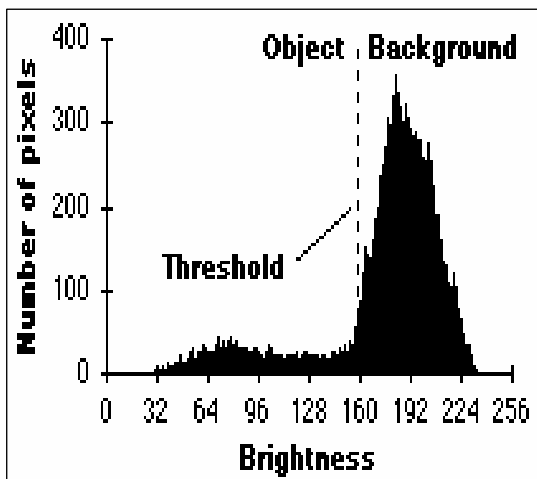


Figure 4.10. Thresholding Operation used to Separate Object from Background

The most common way to choose the threshold is by using the mean gray value in the image, but it is not always useful, especially when is used in a radar image where the gray level values have a great variability. However, in this case, because the image is already processed, thresholding by the mean value is well suited.

4.2.5.2 Application of Land-Water Segmentation

In real data, and especially in radar images, the object and background pixels have overlapping gray level values.

In coastline extraction, it is important to discriminate land from water. Because of the speckle and environmental noise, the simple use of segmentation techniques does not work too well over radar images as is shown in Figure 4.11, where segmentation is applied.

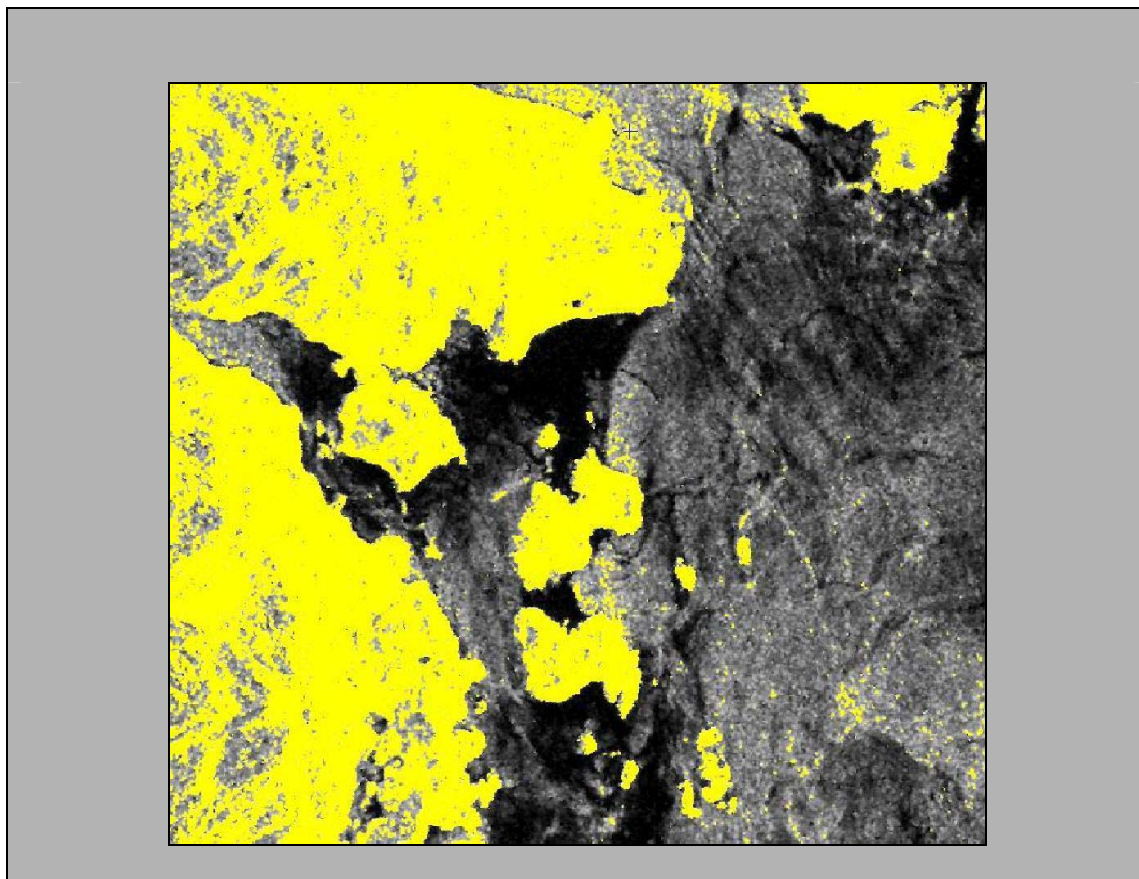


**Figure 4.11. Application of a Single Threshold Operation to the Radar Image
Even when the image was filtered to remove the speckle, there is no good land-water
discrimination.**

The single use of segmentation is a bad approach, but combined with different spatial procedures it should give acceptable results in land-water separation and finally in coastline extraction.

The threshold must be carefully selected by the operator in order to remove backscatter coming from the sea surface and to avoid missing land. In this case, the critical areas in the image were examined.

The threshold used was the mean value of land pixels after the histogram was computed (in this case was 179). Of course, the operator's analysis is important here to determine the value of threshold to be implemented. Figure 4.13a) shows the results of the segmentation using that threshold. To eliminate noise from sea surface, four adjacent pixels are considered for the connectivity. Each connected region, or segment, is given a unique DN value in the output image.

After the whole process, the result of segmentation is poor. The noise over sea surface is too high to achieve a proper land-water separation, and further coastline detection. The problem is that there is still too much environmental noise close to the shoreline in the original image, which will be misinterpreted with the shoreline itself. Also in Figure 4.13b), the same problem is present over an image of the same area but acquired at a different date.

Because of the noise problem, the coastline detection step cannot be achieved well enough to obtain acceptable results.

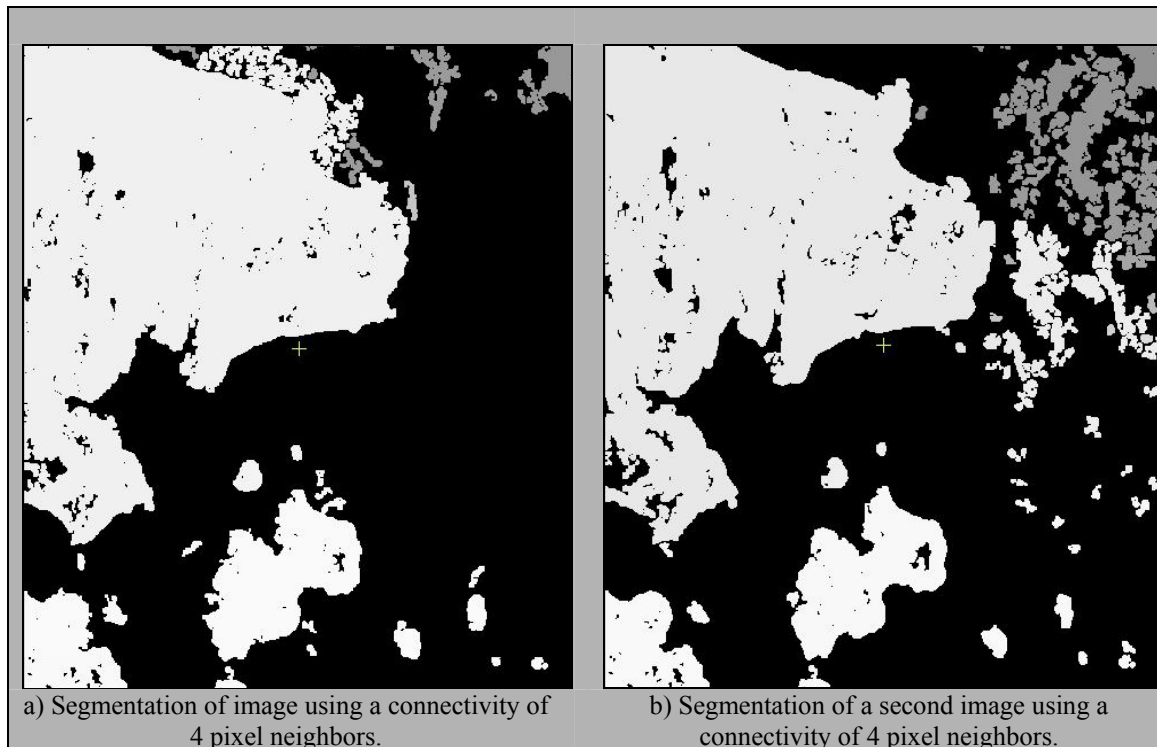


Figure 4.12. Results on Segmentation using Single SAR Images

4.3 Summary

In this chapter, rough land-water segmentation was achieved using the most common procedure based in essential operations focused on the enhancement of the land-water boundary and the reduction of grey-level value in the unnecessary edges, while keeping the most important edge: the shoreline.

However, the results were not good. Hence, the high backscatter of rough sea surface proved to be a problem that needs to be solved using a different approach.

Chapter 5

DEVELOPMENT OF A NEW METHOD FOR LAND-WATER SEPARATION

5.1 Introduction

The principal problem encountered in chapter four was caused by the presence of rough sea surface due to wind conditions at the time of image acquisition. The backscatter from that rough sea surface can usually equal or exceed the backscatter from a portion of land close to the coastline, resulting in a detrimental factor to achieve land-water separation.

To solve this problem this research uses two images from the same areas, but acquired in different time. Certainly, one of those two images will present better sea surface conditions than the other.

This chapter presents a novel methodology based on operations between multitemporal images to enhance the input image to the point that backscatter over sea is reduced to a point where it is so far below that from land that the differences are useful in discriminating shoreline.

After that, the application of an iterative use of windows designed both to delete the noise and to fill some undesirable gaps caused by shadowing is presented.

5.2 Data Used and Methodology Selected in this Research

The data used was The ERS - SAR Precision Image product, which is well suited for quantitative analysis, photo-interpreting and image processing. Also, multitemporal series are well suited using this product.

ERS-1 SAR looks at the Earth surface with a 23° incidence angle. Due to this, images contain almost no shadow but may contain a large amount of layover and foreshortening. The reduction of shadows is fundamental if the coastline to be extracted is part of a high relief area, such as the area analyzed. Appendix II shows the main characteristics of this product.

The developed methodology is based in two stages:

- A rough land water segmentation stage, which was presented in the previous chapter. However, the use of multitemporal images now improves the land-water segmentation.
- A refinement stage using the Multitemporal Segmentation Method and the iterative use of windows to delete the noise, which is proposed in this chapter.

5.3 The Multitemporal Analysis for Noise Reduction

The multitemporal analysis consists in making image-image mathematical or statistical operations to reduce the pixel values of those areas with high backscatter on sea surface, especially when it is close to the shoreline. Hence, the problem is solved in

some locations of the first image and other locations for the second image. Most researchers could think that just choosing the better image will solve the problem of shoreline extraction, but because the noise coming over the sea surface is random and it presents different characteristics in shape and location, this method certainly helps to eliminate part of the high backscatter coming from sea surface.

To do image-image operations, both images must have the same reference system. First, image-image registration is achieved, using the geocoded reference image or entering manually the coordinates. The RMS has to be low, to ensure a good registration, and care must be taken in the resampling mode (usually cubic convolution used) and the channel used in the input and output. The user has to avoid making changes in the digital value of the original pixels after this operation.

To avoid displacement over analyzed areas, both images must be subseted in a way with both of them starting at the same pixel.

5.3.1 Averaging the Images

Averaging both images reduces the random noise over the sea surface; especially when that noise is high close the coastline. To obtain the average of those images this project uses the program called “*8bits_imgavg.dsw*”, modified from an existing C source code to open and display LAN images¹. To do that, Microsoft Visual C++ was used.

¹ The original code to display images was provided by my supervisor, Dr. Yun Zhang

Figure 5.1 shows the original images where the images acquired on different time present problems in some areas close to the shoreline, due the effect of wind. The left image was obtained on 03 Nov 1995, and the right on 25 Nov 1992. Figure 5.2 shows the effect of averaging the pixel value between two images, where the corresponding averaged image solves the problem of random noise close to the shoreline over sea surface. The averaging operation was performed after image scaling to 8bit.

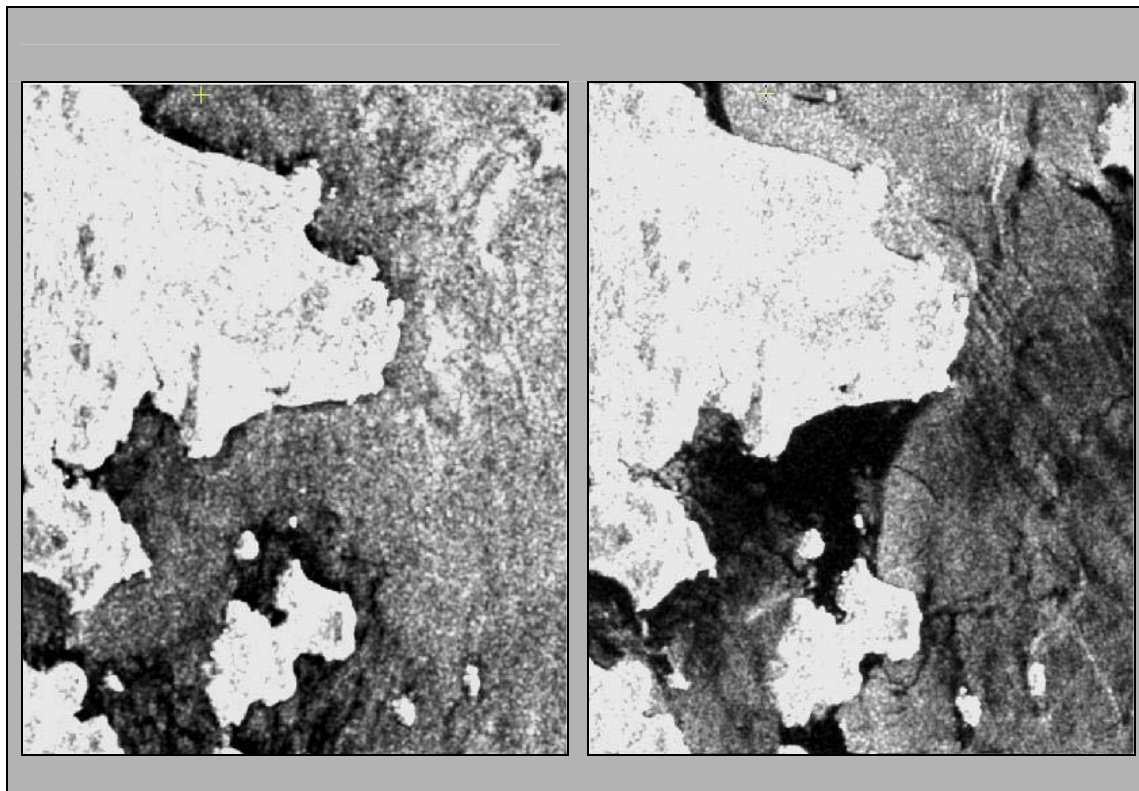


Figure 5.1. Multitemporal Images

The same procedure was made over different areas, obtaining good results in the land water boundary separation. The random noise over sea surface is solved using this image-image operation. After doing this operation between multitemporal images, the

algorithm described in this chapter can be applied over the image, improving the operations for land-water enhancement.

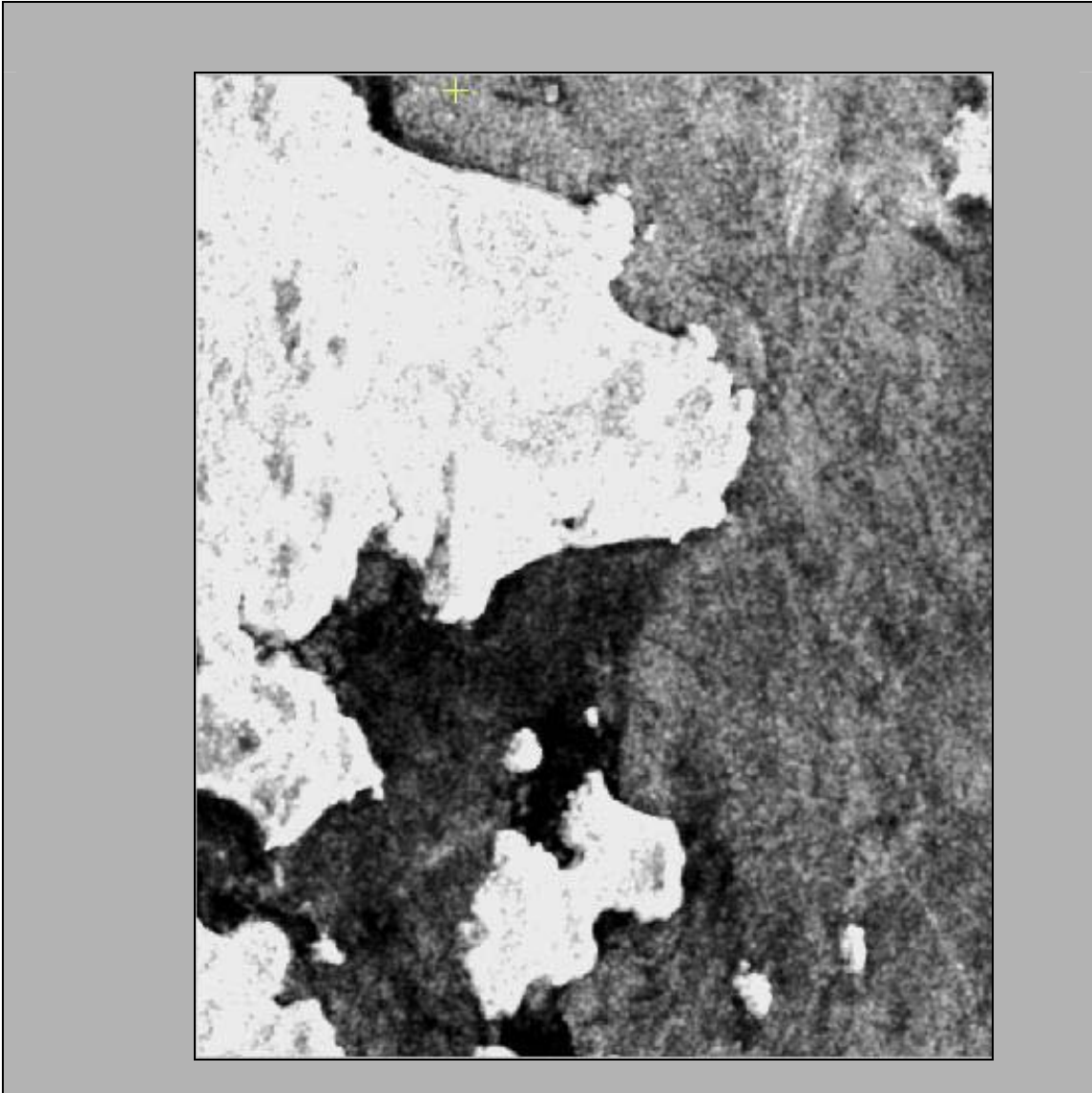


Figure 5.2. Result in Averaging two Images

5.3.2 Principal Components Analysis (PCA)

The multispectral or vector character of most remote sensing image data renders it amenable to spectral transformations that generate new sets of image components or bands [Richards and Jia, 1999]. These components then represent an alternative description of the data, in which the new components of a pixel vector are related to its old brightness values in the original set of spectral bands via linear operation [Richards and Jia, 1999].

The most common way to use multispectral transformation is using satellite images containing multiple channels to acquire the data in different wavelengths each one. The multispectral or multidimensional nature of remote sensing image data can be accommodated by constructing a vector space with as many axes or dimensions as there are spectral components associated with each pixel [Richards and Jia, 1999].

Each channel provides different dimension in the vector space, in which each pixel can be associated. Vectors, whose components are the individual spectral responses in each band, describe the position of pixel points in multispectral space [Richards and Jia, 1999].

The mean position of pixels in the space is defined by the expected value of the pixel vector x , according to equation 5.1:

$$m = \xi \{x\} = \frac{1}{K} \sum_{k=1}^K x_k \quad \text{Equation 5.1}$$

Where m is the mean pixel vector and x_k corresponds to the individual pixels vectors of total number K ; ξ is the expectation operator.

The main steps in a Principle Component Transformation are:

- Assembling the covariance matrix of the image to be transformed, using the following formula in equation 5.2:

$$\Sigma_x = \frac{1}{K-1} \sum_{k=1}^K (x_k - m)(x_k - m)^t \quad \text{Equation 5.2}$$

- Determining the eigenvalues and eigenvectors of the covariance matrix. At this stage the eigenvalues are used simply to assess the distribution of data variance over the respective components.
- Forming the components using the eigenvectors of the covariance matrix as the weighting coefficients.

By examining the covariance matrix between the output eigenchannels, we observe that the most consistent data of the transformed image from the original bands is in the first principal component PC1. Then PC2 and the rest are in the remaining PCs. In this case, the last PC contains the data, which is not correlated (see Figure 5.3).

The practical benefits of this application are:

- User can analyze any of the principal components individually or in combination as a false color composite.
- Relationships between groups of pixels representing different land cover types might become clearer if they are viewed in the principal axis reference system rather than in terms of the original spectral bands.
- Can be used in the analysis of multitemporal images in order to identify areas of change.

In this research PCA can be used to keep the homogeneity of the image, removing the random noise coming from sea surface.

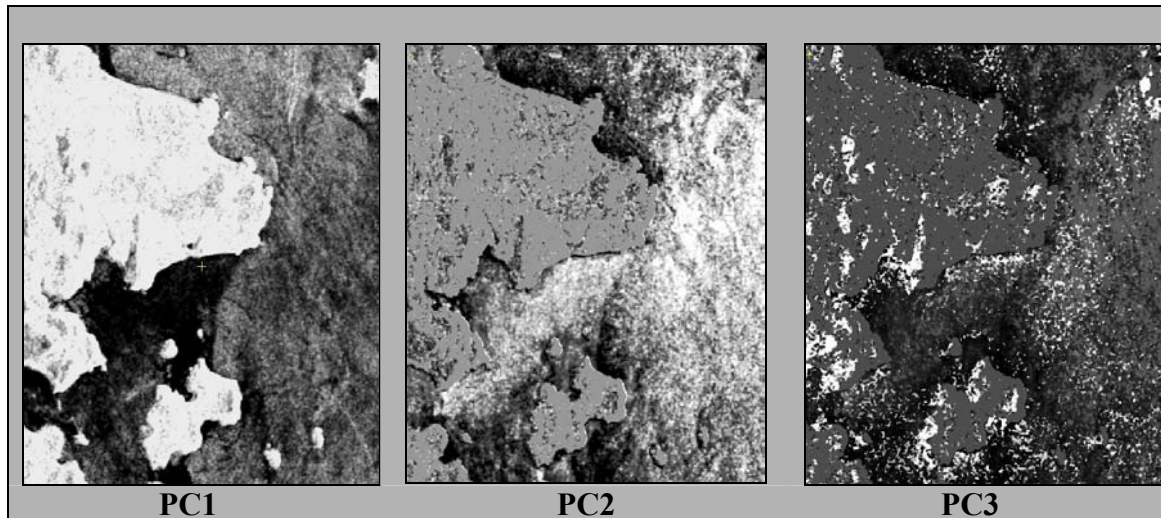


Figure 5.3. Results on Principal Components Analysis
From left to right the PC1, PC2 and PC3 respectively, where PC1 contains the most redundant data and PC3 contains noise.

5.3.3 Multiplying the Images

Another tested image-image operation that gave good results was the multiplication of both images. Because of the effect of multiplication, the image is transformed from 8 bits to 32 real bits to support the resulting grey-level values. The final result looks better than the averaged image, because there is a bigger enhancement between land and water or stretching of the range of grey level values. In this case most of the noise over the sea surface is reduced compared with the high grey-level values of the resulting pixels in land due to the effect of multiplication. While in land the multiplication is similar to the effect of squaring the pixel value, in water the high grey-level value of the first image

(noise) is multiplied by a low grey-level value of the second image. However, even when the images seem looking better, the great amount of information stored in 32r bits is too large to perform the operations of getting rid of the edges in the land (gray level morphological operations). Hence, the image multiplication was not used in the general procedure.

5.3.4 The Modified Algorithm using Multitemporal Images

Because there was an improvement using multitemporal images, then this procedure was included in the general algorithm as shown in Figure 5.4.

In this case, averaging the images was used to avoid too much cost in computation process. Then, these new images will be used in the process of getting rid of the edges in land while preserving the coastline.

After the multitemporal analysis consisting in averaging the pixel values between two images of the same area but acquired at different dates, or using the principal components analysis procedure, the procedure used before can be applied, obtaining better results.

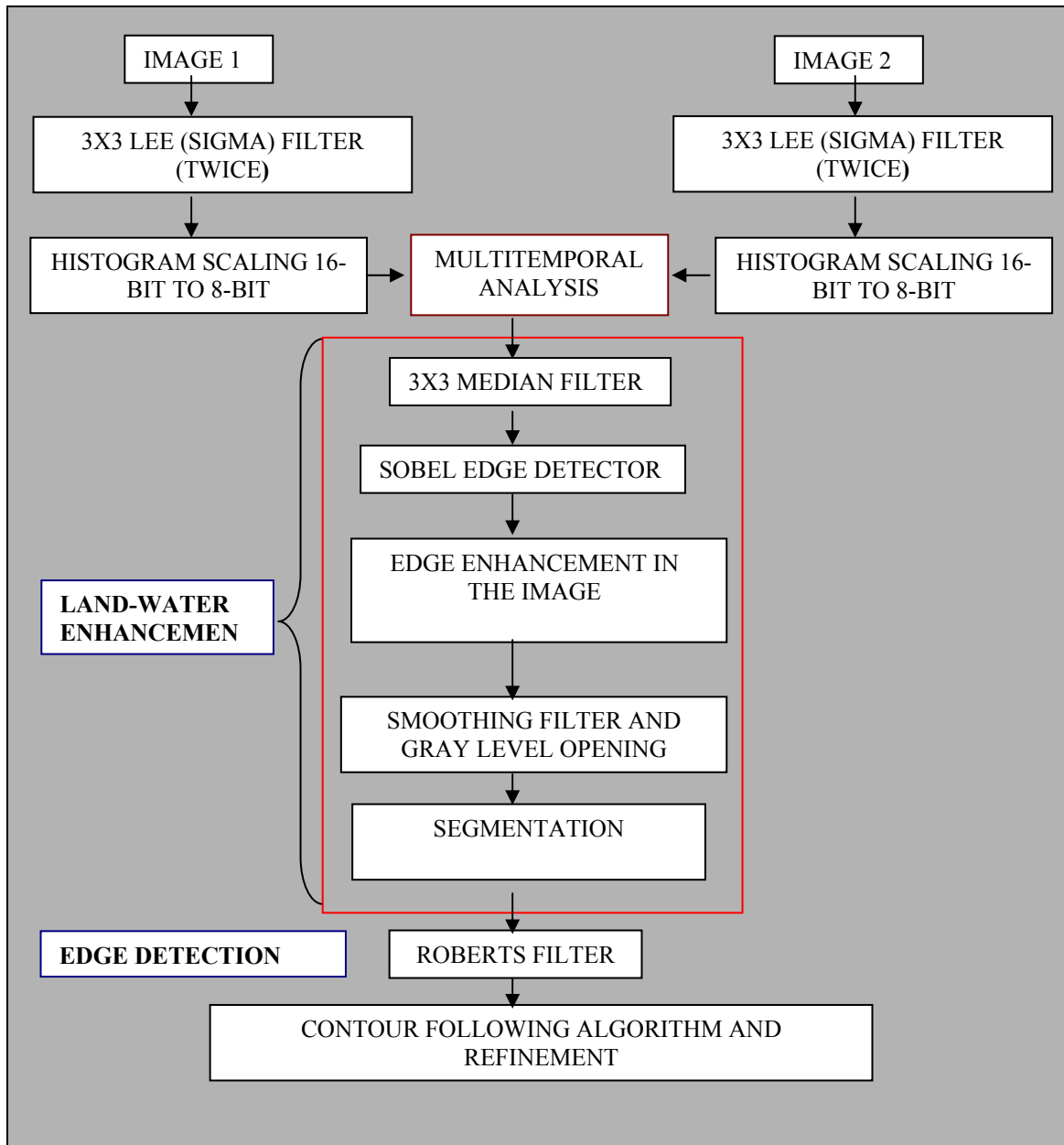


Figure 5.4. Multitemporal Analysis in the use of Most Common Filters to Detect Edges

5.4 Results in Coastline Detection after the Multitemporal Analysis

After improving the general procedure with the use of multitemporal images to reduce the noise, the final step is the detection of the edges. This step provides the coastline generation from the enhanced image.

Analyzing the previous work, Lee and Jurkevich [1990] apply the Roberts edge detection to produce a thinner contour image of the land-water boundary. The reason for applying Robert's operator is that the edges generated are 1-pixel wide, making the edge tracing more precise. Because of the effect of the mean filter applied in the enhancement stage, they need to refine the coastline position due to the resulting offset. To refine the coastline, mean filter is applied twice after the Roberts filter, followed by threshold. Then, the coastline is retraced using a contour following algorithm on the inside edges of the dilated coastline. After refinement, the new coastline matches that of the original image to within a pixel or two.

In this research, the Roberts operator is applied to the binary image, detecting all the edges present in the processed image. Because the image enhancement in the previous chapter focused the image processing in getting rid of the edges in land, the coastline is well defined if there is not rough surface water close to the shoreline.

Figure 5.5 shows the effect of using multitemporal images, improving the shoreline detection. After this edge detection process, the new coastline using the procedure described in chapter four has an average offset of two pixels comparing the position of the coastline with the original image.

If applying the refinement made by Lee and Jurkevich [1990], this offset was reduced to 1 pixel.

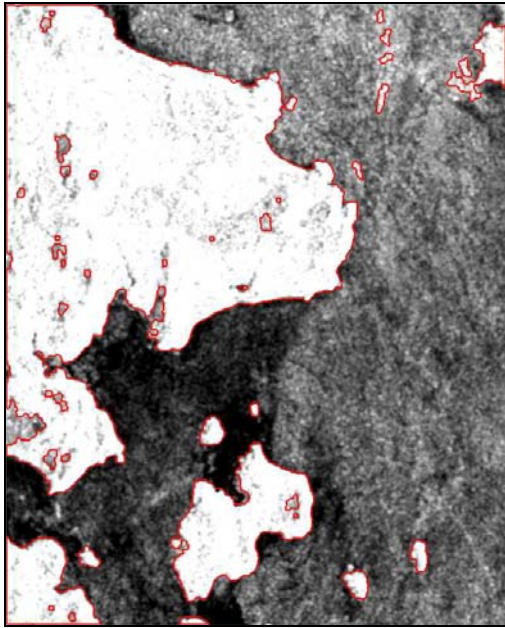


Figure 5.5. Final Edge Detection over the Averaged Image

The procedure used until now to detect coastline gives good results except over few areas, where the backscatter in land is too low. However, some noise still remains in the sea surface. Also, some misinterpretations of the shoreline occur due to a lack of land-noise discrimination procedure. Therefore, there is a need to upgrade this methodology in order to eliminate that undesirable remaining noise.

5.5 Multitemporal Segmentation for Island-Noise Discrimination

The Multitemporal Segmentation proposed in this research is the main improvement achieved. The Multitemporal Segmentation Method consists in a series of operations using two images at different processing level. This section aims to solve the visually observed discrepancies between the detected coastline and the coastline in the original image.

After the application of the basic operations presented in chapter 4, the first problem encountered is the detection of false islands caused by the remaining noise even after the noise reduction using multitemporal images (see Figure 5.6). The left image shows the detected coastline with undesirable false edges. The right image shows the aerial

photography of the study area clearly showing that some islands detected in the left image are misinterpreted because of the high backscatter on the sea surface due to the wind and surface roughness caused by the strong current in the area.

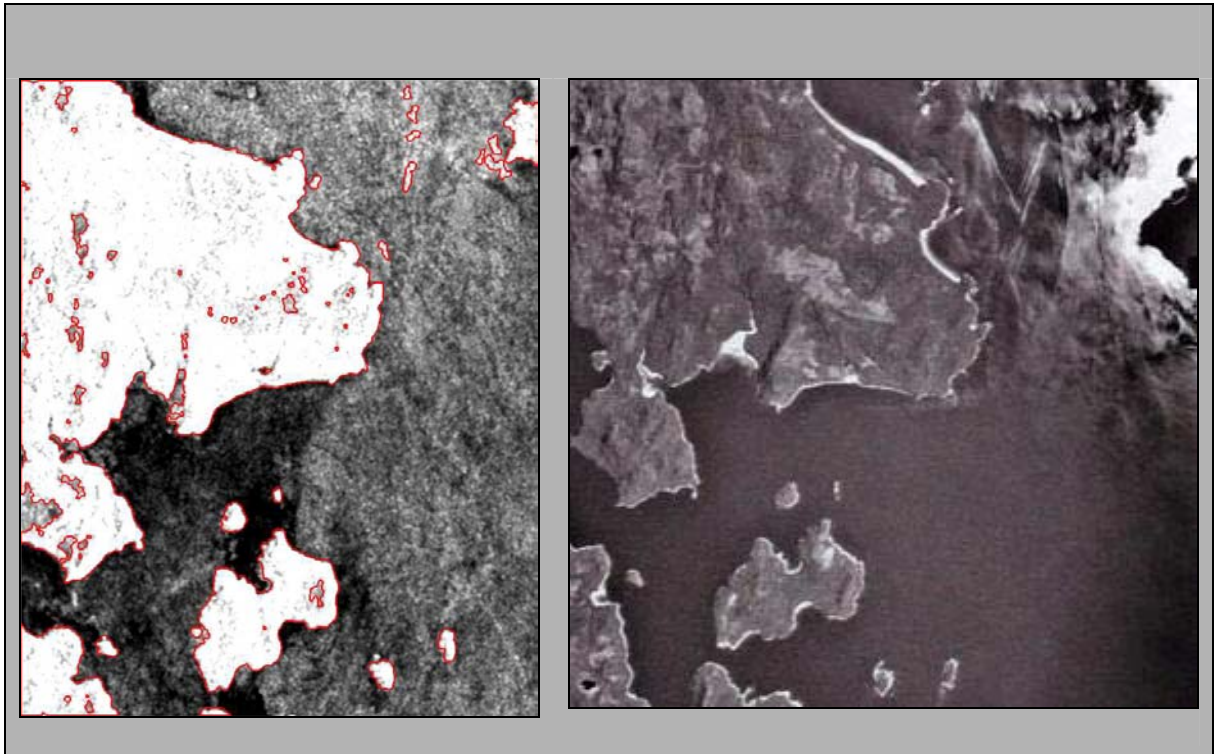


Figure 5.6. Visual Analysis of the Remaining Noise After the Multitemporal Analysis

The second problem encountered is regarding the offset in the detected coastline if compared with the original image. This offset is caused by the characteristics of the filters and the operations described in chapter 4.

5.5.1 Removing Noise and Refining the Coastline Detection

A simple and widely used method to link broken lines and remove noise refers to the mathematical morphological operations. Broken lines can be linked with dilation and noise can be removed with erosion [Sternberg and Serra, 1986; James, 1987; Serra and Vicent, 1992; Noble, 1996; Zhang, 2000]

However, if applying morphological operations directly to the image, the coastline boundary to be linked must be close to each other. Because the gaps to be closed in land and the noise to be removed over the sea surface are often too large, the direct application of morphological operations is not recommended [Zhang, 2000].

Because those noises are locally distributed over the image, the application of general transformation such as the Fourier doesn't give good results. Also because the shoreline consists of many different and complicated curves, techniques such as Hough transformation don't give acceptable results [Zhang, 2000].

Hence, the approach used to get rid of that noise consists of two stages:

The first consideration is the improvement of the input image using the pixel information that the original 16-bit image gives, especially over the sea surface.

Secondly, after the improvement of the input image, the application of windows to remove the noise depends on the gray-level value of the pixel and their neighborhood.

So, to solve these problems, the algorithm was modified as it is shown in Figure 5.7.

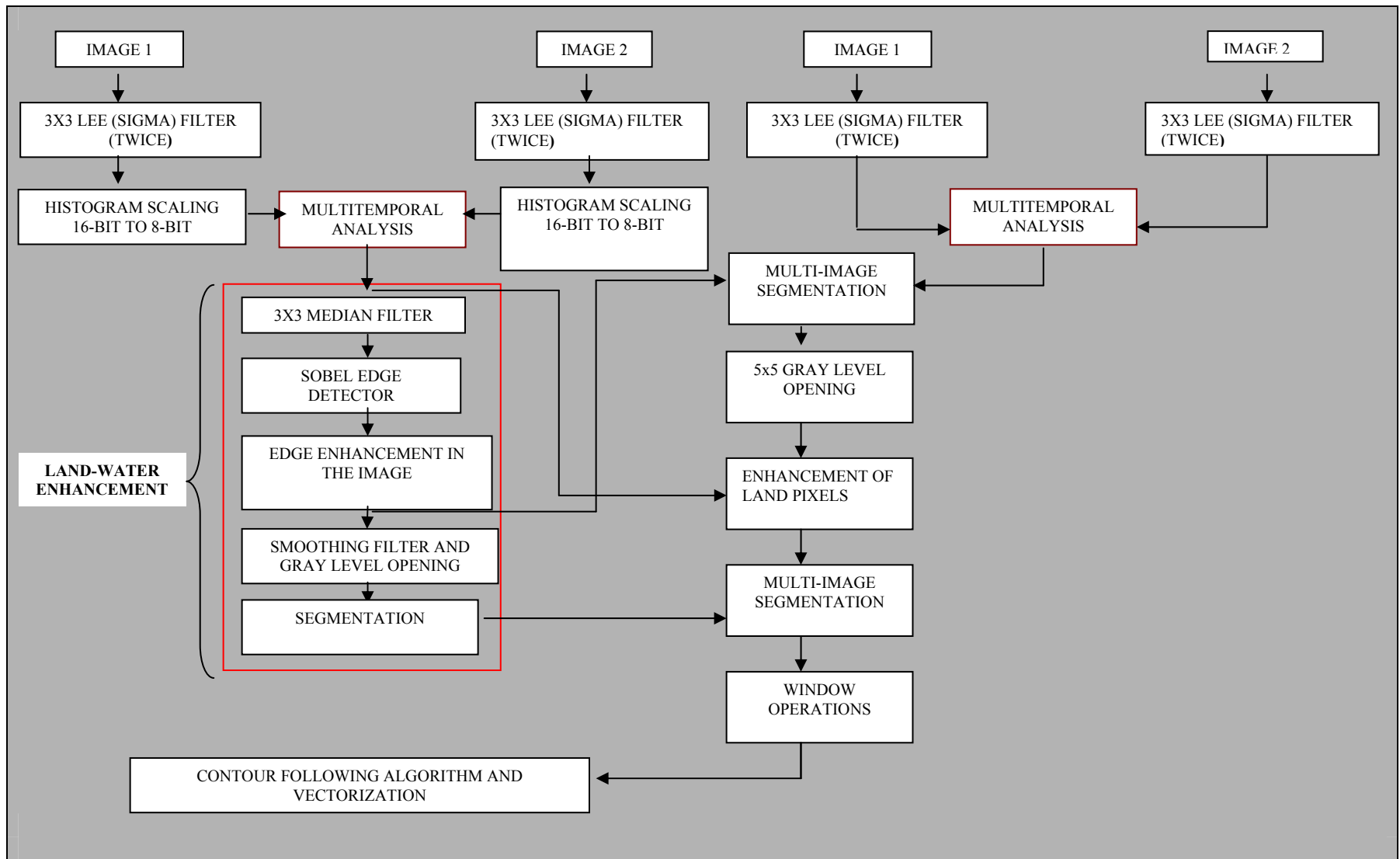


Figure 5.7. Final Proposed Method to Detect Coastline using the Multitemporal-Segmentation Method

5.5.1.1 Analyzing and Removing Noise

To analyze and solve the problem regarding the remaining noise in the images, the approach consists of comparing the 8-bit image after land-water enhancement with the 16-bit original image, achieving grey-level segmentation.

5.5.1.1.1 Island-Noise Discrimination

During the experiment with the images, it was noticed that the operation of scaling from 16-bit to 8-bit produced an enhancement in land pixels, making land more homogeneous. Hence, the multitemporal analysis was made using two 8-bit images. The multitemporal analysis using the 16-bit image did not give good results because of the high range of gray-level values, especially for those pixels corresponding to the land. This high variability produces some induced noise, even when the island-noise discrimination is good enough. Then, scaling the image from 16-bit to 8-bit was highly recommended to achieve land-water enhancement. The effect of multitemporal analysis within two 16-bit images is shown in Figure 5.8.

Even when, the multitemporal analysis using the original 16-bit images did not give good results in land pixels, the radiometric characteristics of the pixel values gave important information if comparing gray-level value in island with gray-level value over the rough sea surface. As shown in Figure 5.9, the gray-level value over land (island) is

always greater compared with the noise caused by rough surface. Hence there is better discrimination between noise and real islands.

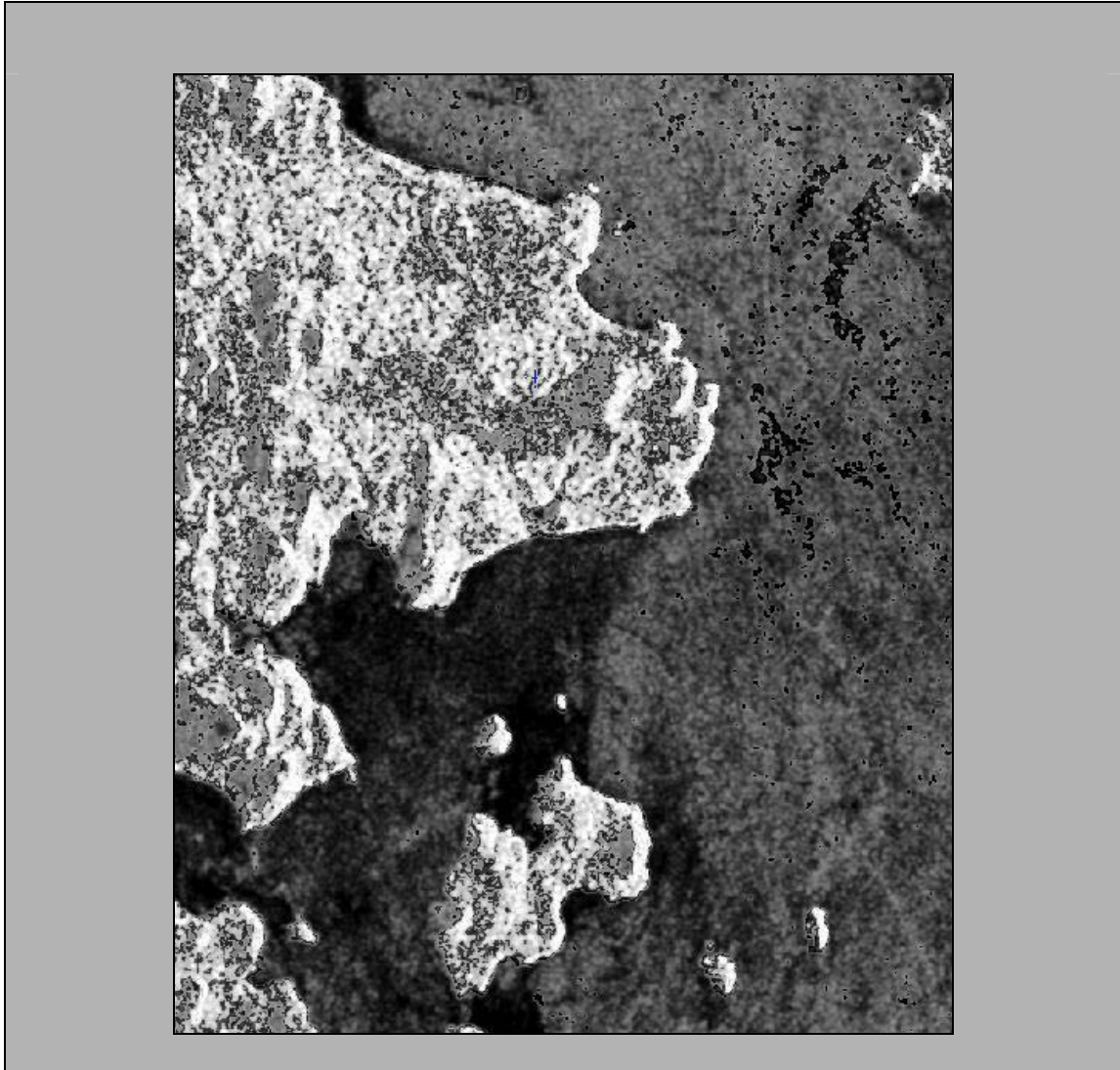


Figure 5.8. Effect of Multitemporal Analysis between two 16-bit Images

These special characteristics of 8-bit image (land homogeneity) and 16-bit image (island and noise discrimination) are valuable information, which were used to solve the problem detected after running the procedure described in chapter 4.

Hence, to solve the problem this thesis presents a subroutine to analyze and compare two images in a so-called multitemporal and multiscale method. The program is called *contrasting_16bits*.

After testing different inputs to run the algorithm, the best results achieved were using the 8-bit image after the image addition consisting of 30% of Sobel and 70% of the original image as the 8-bit input image. That combination of Sobel and the original 8-bit image provides a better enhancement in shoreline, if compared with the use of the single original 8-bit image as one of the inputs.

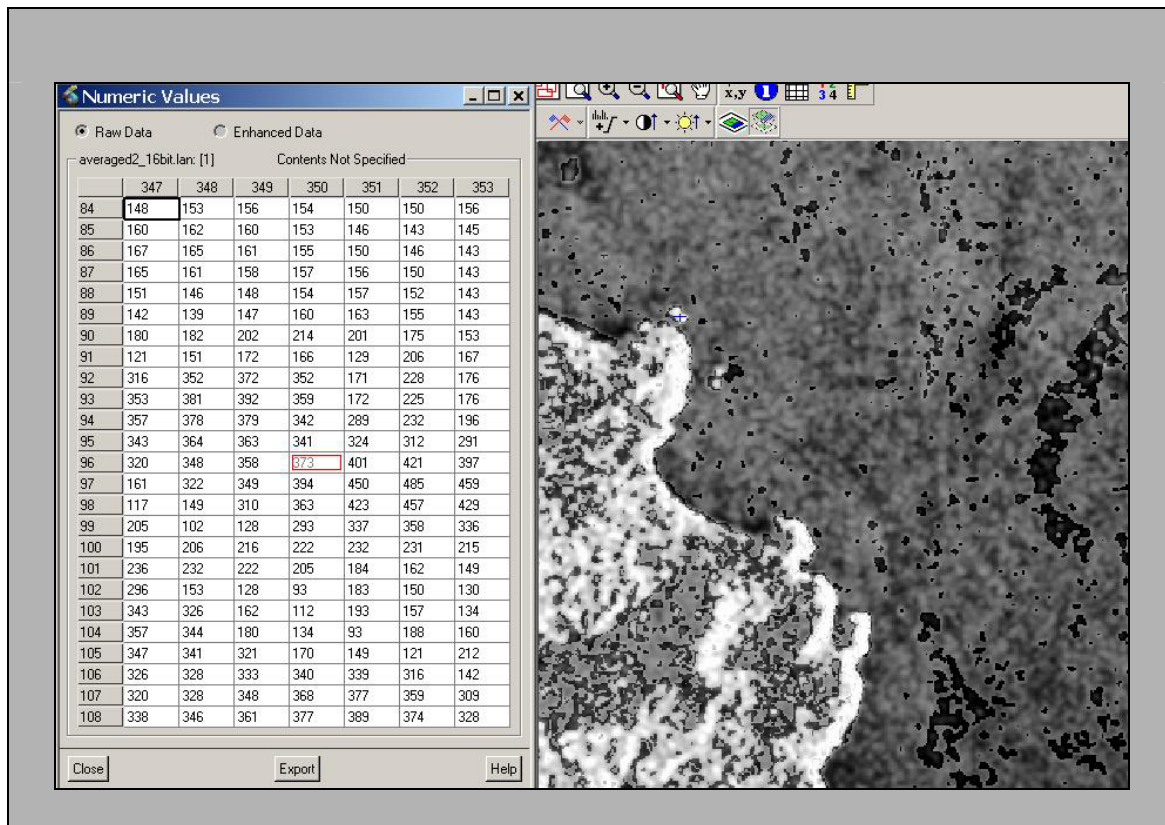


Figure 5.9. Island and Noise Discrimination after the Multitemporal Analysis between two 16-bits Images

The operator must analyze the critical areas and chose a threshold in the 8-bit image and the 16-bit image. The program first reads the enhanced Sobel 8-bit image, and then if the pixel value is above the threshold, it analyzes the second image. Otherwise, it sets the pixel to zero (rough land-water segmentation). Then, in the second image, if the pixel value is above the threshold, the pixel value in the output is set as the pixel value in the 8-bit image (keeping most of the land radiometric characteristics), otherwise, a mean window is applied over the center and its neighboring pixels in the 8-bit image (smoothing the noise over the sea surface).

The effect of comparing an 8-bit Sobel enhanced image and a 16-bit image is shown in Figure 5.10. This procedure performs a kind of segmentation, setting most of water pixels to zero while smoothing the pixel corresponding to noise in water and maintaining the enhancement of most of the pixels corresponding to land. The ideal threshold should not affect the pixel values corresponding to shadow or wetland areas (practically an impossible task because the radiometric and geometric characteristics of radar images).

This time, the threshold was chosen according to the mean value for both 8-bit and 16-bit images. It gives a desirable separation between land and water.

After this procedure, opening operation (digital morphology) is applied to the image to destroy and smooth most of the edges in water (noise), giving acceptable results.

Once the opening operation has been done, the resulting image is contrasted again with the 8-bit image, but this time the effect of this operation is to enhance most of the land pixels with respect to the noise pixels over the water. This new subroutine is called "*island enhancement*".

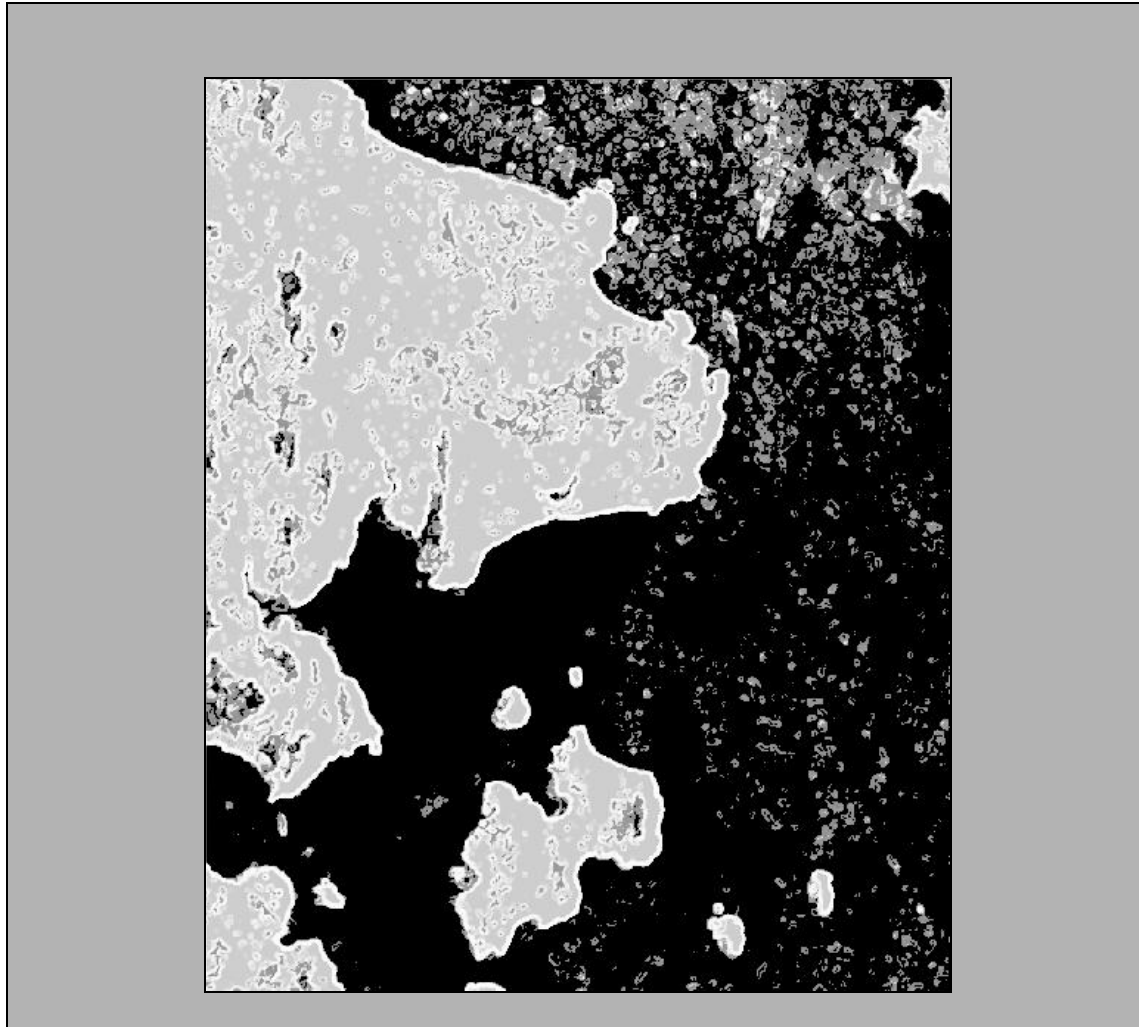


Figure 5.10. The Resulting Image after Applying Multi-Image Segmentation

In this case, the output from the opening operation is used together with the original 8-bit image in the new module called *island enhancement*. This sub-routine enhances the values over land while keeping the gray-level value of the noise after the opening operation.

The enhancement of pixels having 255-value is done according to the values of the pixels in its neighborhood. If the pixel corresponding to land is connected at least with three pixels with value corresponding to 255, then the center pixel and the complete 3x3

surrounded window is set to 255 unless the neighbor pixels correspond to water (pixels with value equal to zero). The results of this operation were good because it made the island-noise discrimination better. Also, pixels having zero gray-level values are not affected by this operation. Consequently there is no offset in the shoreline

The result of this operation is shown in Figure 5.11. Most of the land pixels have again 255 gray-level values, while the gray-level value in the pixels corresponding to noise remains smoothed and with lower value if compare with islands.

Figure 5.12 shows also a zoom and numeric values to display the effect of this operation that increases most of the gray level pixel values of land and islands.

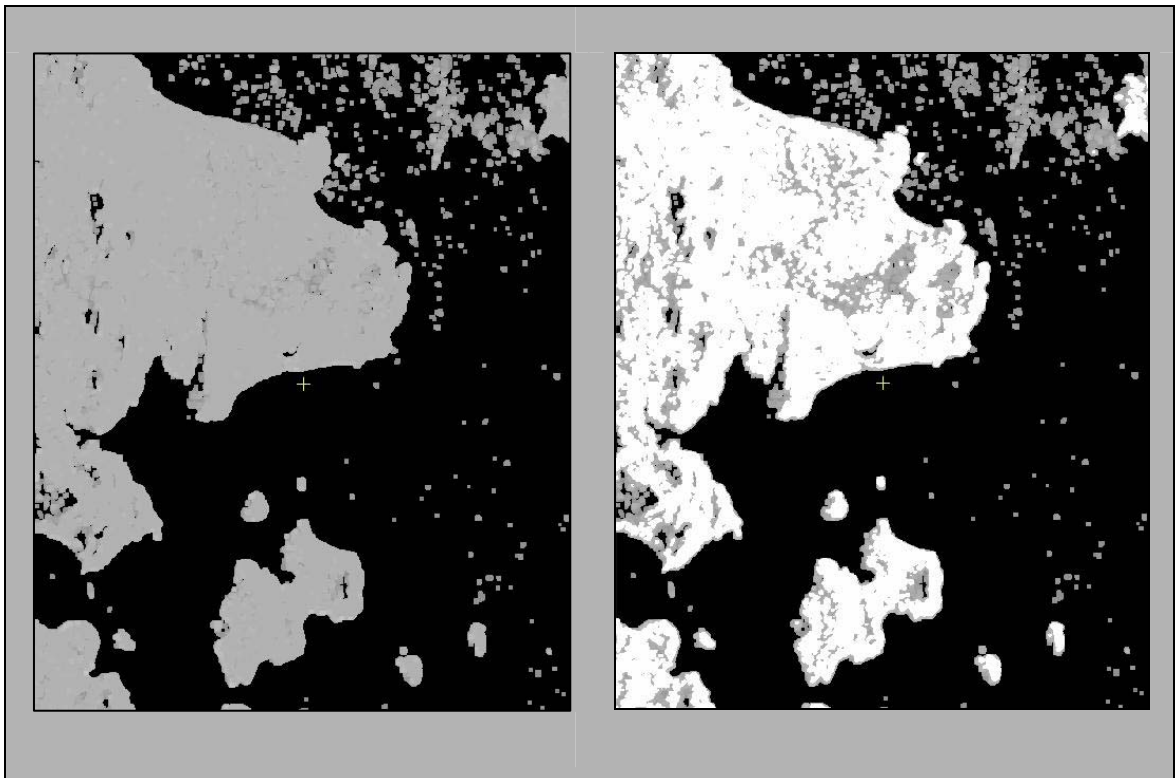


Figure 5.11. The Effect after Enhancing Land Pixels
The pixels in the image after opening operation (left) are enhanced as shown in the right image.

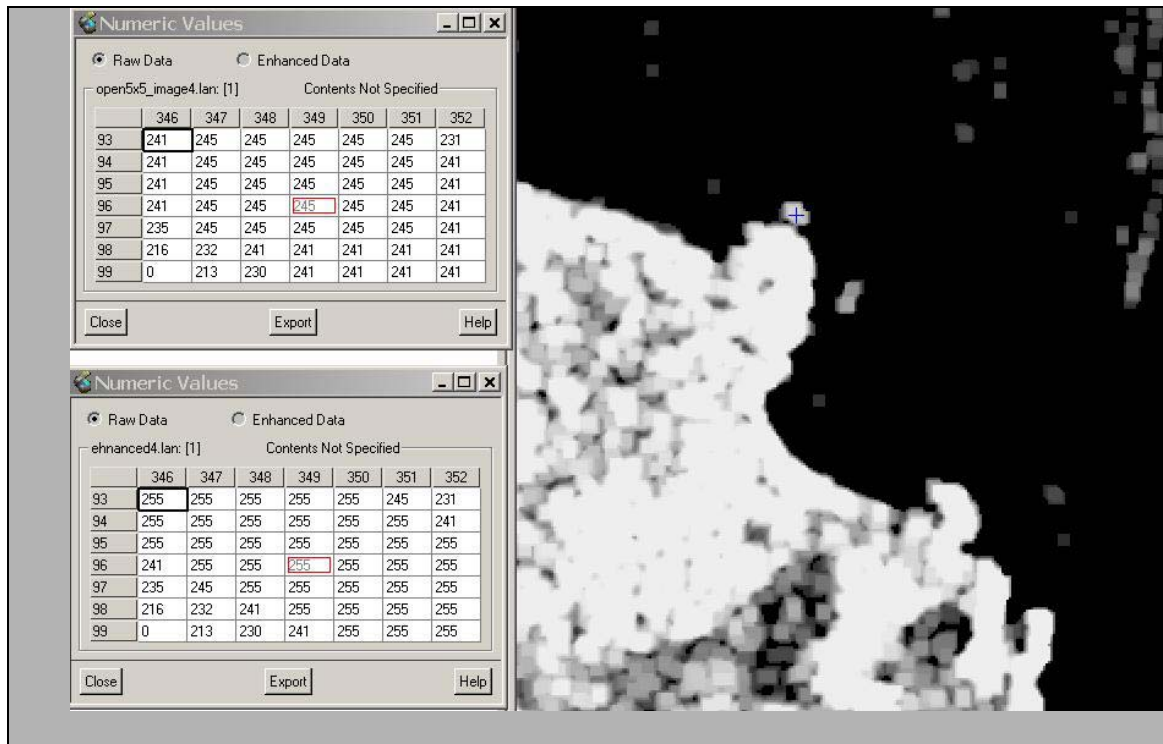


Figure 5.12. Numeric Values of Pixels in Land and Noise

However, there is still too much noise present in the sea, which could be misinterpreted as false islands. In the process of reducing that noise, again the image after being enhanced is compared with the segmented (binary) image obtained after the application of common filters.

Using the subroutine called “*contrasting bitmap*”, if zero-values are found in any of the input images, the output is set to zero. This operation ensures the reduction of the noise when it is excessively large in the image. If the noise is not too big, this stage could be jumped and the direct application of windows to delete noise proceeds.

The effect of this operation is displayed in Figure 5.13. The most important achievement of this operation is that the noise now has a gray level value different from the gray-level value of islands in the image.

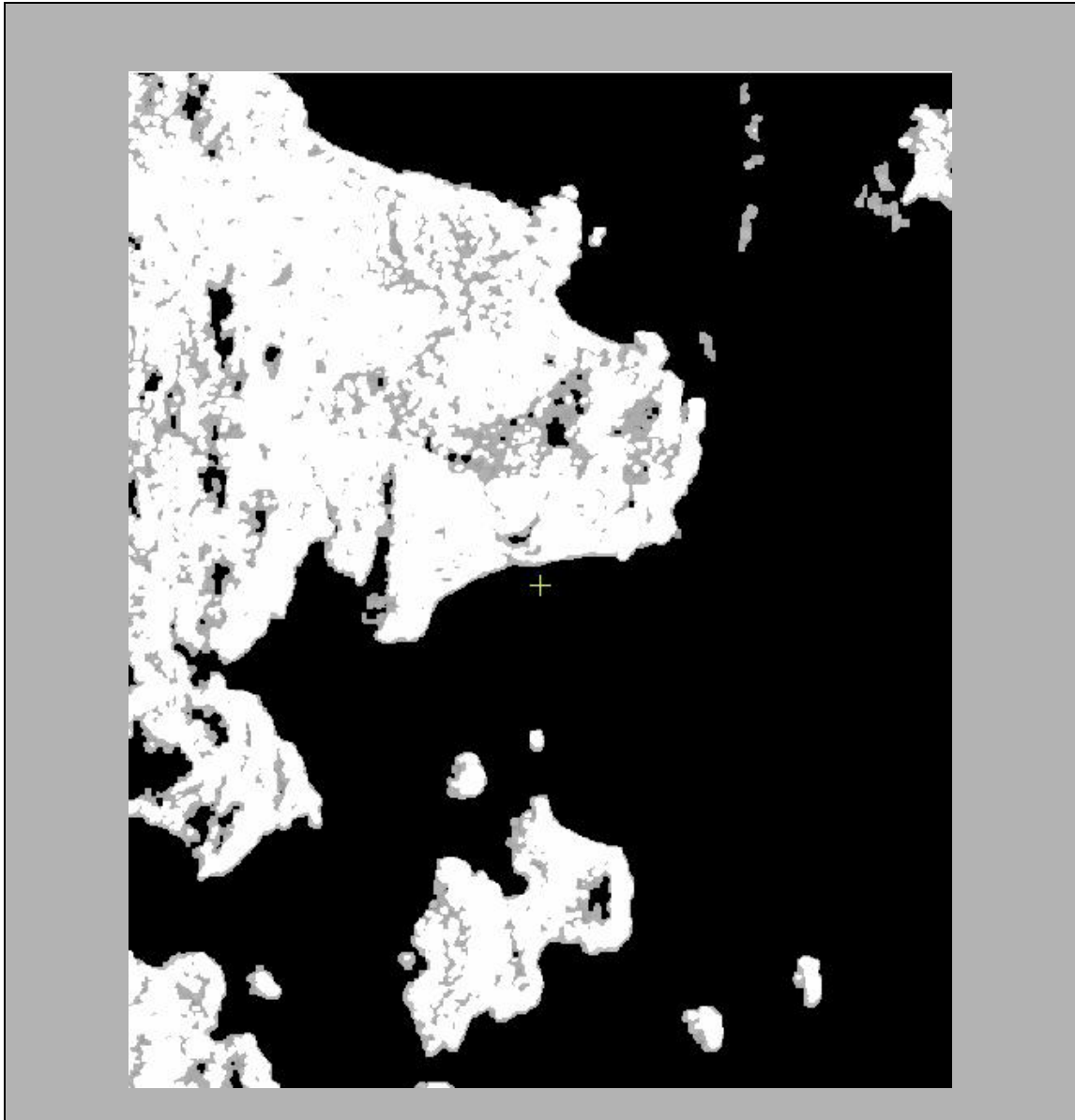


Figure 5.13. The Enhanced Image after the Multitemporal Segmentation Method

After the operations described in this section, the input image is improved and now it is ready for the application of windows designed to delete the remaining noise over the sea surface.

5.6 A Window-based Algorithm to Eliminate the Noise

After the enhancement of the input image, the next task was to improve a procedure to remove the noise while keeping the pixel values in land.

Because that noise is local and it could be easily confused with islands, this approach was achieved using a basic “star-shape” (Figure 5.14) window analyzing the presence of zero-values in the neighborhood of the center pixel, considering vertical horizontal and diagonal directions. The size of the window depends of the size of the noise to be removed. The size of the window is usually large (15x15 and up) to remove large extensions of noise.

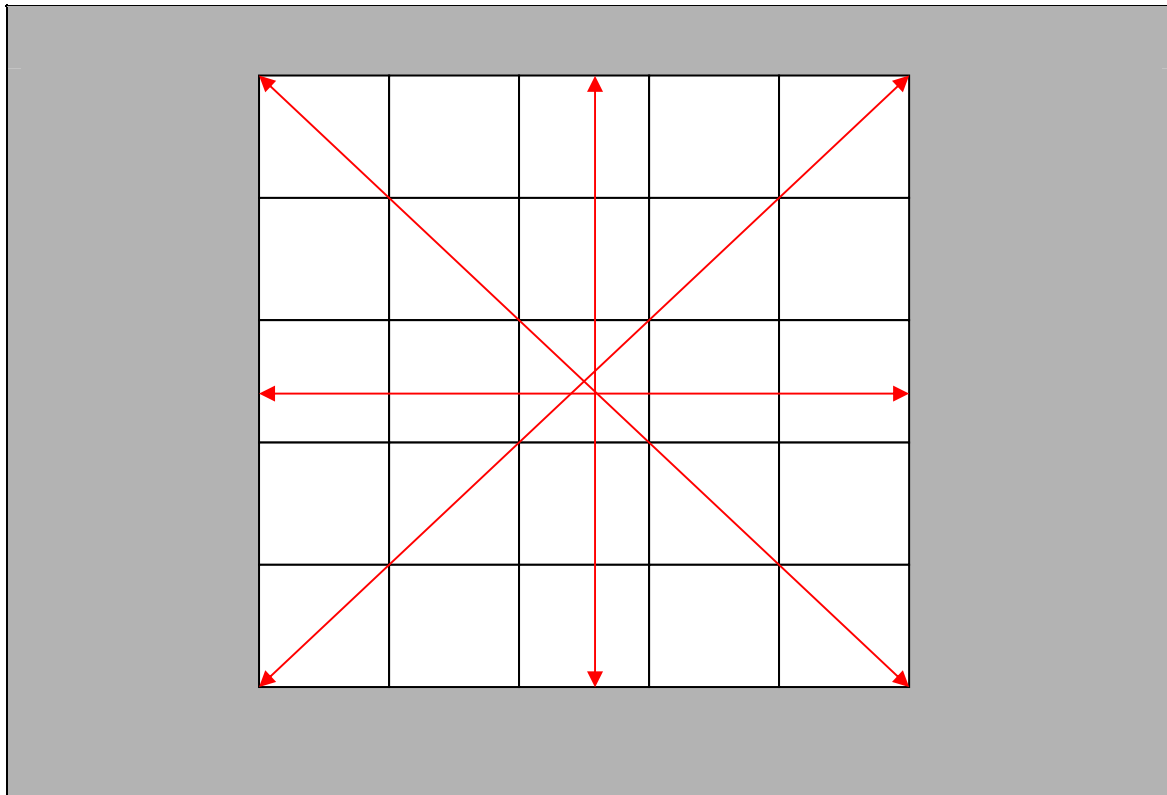


Figure 5.14. The Window used to Remove Noise and to Fill the Gaps
This window is based on the analysis of pixel values in the vertical, horizontal and diagonal directions.

As a result of the analysis in eight directions, a great amount of noise has been removed, but as seen in Figure 5.15, some portion of the coastal zone is deleted too. To refine the window, now sixteen directions were analyzed. Hence, the noise is removed just when the analyzed pixel is different to zero (of course water) or 255 (enhanced islands and most of land pixels).

The window analyzes in the first direction, if zero value is not found the pixel remains with the same value and the next pixel is analyzed. If zero value is found in the first direction, it initiates a counter and the second direction is analyzed. If the counter reaches sixteen, then the central pixel is set to zero, otherwise no changes are made to the analyzed pixel.

Especially, close to the land, some remaining spots will still remain in the output image. That noise can be deleted using a small window as shown in Figure 5.16.

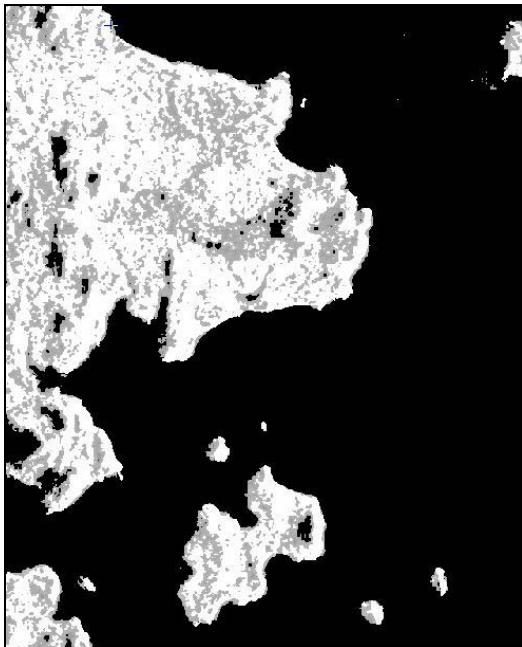


Figure 5.15. Application of Basic Star-shaped Window

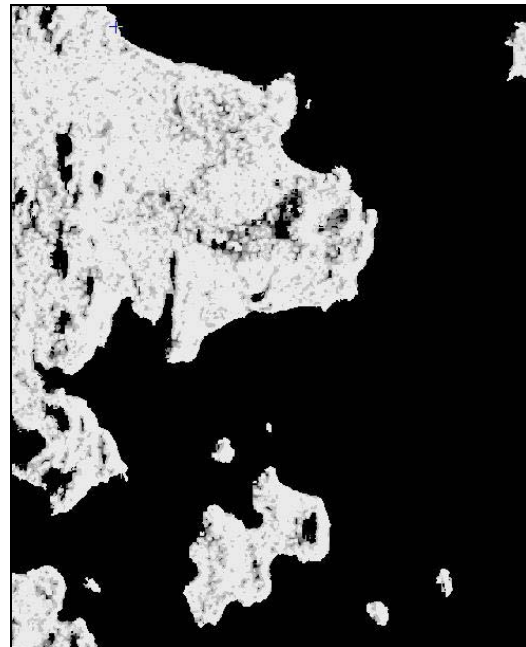


Figure 5.16. Application of Small 3x3 Window

After the noise is deleted, morphological operations (dilation and closing) can be used to fill the gaps and join the broken segments in the bitmap image as shown in Figures 5.17 and 5.18.

At this stage, the results are more acceptable in shoreline detection. However, while testing the results in different areas, the excessive amount of gaps caused by this operation was detrimental in the final results. Therefore, it was necessary to refine the window used to delete noise and to find the way to fill most of the undesirable gaps in land.



Figure 5.17. A 5x5 Dilation Operation



Figure 5.18. A 3x3 Closing Operation

5.6.1 An Iterative Method to Delete Noise and to Fill Gaps

As described by Zhang (2000), methods for connecting broken linear segments and eliminating noise are important. Especially in the case of radar images in which the pixel values depend of land or water roughness, that noise should be eliminated to achieve continuous feature extraction.

Zhang (2000) describes a method to extract urban rivers. The continuous extraction of linear objects, such as rivers, roads or boundaries, from digital images can hardly be achieved using automatic methods. Line extraction algorithms usually break down linear objects into segments with significant noise.

The same problem is present in shoreline extraction. After processing the image, there is some noise in water as well as some gaps in land due to shadows in the image or simply wetlands or lakes. Hence, the application of an algorithm to fill those gaps in coastline segments and to remove the noise in the sea surface is applied to the image.

Therefore the process of segmentation and connection has to be carried out iteratively. Noise is removed step by step and coastline segments are also restored step by step. This procedure is based in windows designed to operate over the image deleting the noise and filling some holes in land.

The key to achieve this window operation was the enhancement of input image described early in this chapter. After that enhancement, the reduction of noise in water and the process to fill the gaps in land are made iteratively until the noise is gone. After that, the continuous application of the function to fill the gaps could be applied to the image combined with closing operations if necessary.

The result of this operation will produce a new image without noise and with most of the gaps closed.

The whole process of this window operation is described in Figure 5.19 and the result of the application of the windows is shown in Figure 5.20.

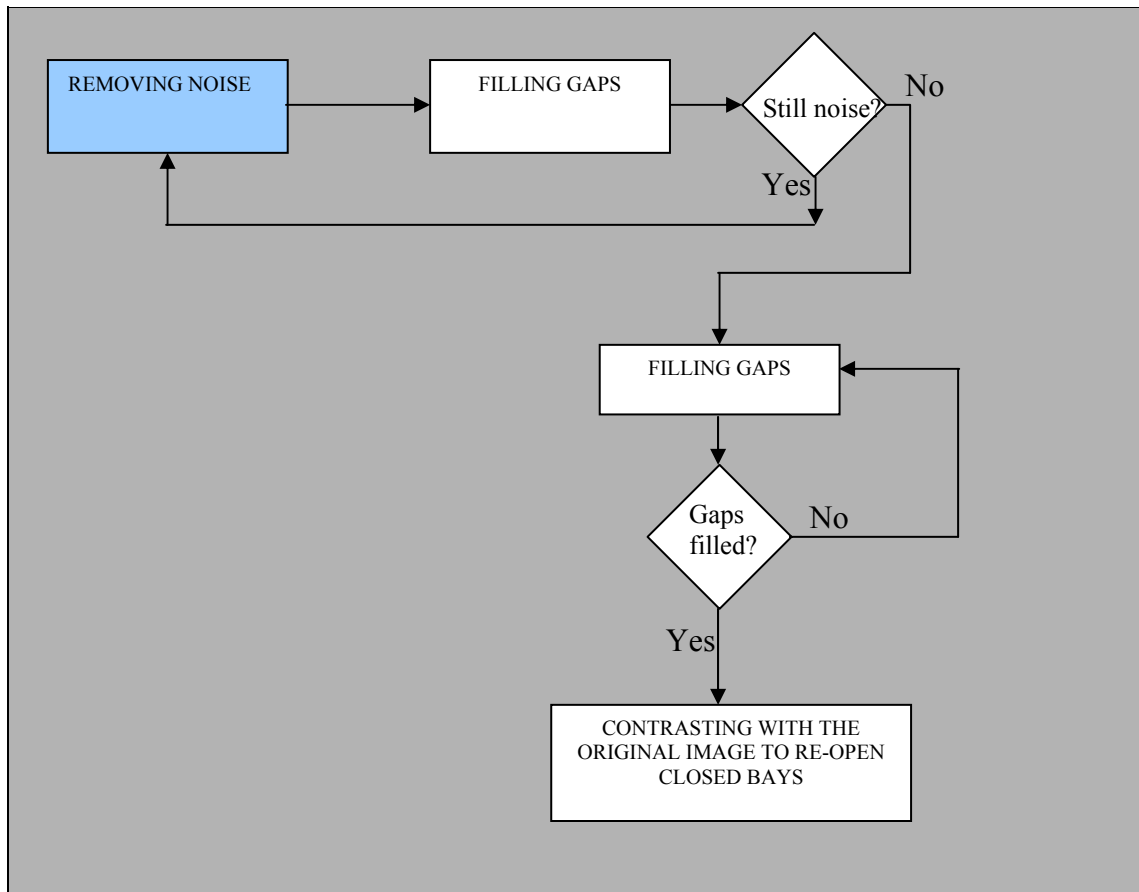


Figure 5.19. Iterative use of Windows to Delete the Noise and to Fill the Gaps

Because the size of the window is sometimes not enough to close completely the largest gaps, usually there are some remaining gaps after this processing stage. These remaining gaps could be undesired, especially if they are still close to the shoreline. To fill those rectangles, a simple closing window (morphological operation) could be used. The result of this closing operation is shown in Figure 5.21.

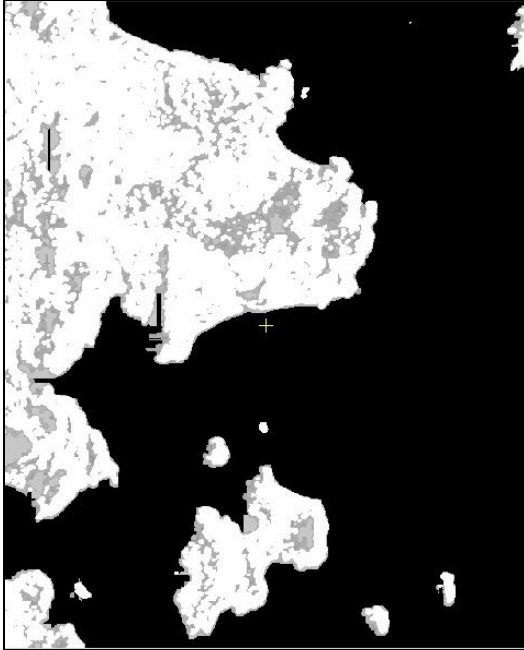


Figure 5.20. The Image after Most of the Gaps are Closed.

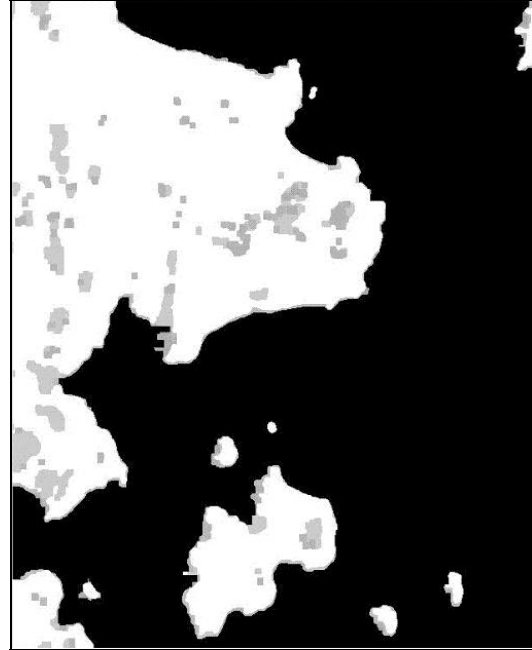


Figure 5.21. The Image after Closing Operation using Digital Morphology.

Because filling gaps or closing operation could affect little indented bays, rivers or deltas, the image is contrasted again with the original image to open those areas with a pixel value that approximately corresponds to the mean pixel value in water areas (enclosed bays).

The original image usually has no problem of noise in enclosed bays (less wind) as it has in the open sea areas. Because some gaps filled in the image correspond to real lakes, bays or rivers, they are restored again using the original image.

After this procedure, it is possible to segment the image to finally detect the shoreline without the problem of noise. Also, most of the problems in shoreline detection are solved with the exception of some little problems because the presence of

shadow areas, which is the most common problem in radar images and it's still not totally solved.



Figure 5.22. The Resulting Image after Contrasting with the Original Image

Because the closing operation, some small bays are closed. To re-open that bays, the segmented image is contrasted with the image obtained after the multitemporal analysis. The result of this operation is shown in Figure 5.22.

After the refinement of the algorithm presented in this thesis, the detected shoreline was improved, as shown in Figure 5.23.

5.7 Results in Coastline Detection after the Multitemporal Segmentation Method

After the detection of edges using the Roberts operator, the qualitative comparison between the shoreline before and after refinement gives a good improvement. The undesirable noise obtained using the general procedure described in chapter four was eliminated, while the detection of shoreline in islands was properly achieved.

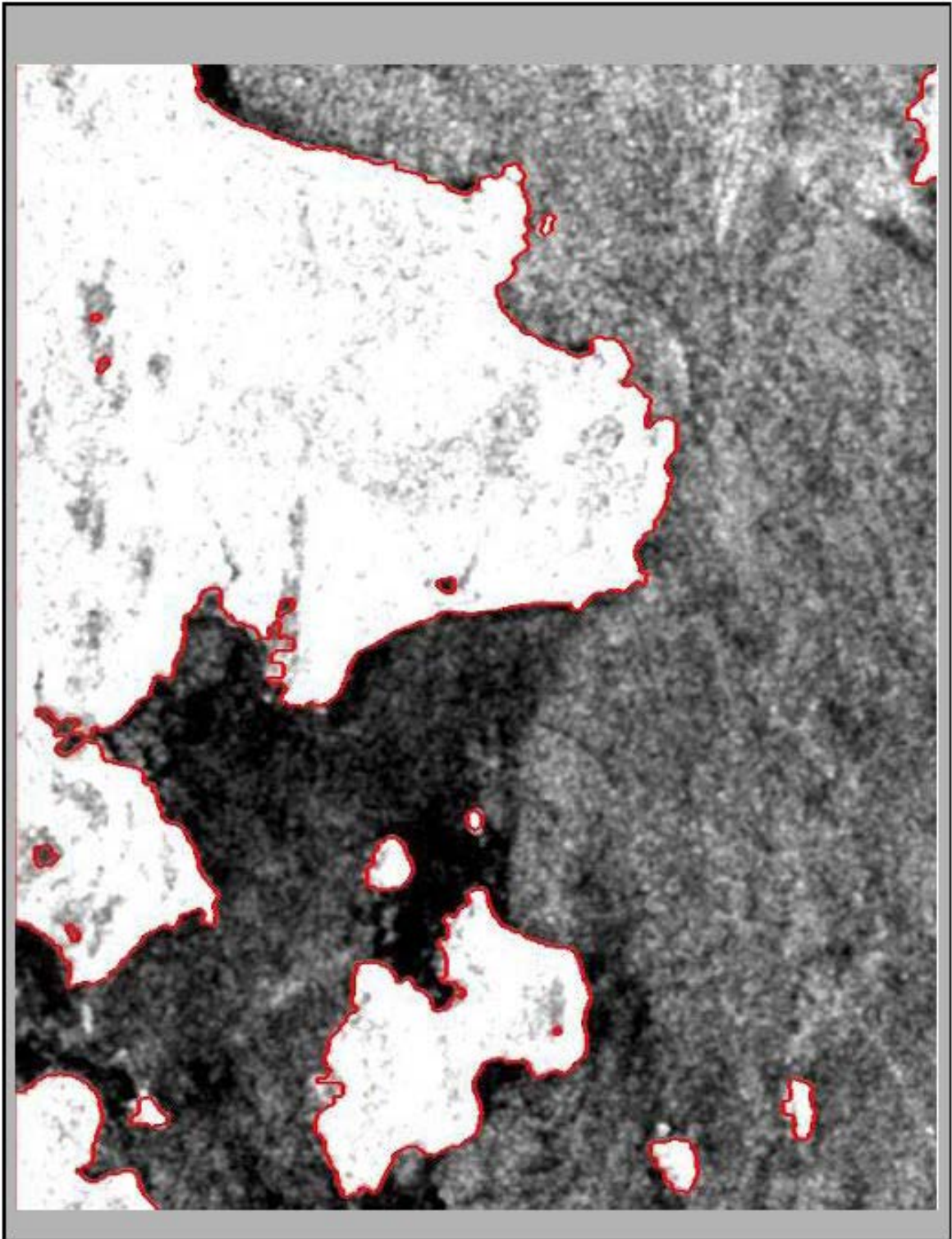


Figure 5.23. The Detected Coastline after using the M.S.M. Developed in this Research

5.7.1 Testing the Refined Algorithm in Different Areas

Except a little problem caused by the inevitable shadow caused by a steeper hill, the algorithm seems to work properly in the area tested during the previous section. However, to ratify the efficiency of the algorithm it is absolutely necessary to test other areas with different geographic characteristics.

The same procedure described in this chapter was applied to other areas with different environmental and geographic characteristics. Areas with indented fiords and bays, mountains causing undesirable shadows and wetlands, which produce low backscatter in the returning signal, were tested.

After the refinement performed in this chapter, the noise in the sea surface has been solved, but there are still gaps in the land areas because the radiometric characteristic of radar images related to geographical relieves.

Also, because this procedure attempts to find a solution for coastline detection, those gaps present in land are not totally solved but improved using this algorithm.

It is important to mention that this algorithm is based in the land-water enhancement. Hence, this algorithm is enhancing the shore areas using a technique based in the destruction off most of the land edges, while preserving the most important: the coastline.

During the analysis of the other areas, the results were not perfect if compared with the result achieved in the study area presented before in this chapter. Because their size, some gaps could not be closed; however they rarely affect the correct delineation of the

shoreline. To avoid that, closing operations can be performed if necessary, unless the area is indented, and it presents high backscatter of the sea surface close to the land.

As shown in Figure 5.24, the results observed in those four different areas are quite good output to delineate the coastline because the edge corresponding to the shoreline has been isolated from other edges of the image. The unsolved gaps encountered in landward directions are just visually negative because they are not affecting the final shoreline extraction. The coastline has been well defined, without the influence of undesirable noise that could produce misinterpretation of that required edge. Even in the top-left image (Area 1), which is the most difficult scenario to detect the shoreline because the amount of small fiords and the fuzzy shoreline definition in another areas, however, the coastline is continuous over its extension.

The last step in this method is the extraction and vectorization of the detected shoreline in the raster image, as described in chapter 7.

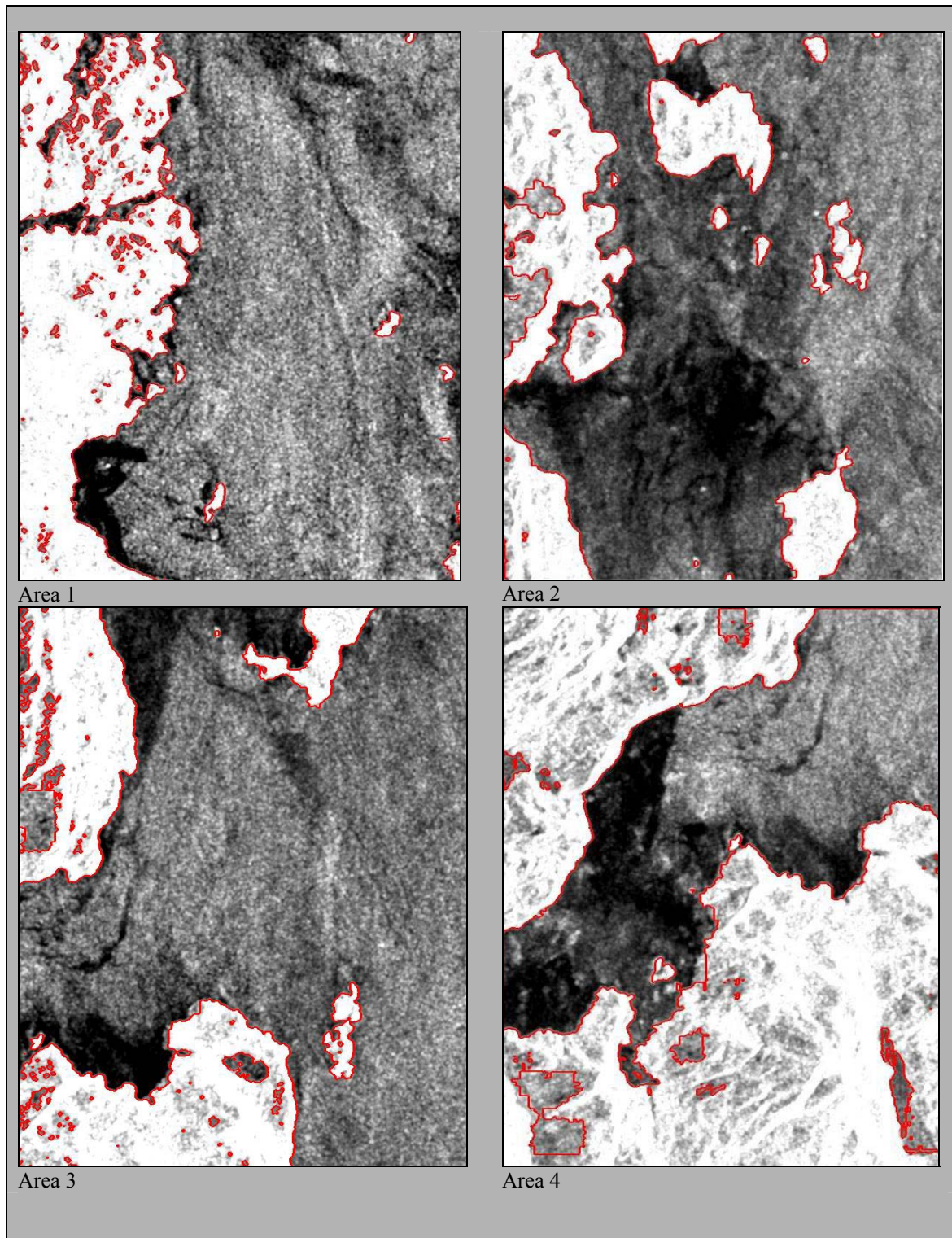


Figure 5.24. Four Different Areas where the Algorithm was Tested

5.8 Summary

The Multitemporal Segmentation Method was successfully used to achieve a proper land-water separation in critical areas subject enormous influence of environmental conditions such as wind.

The success achieved in land-water segmentation was fundamental for further delineation of the coastline in the analyzed images.

Even when, other small edges were detected in land areas, those edges do not affect the delineation of the coastline, because of the enhancement applied to the shore areas.

After the enhancement using the Multitemporal Segmentation Method, the use of windows to get rid of the noise caused by the strong backscatter in the sea surface, achieved the main objective stated in this thesis.

Chapter 6

RESULTS AND DISCUSSION

6.1 Introduction

Like any scientific measurement, some inherent errors are associated with shoreline position data. Quantifying shoreline position and change requires a thorough understanding of coastal processes, mapping fundamentals, and measurement theory. The challenge for quantifying change is that researchers must not only know the most modern methodologies, but they also should have a thorough understanding of how historical shoreline data were captured.

All maps and digital geospatial data are abstractions of reality and, therefore, they have inherent uncertainties.

In order to apply the detected coastline for GIS purposes, in this chapter the average error in coastline detection using M.S.M. is analyzed and compared with the average error obtained if the coastline is detected after the application of common filters and the reduction of noise using multitemporal analysis described in section 5.3.4, showing the improvement achieved in coastline detection.

6.2 Quantitative Analysis in Coastline Detection

To avoid inherent offsets caused by tide conditions, the detected coastline was compared with the original image after the multitemporal analysis to reduce the noise.

If the coastline is detected after the rough land-water segmentation process using multitemporal images presented in section 5.3.4., the offset of the land boundary would be near to two pixels. This is an acceptable result, but still there are large offsets over some areas where the backscatter in land areas is too low.

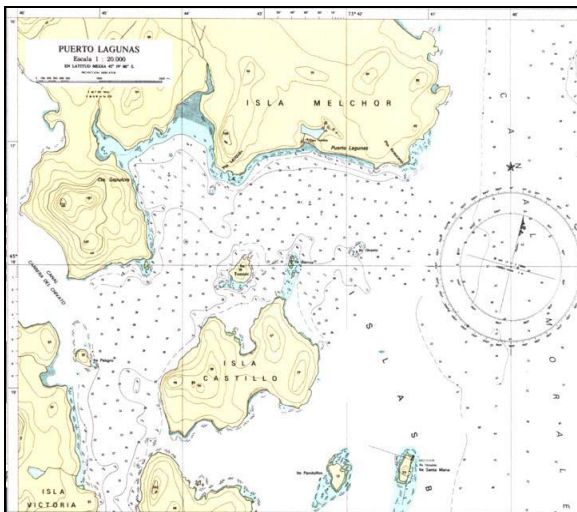


Figure 6.1. Nautical Chart of the Area used to Analyze the Coastline

Usually, the analysis of the available nautical chart can give some answers about the nature of some inherent uncertainties after the coastline detection. For example, analyzing the contour lines from the nautical chart of the area in Figure 6.1, there is a remarkable slope of a hill, which produces a low backscatter in the image.

To analyze the offset of the detected shoreline a set of 205 samples were measured over an area of 80 km². The average error was calculated from the data set. The resulting bias was nearly 2 pixels (1.712195 pixels) comparing the position of the coastline with the original image. The standard deviation was 1.04 and the confidence calculated at 0.95 was 0.00459.

There were several outliers caused by the strong sea backscatter close to the shoreline and the failure of the rough method using common filters to detect the shoreline. This situation is incremented over sinuous coastline configuration, especially when rough sea surface is close to the shoreline.

Without considering the outliers, and after the application of dilation procedure presented in section 5.4 [Lee and Jurkevich, 1990], the same 205 pixels used to calculate the average error were again analyzed. This time, the bias over that “wind-forced” noisy image was nearly one pixel offset (1.009), the standard deviation was 0.99 and the confidence calculated at 0.95 was 0.0043. However, the outliers are still present in the detected shoreline.

After refining the coastline detection with the algorithm proposed in this thesis, the same analysis over the 205 pixels was done, minimizing the average error and consequently giving more precision in the coastline extraction.

The achieved one-pixel offset means a shifting of 12.5 metres in reality. If it is represented in a nautical chart with a scale of 1:60,000, this offset represents a shifting of 0.2 mm.

The following table gives the bias in coastline before and after the algorithm proposed in this thesis. The samples were analyzed every 5 pixels in the coastline. The average error or bias using the M.S.M. in the images was considerably lower than the resulting coastline using common filters and the refinement used by Lee and Jurkevich [1990].

Table 6.1. Comparison between the use of Most Common filters and the M.S.M

ANALYZED AREA	Average error after using common filters	Average error after the M.S.M. and the iterative use of windows
Area 1	1.073	0.909
Area 2	1.009	0.825
Area 3	0.834	0.775
Area 4	0.790	0.741
Area 5	1.892	0.985

6.3 Qualitative Analysis in Coastline Detection

After the analysis of the images it was possible to identify some critical situations regarding the configuration of the coast and environmental parameters, which affect the automatic delineation of the coastline. The most critical topographic features and environmental processes in the detection of shoreline can be described as follow:

- *Shadows areas caused by hills close to the shoreline*

The main problem of radar images (shadowing caused by relief) is present here and it is the most difficult problem to solve in automatic delineation of shoreline when it is close to the land-water boundary.

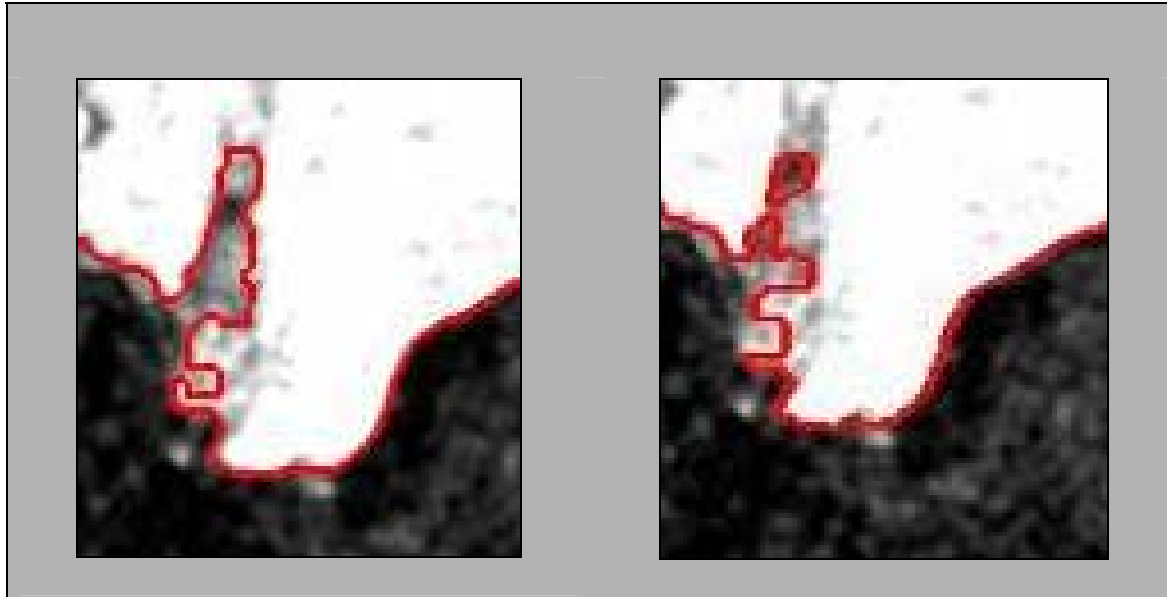


Figure 6.2. The Effect of Shadow Caused by Step Relieves such as Hills or Trenches
Left: The detection of shoreline using the most common procedure.
Right: The detection of shoreline using the M.S.M.

After the coastline detection using the M.S.M. this problem is partially solved. However the operator still must pay attention to this kind of problem.

- *Wetlands, which produce low backscatter*

Another unsolved problem is the low backscatter coming from flooded areas or wetland. In fact, the coastline is in the place where water ends. If the wetland is close to the shoreline, that shoreline will be placed where the land starts. The operator must analyze quite well the areas with an optical image or analyzing the old map to verify the presence of beaches, salty and shallow lagoons, deltas etc. Figure 6.3 shows the effect of coastline delineation considering a flooded area with the connection with a small river. Figure 6.4 shows the map and photography of the area with problems.

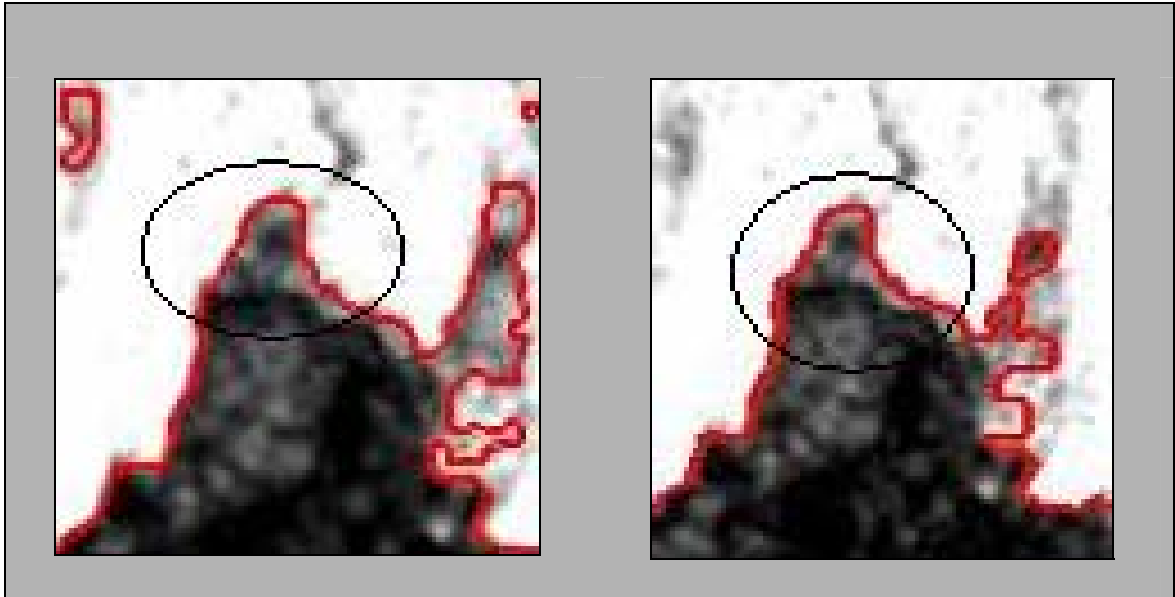


Figure 6.3. The Low Backscatter of Flood Areas or Wetland Produces a Misinterpretation of the Shoreline

**Left: The detection of shoreline using the most common procedure.
 Right: The detection of shoreline using the M.S.M.**

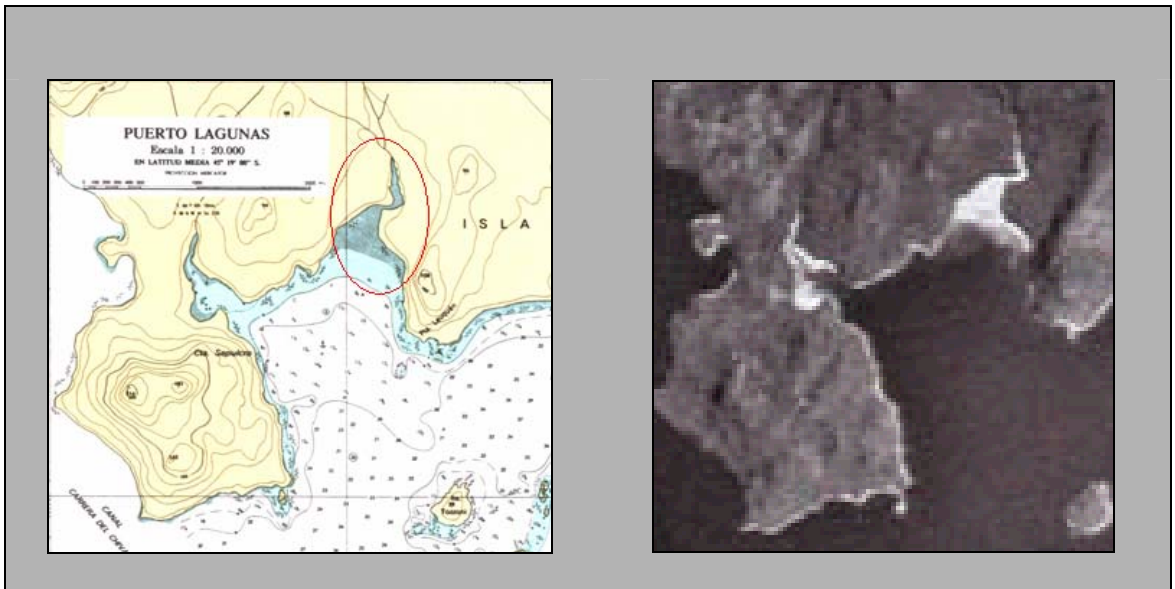


Figure 6.4. Information used to Visually Analyze the Coastline in Areas with Problems

**Bottom Left: The area illustrated in the nautical chart.
 Bottom Right: The same area from the aerial photo.**

- *Islands close to the main shoreline*

Due to the spatial resolution of the image, while the enhancement of land-water boundary is taken effect, the shoreline is displaced seaward in most of the spatial methods used to delineate the shoreline. This is the case of Erteza [1998] method or Lee and Jurkevich [1992] method (1 pixel or two). Figure 6.5 shows the improvement made over areas where islands are too close to land, if using the M.S.M.

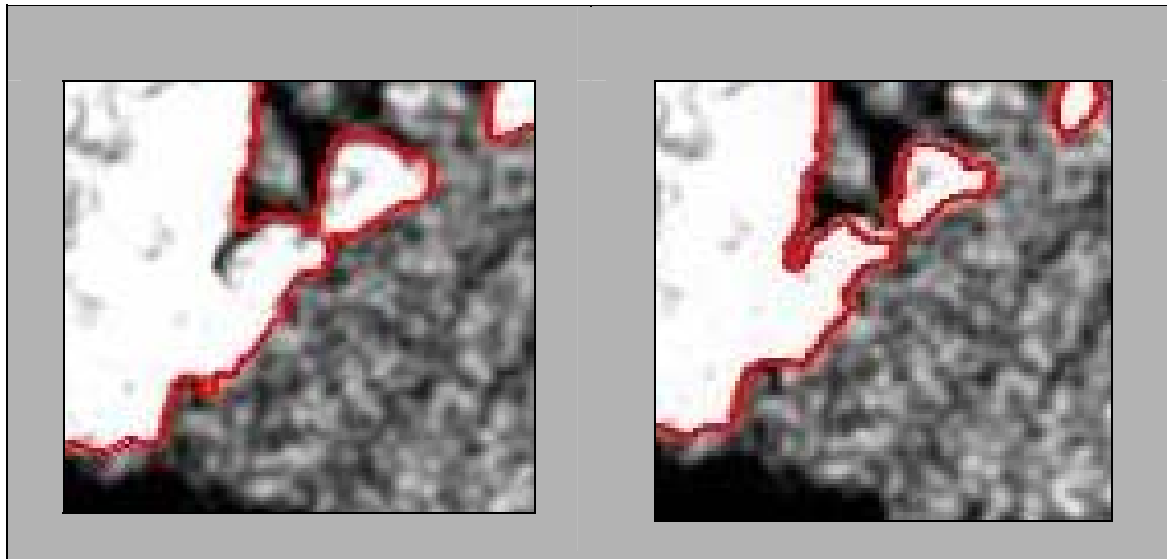


Figure 6.5. The Effect of Shoreline Delineation in Cases where the Islands are Close to the Main Shoreline

Left: The detection of shoreline using the most common procedure.

Right: The detection of shoreline using the M.S.M.

Using the proposed method to detect the shoreline, the offset is reduced. Hence, most of the islands close to the land are detected without merging them. Also if the resolution of the image to be used is better, this problem could be further solved.

- *Narrow channels or straits, with indented shape*

As the same situation of the islands close to the land, narrow channels could be closed and misinterpreted. With the M.S.M the offset of the shoreline is solved in most of the cases. Figure 6.6 shows how a narrow channel is correctly delineated. Hence, the shoreline can be automatically vectorized successfully.

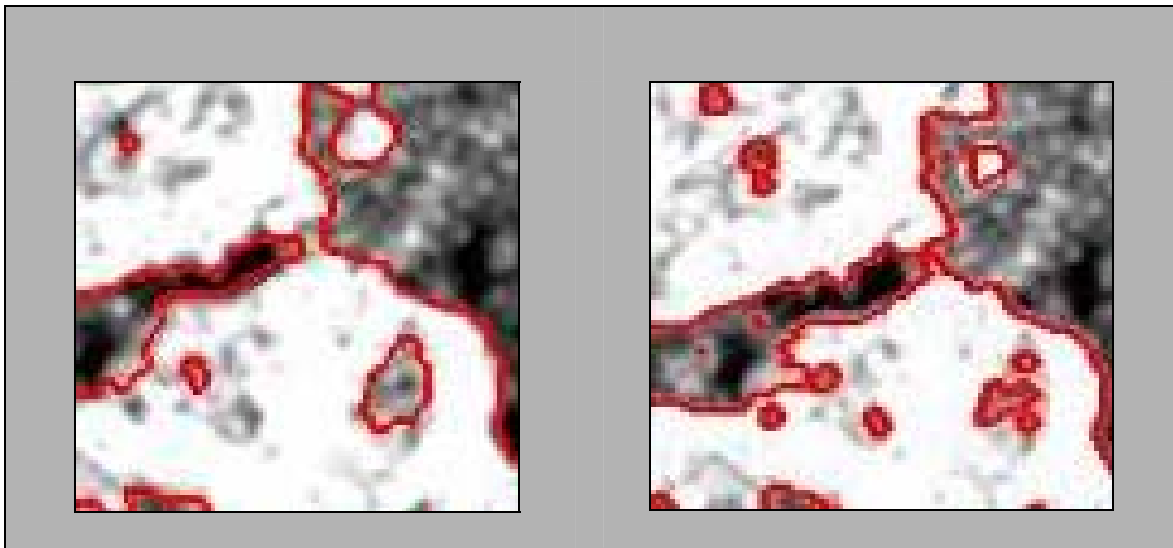


Figure 6.6. The Effect of Shoreline Delineation in Cases of Narrow and Indented Channels
Left: The detection of shoreline using the most common procedure.
Right: The detection of shoreline using the M.S.M.

- *False edges on the sea surface caused by wind*

Noise over the sea surface can be presented in ways such as small dots, large spots with regular or irregular shape, etc. However, one of the most complicated types of noise is the one that produces a well-defined edge in water surface caused by local stream wind. If one of the images used in the multitemporal analysis has too much noise, that noise is just smoothed a little bit and the resulting image will still have this “false edge”. After the refinement using the M.S.M. this problem is solved.

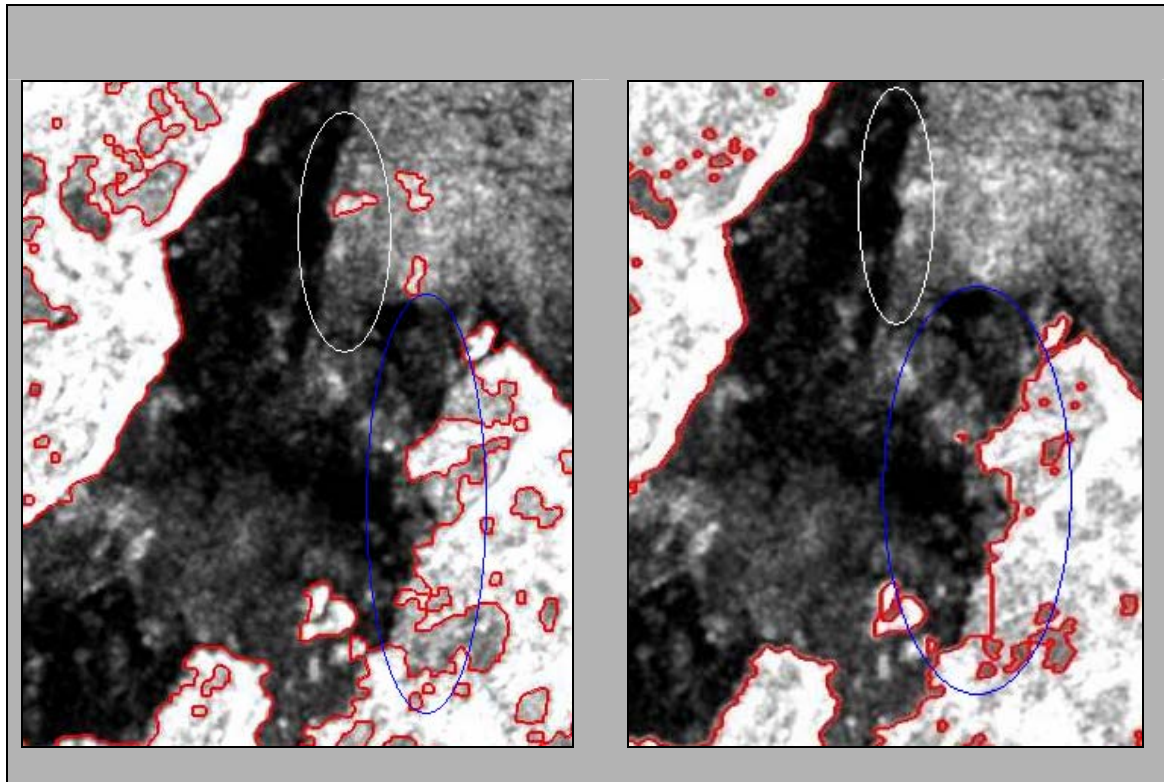


Figure 6.7. The Effect of False Edges in Water Areas and how the Algorithm can Discriminate False from Real Edges

Left: The detection of shoreline using the most common procedure.

Right: The detection of shoreline using the M.S.M.

This effect can be observed in Figure 6.7. If using traditional filters, there is still an excessive noise in the middle of the canal and an undesirable edge caused by the contrast of rough surface (wind) and calm water. Hence, the main shoreline was delineated with a large offset. However, applying the M.S.M., the gray-level value of that noise is lower than the gray-level value of land in the canal.

After the refinement, and because this thesis uses the radiometric characteristic of images in 8-bits and 16-bits, this problem was solved.

The principal problems in the detection of shoreline after the application of common filters are the use of relatively large windows (5x5 smoothing and closing principally).

After the segmentation and 5x5 binary closing coarse land-water segmentation was achieved. That segmented image is further used just to eliminate most of the wind-forced noise in the M.S.M presented in chapter 5.

Besides the better results in the bias obtained in shoreline extraction, most of the shoreline delineation over those critical areas was solved with the refined algorithm, solving a great amount of the outliers detected during the first approach.

Also, it is obvious but necessary to mention that the land-water enhancement and discrimination produces the elimination of all the image features except the shoreline. Hence, after histogram scaling, most of the land features are gone and land analysis could not be performed.

6.4 Summary

In all the areas tested, the problem of excessive noise over the sea surface was solved using the Multitemporal Segmentation Method. Also the offset of the detected shoreline was improved.

Because the algorithm fails in few cases mentioned above and some coastlines are misinterpreted causing some offset in few areas, the analysis of the operator in this semi-automatic algorithm is very important to correct those errors during the vectorization procedure.

Chapter 7

APPLICATION OF THE DETECTED COASTLINE FOR GIS PURPOSES

7.1 Introduction

The detected coastline now can be extracted using a contour following algorithm. In this project, the shoreline was exported to a GIS environment and vectorized using CARIS SAMI.

However, the vectorized coastline must be referenced to a tidal level. This concept is just outlined in this chapter, but must be taken in account when using the shoreline to update nautical charts.

7.2 Vectorization of the Coastline using CARIS SAMI

CARIS SAMI is an interactive program designed to create and edit digital maps. A digital map is a computerized version of a traditional map. CARIS (Computer Aided Resource Information System) stores a digital map as a CARIS file.

An efficient method of converting large volumes of paper maps into a digital vector format is to scan the map sheets and convert the resulting raster data to vector

Raster data consists of rows and columns of pixels (rectangular cells with a single grey level value between 0 and 255 with 0 being black and 255 white). CARIS SAMI requires a single bit file where the pixel value is either 0 or 1.

Vector data consists of lines, points and text. The vector format is used in most Geographic Information Systems (GIS) and computer aided drafting (CAD) systems. CARIS SAMI has integrated the two formats to efficiently handle the conversion of large volumes of data.

The vectorization of the coastline information is fundamental to insert the extracted coastline in a vectorized environment such as the Digital Nautical Chart (DNC).

One of the purposes of extracting the coastline from a satellite image is the updating of this important feature in existing nautical charts. Hence, the vectorization of the coastline using CARIS SAMI gives an important solution to update the coastline information in the same software used to compile the DNC.

7.2.1 Procedure to Export the Image as CARIS SAMI File

CARIS SAMI is a Microsoft Windows based application. The software is user-friendly and it has a wide range of options and functions to work with raster data.

After the detection of the shoreline and the other few remaining edges, there are two alternatives to do with the data:

The first one consists in transforming the data to DXF vector format. A DXF file is a drawing interchange format file developed by Autodesk. This is a file type used for facilitating data exchange between CAD systems.

Just as CARIS has visibility parameters, DXF has layers to allow users to define what is displayed on screen. Because AutoCAD is primarily a drafting tool and CARIS is meant for information management, there are differences in the approach to separating data. AutoCAD uses a similar approach to clear acetates, overlaid one on top of the other. CARIS can group data in a similar manner (using themes) but, because it is a GIS, it also has the capability to group features by other means, such as geographic data type (contours, coastlines, etc) [CARIS GIS manual].

The second alternative is exporting the data as TIFF (GeoTIFF) file, and using that raster file to vectorize the data in SAMI. "GeoTIFF" refers to TIFF files, which have geographic (or cartographic) data embedded as tags within the TIFF file. The geographic data can then be used to position the image in the correct location and geometry on the screen of a geographic information display.

I used the second option because instead of having all the edges transformed to vectors, the aim is to vectorize just the usable edge, which is the shoreline. Therefore, once in SAMI environment, the coastline is selected and the contour following algorithm is applied as follow.

After the shoreline detection using the algorithm presented in chapters 5, the resulting raster image is transformed into TIFF format. However, it is necessary to manipulate the pixel values using image processing software such as Photoshop applying contrast and converting the image into bitmap image (0 and 1).

After that, using the tools mode of CARIS SAMI, the image is exported into *.DES file, which is the standard file format for CARIS. Once converted to *.DES, it is possible to use CARIS SAMI to open the raster file and to start using the line following or contour following function in case of island or linear shoreline respectively.

Thinning operation in CARIS SAMI is not necessary because the edges detected are 1-pixel wide after the application of Roberts algorithm.

The procedure is very easy to implement and the operator should concentrate just in the vectorization of the required edges in the image.

After the vectorization of each completed line, it is important to assign the corresponding user number to the feature to be vectorized. In this case, the feature code used for coastline of the coastline was entered as CLSL when required.

Since the coastline was well defined after the application of the algorithm described in this thesis, the vectorization using the contour following algorithm was done very fast and straightforward. The generated coastlines after the vectorization are displayed in Figures 7.1 to 7.5.

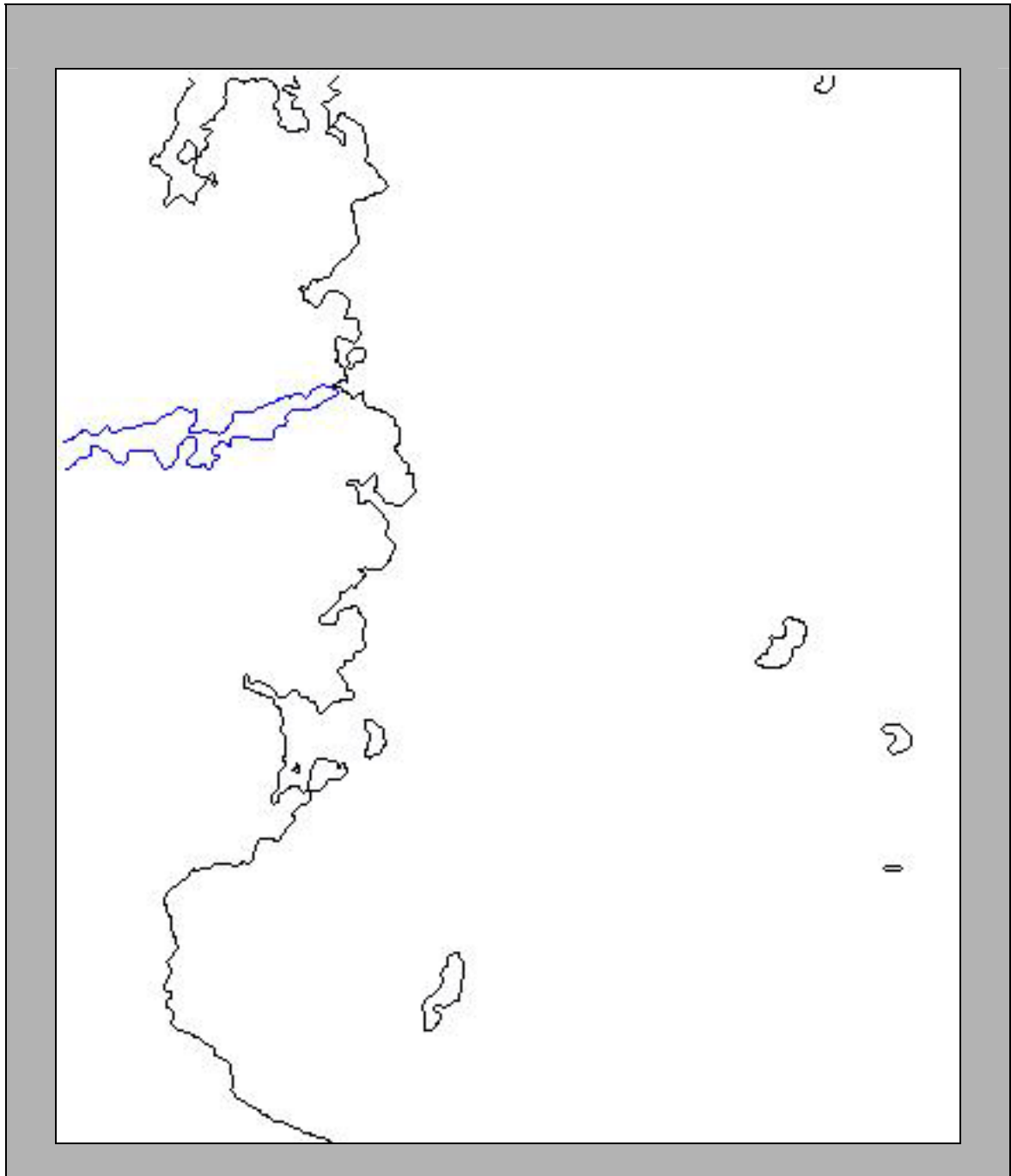


Figure 7.1. Shoreline Vectorization of Area 1 after using the Contour Following Algorithm

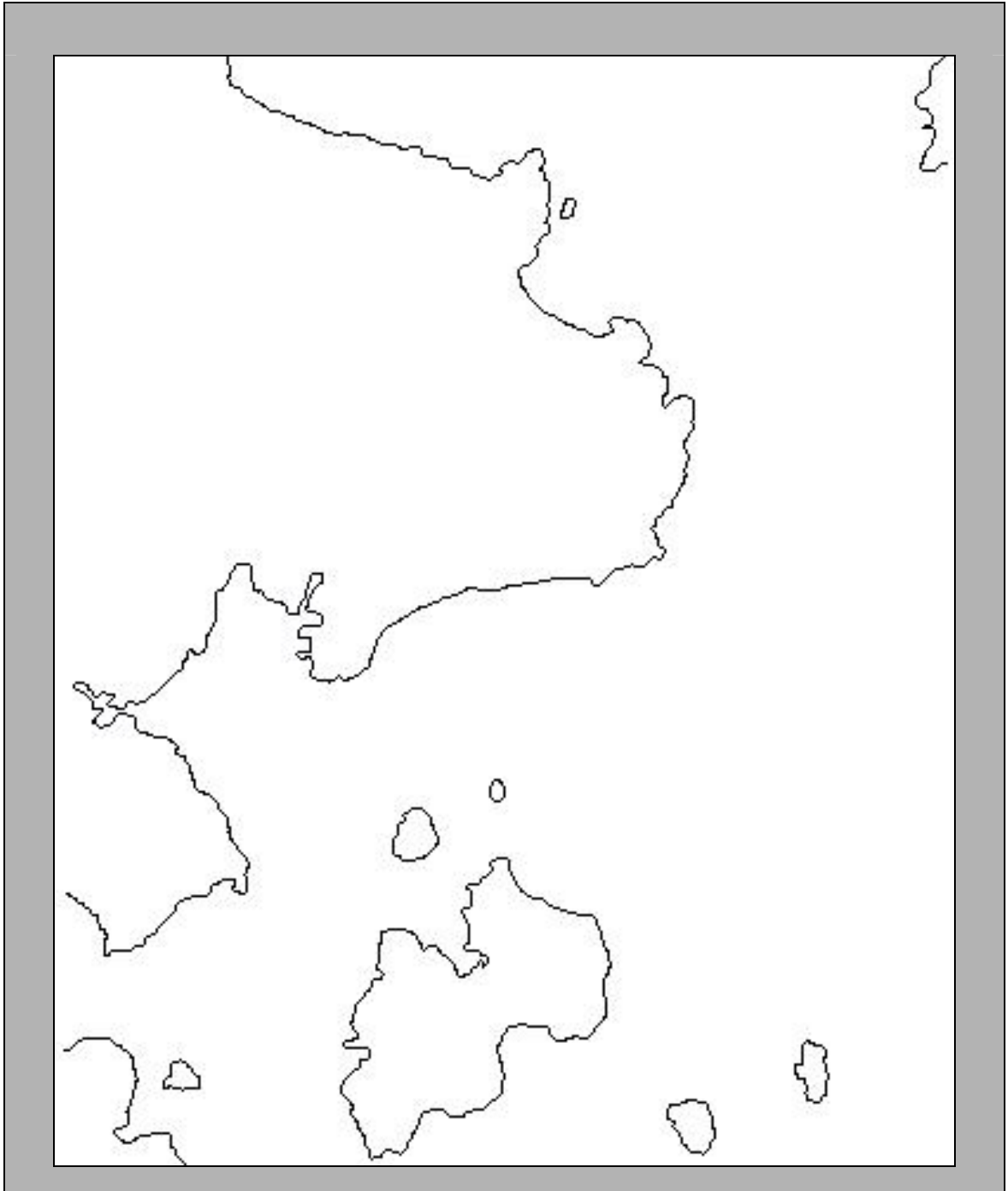


Figure 7.2 Shoreline Vectorization of Area 2 after using the Contour Following Algorithm

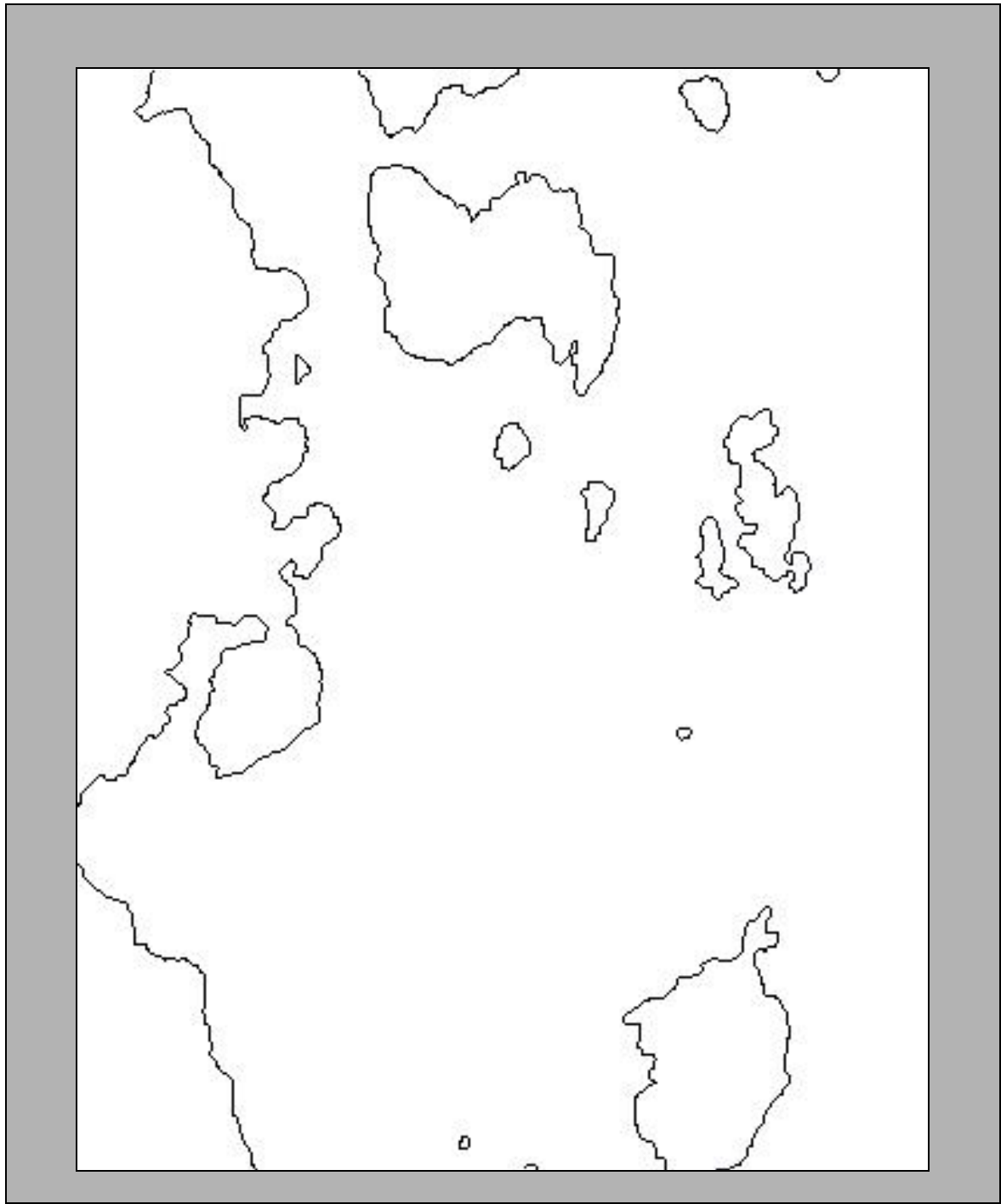


Figure 7.3. Shoreline Vectorization of Area 3 after using the Contour Following Algorithm

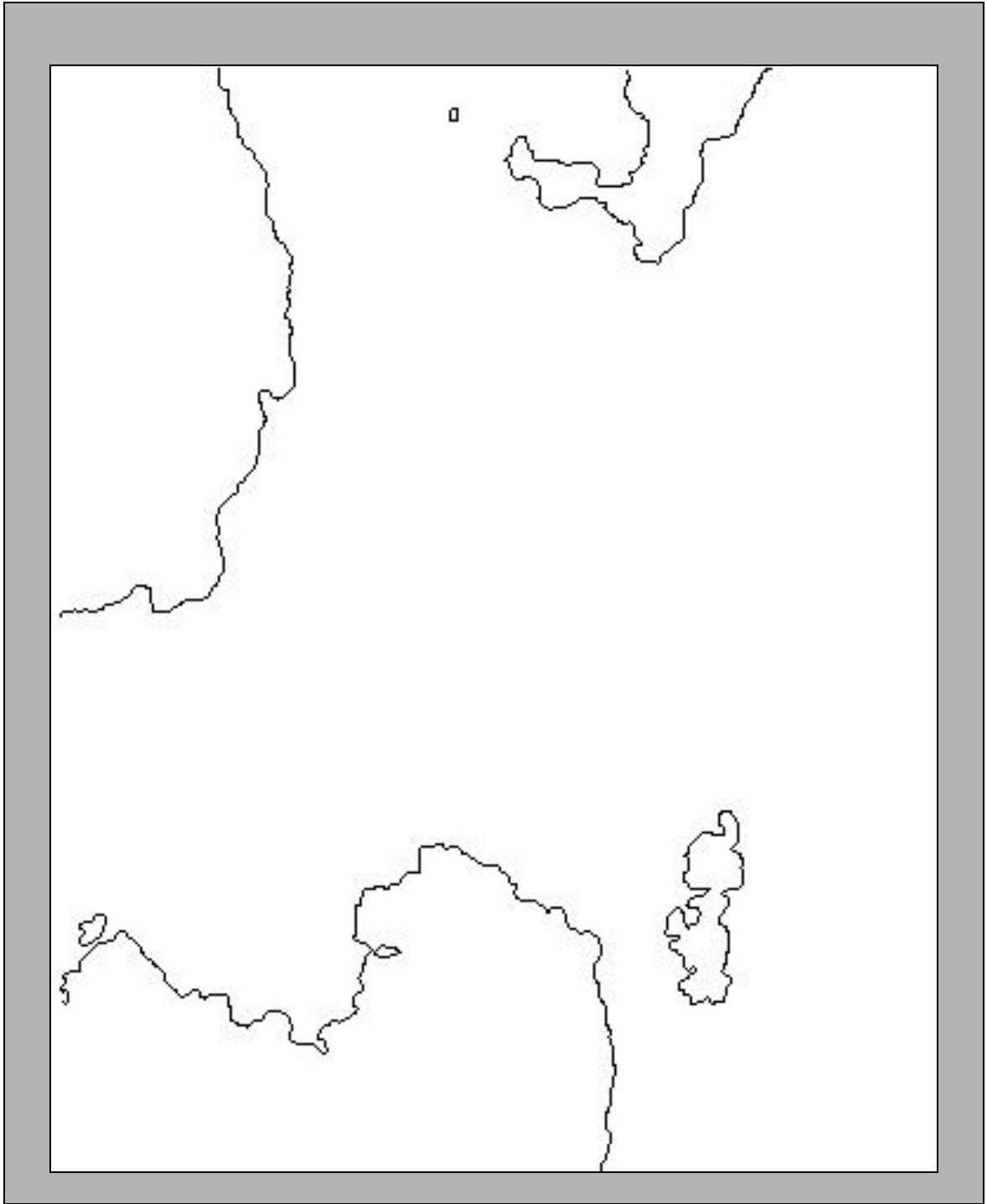


Figure 7.4. Shoreline Vectorization of Area 4 after using the Contour Following Algorithm

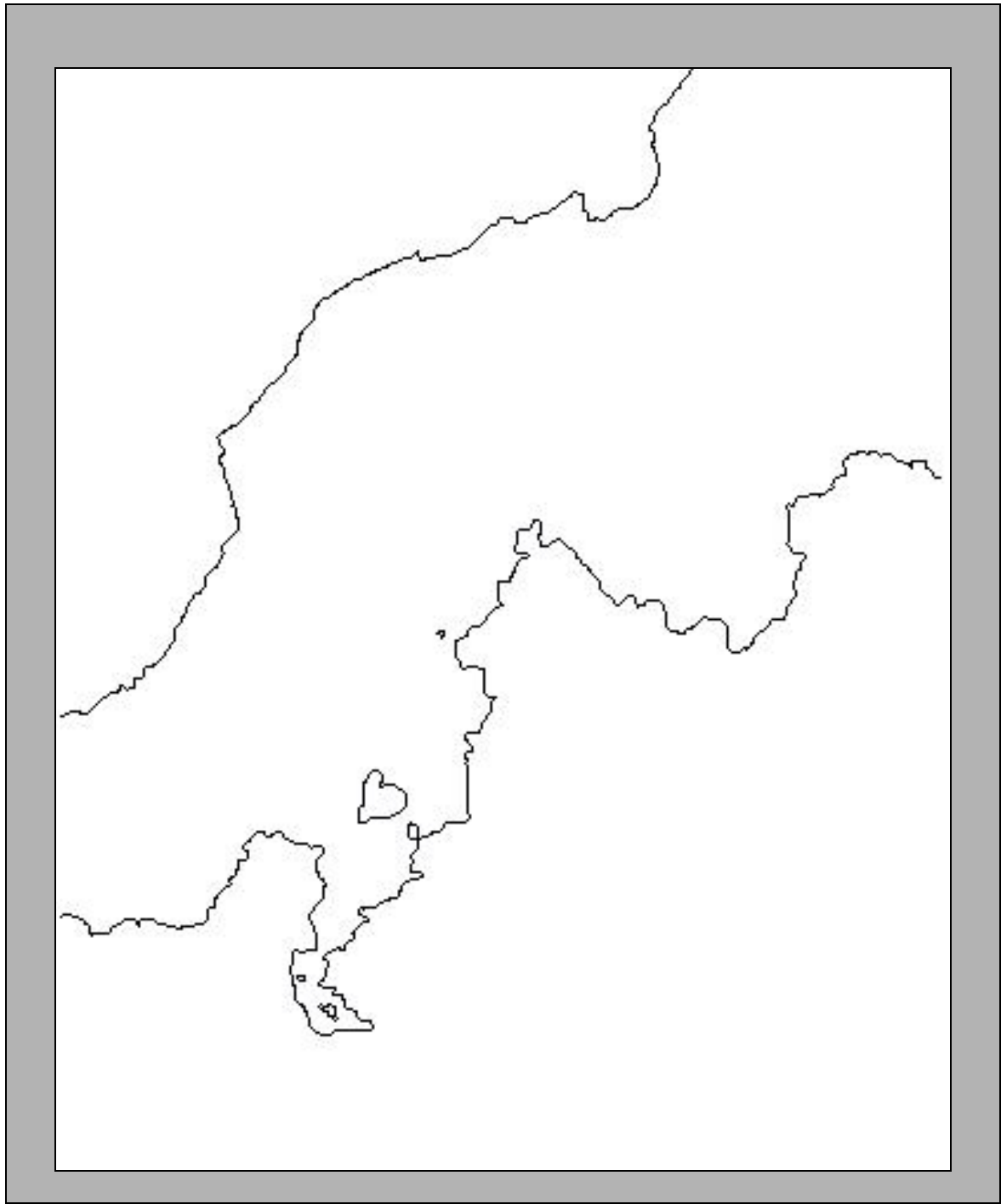


Figure 7.5. Shoreline Vectorization of Area 5 after using the Contour Following Algorithm

7.3 The Needs to Adjust the Shoreline with a Tidal Model

For nautical cartography, the desired product is to develop a method for extracting a Mean Low Low Water (MLLW) vector estimate from imagery. By definition [NOAA, 2004], MLLW is the horizontal vector shoreline determined at an elevation, which is average of the lower low water height of each tidal day observed over the National Tidal Datum Epoch (NTDE).

The distance between MLLW and *in situ* waterline is dependent on the tidal stage and the daily tidal variability. At high tide, the distance is small (large) for steep (shallow) shore slopes. Capturing an image near low tide usually reduces this error. However, low tide elevations are seasonal and can be quite variable. Also, perturbations from tidal models occur regularly due to environmental conditions [Jeremy et al., 2001].

For a project like shoreline mapping the logistics of acquiring satellite images at the local low tide could also be very difficult. Instead, if more accurate shorelines are required, a waterline estimate can be improved to an MLLW estimate, provided the appropriate information is available. In particular, the shore slope and a tidal model, which is geo-referenced (with accurate elevation information), are required. If possible, local tidal elevations at the acquisition time would also improve the estimate and remove errors caused by temporal variability [Jeremy et al., 2001].

The requirements to achieve a shoreline extraction referred to the required datum are summarized as follow [Jeremy et al., 2001]:

- Image data.
- Ground truth (extracted waterline could be compared with in-situ measurement).
- Contrast enhancement methods for accentuating the land-water edge in the imagery (achieved in this thesis).
- A procedure developed for extracting shorelines from this enhanced image data (achieved in this thesis).
- A method to extract shore slope information.
- Shore slope data potentially can improve a shoreline estimate to MLLW estimate.
- Tidal models referenced to chart datum must be included.
- The addition of *in situ* tidal elevation data at the image time would also improve the results.

As shown in Figure 7.6, a simple geometric model can be applied to reference the extracted shoreline to the desired datum (in this case, the MLLW).

If a shore slope estimate can be determined, then with a sufficient tidal knowledge the elevation difference (z) between the elevation of the MLLW and in-situ waterlines provides a distance, which can be projected onto the shoreline.

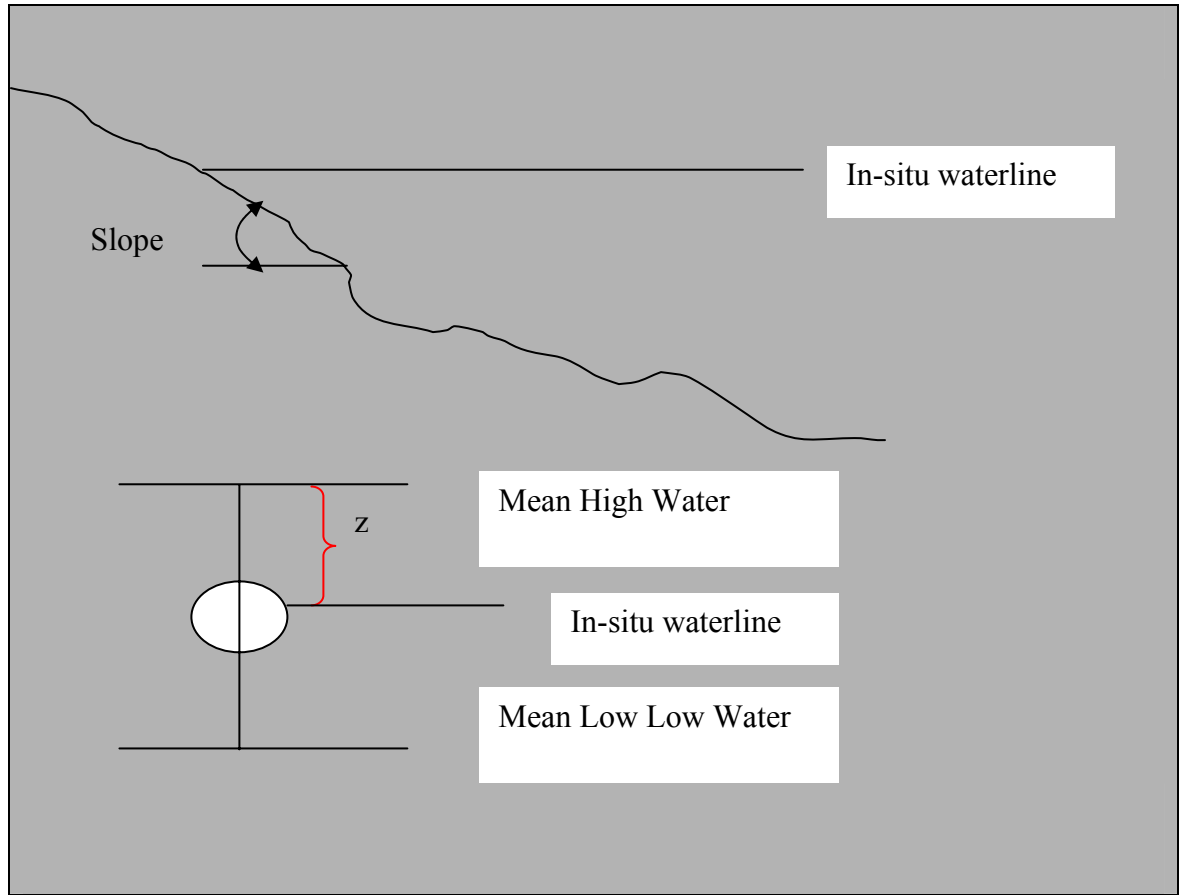


Figure 7.6. Geometric Model to Reference the Extracted Shoreline into a Tidal Datum [after Jeremy et al., 2004]

Capturing a waterline from imagery introduces an error which is dependent on the shore slope and tidal elevation variations. Provided the shore slope is not shallow, the horizontal discrepancy between low and high waterlines is often within the mapping errors limits. For instance, a typical daily tidal elevation difference of 2 m for a 7dgs shore slope represents a maximum horizontal error of about 16m which is within this project mapping limitations. However, for shallower slopes, the error from the MHWL can be quite large, and corrections should be considered [Jeremy et al., 2001].

In this project, the study area presents high topographic variations. Also the slope of the beach is very steep. After the application of a tidal model, this situation should provide small offset between the in-situ waterline and the desired product.

7.4 Summary

In order to use the detected shoreline in a GIS environment, some requirements are necessary. First, the appropriate extraction of the detected shoreline must be achieved.

Once the shoreline is vectorized, the application of a tidal model is highly necessary to connect the shoreline to a reference system.

Chapter 8

CONCLUSIONS AND RECOMMENDATIONS

8.1 Conclusions

Previous research had been done in shoreline detection. Certainly, the detection of those important features depends on the quality of the image together with the environmental parameters at the time of the data acquisition.

Most of the previous works in shoreline extraction using SAR images use complicated algorithms based in a series of mathematical and statistical procedures to detect the shoreline, obtaining very good results. However, the studied previous works do not show results over areas with high environmental conditions such as the area analyzed in this research.

8.1.1 Regarding the Algorithm

After analyzing the most common procedures used to detect the shoreline, the general approach to detect the coastline is based on:

- Obtaining a rough separation between the land and water, and

- Refining the rough land-water boundaries by edge detection and edge tracing algorithms to extract the accurate shoreline position.

This thesis has followed these two principal stages. The rough land-water separation has been achieved using the most common filters after applying the multitemporal analysis to reduce the noise caused by the strong backscatter over the sea surface.

The second stage was achieved using the Multitemporal Segmentation Method proposed in this thesis, with excellent results and solving the most common problem in SAR images: noise on the sea surface. After the successfully shoreline detection, the edge was extracted using CARIS SAMI.

The M.S.M. is a simple method based in the enhancement of the input image using a series of operations between two images acquired at different dates.

The traditional method described in chapter 4 corresponds to a coarse procedure to detect the coastline. Using this coarse method, in section 5.3.4, after the application of multitemporal analysis to reduce the noise, the shoreline has been roughly detected and there are still some problems to solve.

However, the segmented image resulting from this rough method is still useful in the proposed Multitemporal Segmentation Method. So, the rough and the refined shoreline detection methods are connected and form one single methodology.

The use of windows after the M.S.M., were fundamental to achieve good results. After the enhancement of the input image, noise and land pixels have their own pattern in pixel value and distribution. Therefore, a local window that analyzes the pixel having values different to zero and 255 and their respective neighborhood is used to delete the noise with very good results.

To, fill the gaps in land, the same concept is applied, but in reverse way: detecting pixel-value equal to zero and analyzing their neighboring pixels.

The process of filling undesirable gaps in land is a little more complex and it still requires more improvement. The problem comes when the area is indented and contains small bays and narrow canals. Some gaps cannot be closed and sometimes is necessary to perform morphological operations (closing) to fill gaps close to the shoreline.

8.1.2 Regarding the Data Used

Regarding the data used for feature extraction, amplitude images are the most used. Today the use of polarimetric images gives a very good approach to detect the coastline and it is becoming widely used.

The algorithm applied to the data used in this research can be applied to better dataset, such as polarimetric images or better images in resolution. The spatial resolution of radar images is becoming better and consequently, the applications of using those images for cartography are more and more widely used.

8.1.3 Identification of Main Concepts the Proposed Method

Certainly, the application of the proposed method to detect the shoreline would not be successful without some very important concepts.

The use of multitemporal images was essential to solve the problem regarding the roughness in the sea surface. Statistical correlation or averaging two images has been used to reduce the noise on water while keeping the high pixel value in land, with very similar results. If the available images are more than two, the correlation analysis or PCA gives better result. However the more images are available, the more expensive is the cartographic production.

Doing the multitemporal analysis, most of the original noise has been smoothed. After the noise reduction the sequential application of spatial filters, morphological operations and edge detection filters were applied to the image to roughly detect the shoreline. However, the remaining noise in the sea surface still caused some problems in the shoreline delineation and island detection. That noise usually was misinterpreted as islands producing undesirable detection of false edges.

The stated question was: how to get rid of that noise without deleting islands or low-pixels values features in land areas? Instead of using complicated algorithms to solve that problem and with the fact that usually the pixel-value of that undesirable noise is higher than some of the pixel values in land (shadows, wetland, etc), this research was focused in the use of a simple and straightforward procedure based in the inherent properties of the image and the use of local windows to delete that noise without affecting the land pixels.

The time saved using this procedure if compared with the traditional methods of digitization of the contours constitutes a great improvement in the cartographic production and updates of existing maps.

Even when automatic coastline detection methods give very good results to save time during the tedious process of digitalization, the analysis of the operator in the final revision is very important to avoid wrong interpretation of critical areas.

8.2 Recommendations

A simple and effective algorithm to detect the coastline has been described in this thesis. After the coastline detection, the extraction of that coastline has been achieved using CARIS SAMI, in a fast and reliable procedure to vectorize the shoreline information.

The shoreline that has been extracted should be related to the tide information at the time of image acquisition. So, this shoreline information corresponds to the in-situ waterline.

For nautical cartography requirements, the desired product is the Mean Low Low Water (MLLW) vector estimate from imagery.

To achieve that desired result, one solution is trying to acquire the image in low during low tide condition. The other way is by estimating the shore slope.

8.3 Further work and development

Once integrating tidal information together with the shoreline, an important, but often overlooked issue is: how is the data going to be used? What will be the scale of the map to be updated and the different uses (military, navigational, tourism, environmental studies, etc). Is the area a commercial navigational route? What risks involve the existence of uncertainties in the coastline delineation?

In this case the shoreline can be used to improve existing shorelines or to have shoreline information from unmapped areas. Because of the resolution of the image used (12.5 m) the detected shoreline could be used in charts with a scale of 1:70.000 or less (intermediate to small scale nautical charts).

The development of a semiautomatic methodology to detect the shoreline using single ERS-1 SAR images gives a powerful tool to extract coastline from remote areas for mapping purposes. This application of coastline detection can be extended also to the Antarctic Continent. SHOA is producing nautical cartography over the areas in the Antarctic. Some portions of the Antarctic Coast have never been accurately mapped, and other portions have experienced dramatic changes in position and shapes since they were mapped. Information about geographic position, orientation, and geometric shape of the Antarctic coastline is essential for geographic exploration, and nautical and aerial navigation.

Constructing an accurate coastline map is an important step toward establishing a baseline for the Nautical Chart and also for future change detection studies in order to understand the response of remote and southern areas such as the Antarctic Ice sheet to climate change.

The different subroutines were designed to work with images limited by size 800 x 650 pixels. Further work must be done to work with large amount of data with lower spatial resolution.

REFERENCES

- Alegria L. (2003). "The Military Geographic Institute of Chile as a Tool For National Development." Ordnance Survey. Paper presented in Cambridge Conference. [On-line] 03 February 2004.
<http://www.cambridgeconference2003.com/camconf/papers/3-5.pdf>
- Alvial A. and D. Recule (1999) "Foundation Chile and the integrated management of the coastal zone." *Ocean & Coastal Management*, Vol.42, Num. 5, pp. 143-154.
- Asociacion de Productores de Salmon y Trucha de Chile APSTC (2000). "La salmonicultura en Chile." Unpublished pamphlet. Santiago, Chile: APSTC (AG). [On-line] 03 February 2004.
<http://www.globefish.org/publications/commodityupdate/200201/200201.htm>
- Barret G., M. Caniggia and L. Read (2002). "There are more vets than doctors in Chiloe: Social and Community impact of the globalization of Aquaculture in Chile." *World Development*, Vol. 30, Num.11, pp. 1951-1955.
- Caris GIS V.4.4a.4.0 (2004) CARIS Universal System Limited. Fredericton, N.B., Canada. *Caris SAMI Tutorial*.
- Caris GIS V.4.4a.4.0 (2004) CARIS Universal System Limited. Fredericton, N.B., Canada. *Caris SAMI User's Guide*.
- Chen, L.C. and C.C. Shyu (1998). "Automated Extraction of Shorelines from Optical and SAR Image." [On-line] 10 March 2004.
<http://www.gisdevelopment.net/aars/acrs/1998/ps3/ps3013.shtml>
- Erteza, I (1998) "An Automatic Coastline Detector for Use with SAR Images". Signal Processing and Research Department. Sandia National Laboratories [On-Line] 13 September 2003. <http://www.osti.gov/dublincore/gpo/servlets/purl/1322-XIfWqu/webviewable/1322.pdf>
- European Space Agency (2004). Earth Observation. *Radar Course* [On line] 12 August 2004.
http://earth.esa.int/applications/data_util/SARDOCS/spaceborne/Radar_Courses/Radar_Course_I/image_geometry.htm
- Henderson, F.M., and A.J. Lewis (1998). Vol. II of *Principles and Applications of Imaging Radar*. Third ed., Wiley & Sons, USA.
- Hydrographic and Oceanographic Service of the Chilean Navy (S.H.O.A.). [On-line] 04 February 2004. <http://www.shoa.cl>

- James, M. (1987). *Pattern Recognition*. BSP Professional Books, Oxford, London, Edinburgh, Boston, Melbourne, 144p.
- Lee, J-S and I. Jurkevich (1990) "Coastline Detection and Tracing in SAR Images." *IEEE Transactions of Geoscience and Remote Sensing*, Vol.28, Num.4, pp. 662-668.
- Liu, H. and C. Jezek (2004). "A Complete High-Resolution Coastline of Antarctica from Orthorectified Radarsat SAR Imagery." *Photogrammetric Engineering and remote Sensing*, Vol. 70, Num. 5, pp. 605-616.
- Manfredini J.S. (n.d.). "Aportes del Servicio Aerofotogrametrico en la Produccion y actualizacion de Cartografia." [On-line] 12 March 2004. <http://www.saf.cl/>
- Martin, A. and S. Tosunoglu (n.d.) "*Image Processing Techniques for Machine Vision.*" Florida International University. Department of Mechanical Engineering [On-line] 20 May 2004. http://www.eng.fiu.edu/me/robotics/elib/am_st_fiu_ppr_2000.pdf
- Mason D. and J. Davenport (1996). "Accurate and Efficient Determination of the Shoreline in ERS-1 SAR Images." *IEEE Transactions on Geoscience and Remote Sensing*, Vol.34, Num.5, pp. 1243-1253.
- Military Geographic Institute Of Chile (IGM) (2003). "Report On Cartography In The Republic Of Chile 1999 – 2003". [On-line] 10 February 2004. <http://www.igm.cl/Images/ICAreport.PDF>
- National Oceanic and Atmospheric Administration (2004). [On-Line] 20 July 2004. <http://co-ops.nos.noaa.gov/mapfinder/mlw.html>
- Noble, J.A., (1996). "The effect of Morphological Filters on Texture Boundary localization." *IEEE Transactions of Pattern Analysis and Machine Intelligence*. Vol 18, Num.5, pp. 554-561.
- Parker, J.R. (1997). *Algorithms for Image Processing and Computer Vision*. First ed., Wiley & Sons, USA.
- RADARSAT International (2004). [Online] 04 April 2004. www.rsi.ca
- Richards, J.A., and X. Jia (1999). *Remote Sensing Digital Image Analysis, an Introduction*. Third ed., Springer, Berlin.

- Schultze, M and Q. Wu (1995) "Noise Reduction in Synthetic Aperture Radar Imagery using a Morphology-Based Nonlinear Filter." Proceedings of DICTA95. Digital Image Computing: Techniques and Applications, pp 661-666. [On-Line] September 13th 2003. <http://www.markschulze.net/docs/pdf/dicta95.pdf>
- Schwäbisch, M., S. Lehner and W. Norbert, 1998. "Coastline Extraction Using ERS SAR Interferometry". [On-Line] 14 September 2004. <http://earth.esa.int/symposia/papers/schwaebisc>
- Serra, J., and L. Vincent (1992). "An overview of morphological filtering." *IEEE Transaction on Circuits, Systems and Signal Processing*. Vol 11, pp. 357-393.
- Sternberg, S.R., and J. Serra, (1986). "Special Section on Mathematical Morphology". *Computer Vision, Graphics and Image Processing*. Vol 3. pp. 279.
- The Alaska Satellite Facility (2004). Radar Distortions [On-Line] 20 July 2004. www.asf.alaska.edu
- Touzi, A., A. Lopes and P. Bousquet (1988). "A Statistical and Geometrical Edge Detector for SAR Images". *IEEE Transactions on Geoscience and Remote Sensing*, Vol.26, pp. 764-773.
- Yeremi M., A. Beaudoin, J. Beaudoin and G. Walter ([2004). "Global Shoreline Mapping from an Airborne Polarimetric SAR: Assessment for RADARSAT 2 polarimetric modes." Defence R&D Canada. Technical Report. DREO TR 2001-056.
- Yu, Y. and S.T. Acton, (2004). "Automated Delineation of Coastline from Polarimetric SAR Imagery". *Int. Journal of Remote Sensing*, Vol. 25 Num.17, pp. 3423-3438.
- Wolf, P. and B. Dewitt (2000). *Elements of Photogrammetry with applications in GIS*. Third ed., Mc. Graw Hill, USA.
- Xiao, J., J. Li and A. Moody (2002). "A Detail-Preserving and Flexible Adaptive Filter for Speckle Suppression in SAR Imagery". *International Journal of Remote Sensing*, Vol. 24, Num. 12, pp. 2451-2455.
- Zelek J. (1990). "Computer-aided linear Planimetric Feature Extraction" *IEEE transactions on Geoscience and Remote Sensing*. Vol.28, Num.4, pp. 567-572.
- Zhang, Y. (2000). "A method for Continuous Extraction of Multispectral Classified Urban Rivers". *Photogrammetric Engineering & Remote Sensing*. Vol.66, Num.8, August 2000, pp. 991-999.

Appendix I

STEPS TO PERFORM COASTLINE EXTRACTION USING THE MULTITEMPORAL SEGMENTATION METHOD

The proposed algorithm is based in sequential operations using ENVI 4.0 software and a series of developed subroutines stored in attached CD. The procedure is straightforward and easy to implement in any computer having ENVI and Microsoft Visual C++ software.

To run all the programs in the CD, the input images must be 800x650 pixel and *.lan files. The following outline is writing here for easy use of this method:

I. Rough Noise Reduction and Land-water Segmentation

1. Preprocessing of the entire image using speckle reduction (3x3 lee filter recommended).
2. Subsetting the image according to the area analyzed. The new image must be 800 x 650 pixels and exported as *.lan file (image1.lan).
3. Repeat steps 1 and 2 with a second image corresponding to the same area.
4. Image-Image registration between image1 and image2 (image2.lan).
5. Histogram scaling in image1 and image2 from 16 bits to 8 bits.
6. Smoothing and enhancement of edges by 3x3 median filter using ENVI.

7. Multitemporal analysis of two scaled 8-bit images (image 1 & 2) using the workspace: *D:\chapter5\8bits_imgavg\8bits_imgavg.dsw*

This program is designed to work with two 8-bit images

8. Sobel edge detection using ENVI

9. Edges enhancement, adding back the detected edges over the image.

D:\chapter5\Percent\Percent.dsw

This program is designed to work with Sobel and the image after step 7.

10. 5x5 Gaussian filter and 3x3 gray level closing using ENVI.

11. Binary segmentation and 5x5 binary closing using ENVI.

II. Refinement, Land-noise Discrimination and Windows Operations to Delete Noise

II. a) Input enhancement

12. Multitemporal analysis using the two original 16 bits images using the workspace:

D:\chapter6\16bits_img_avg\percent_16bit.dsw

This program is designed to work with two 16-bit images.

13. Multi-scale image segmentation between the image after step 9 and the image after step 12 using the workspace:

D:\chapter6\enhancing input\contrasting_16bit\contrasting16bit.dsw

Note: before doing this operation must ensure that the edges-enhanced image is 8-bit.

14. Perform 5x5 gray-level opening using ENVI.

15. Island-noise discrimination using the image after step 7 and the image after step 14 using the workspace:

D:\chapter6\enhancing input\island_enhancement\ island_enhancement.dsw

16. Get rid of the noise contrasting the image after step 15 with the land-water segmentation image after step 11.

D:\chapter6\enhancing input\contrasting_bitmap\ contrasting_bitmap.dsw

II. b) Use Of Iterative Windows to Locally Delete the Remaining Noise in Water and to Fill Most of the Gaps in Land

17. Deleting noise in the sea surface in the single image after step 16 using the workspace:

D:\chapter6\deleting noise\removing_noise\removingnoise.dsw

18. Filling the gaps present in land areas the single image after step 17 using the workspace:

D:\chapter6\deleting noise\filling_gaps\filling_gaps.dsw

19. Iteratively repeat steps 17 and 18 using the previous image as input. Once there is no more noise in the image, repeat step 18 until no more gaps are refilled.

20. Opening the closed bays in the image after step 19 using the workspace:

D:\chapter6\deleting noise\opening_bays\opening_bays.dsw

21. Roberts edge detection using ENVI.

22. Binary segmentation of the detected edges using the workspace:

D:\chapter6\segmentation\segmentation.dsw

23. The resulting segmented edges must be saved as geo-tiff for further vectorization using CARIS SAMI.

Appendix II

THE ERS - SAR PRECISION IMAGE PRODUCT

The SAR Precision Image product is generated on CCT, exabyte or CD in CEOS format and contains image data (16 bits, amplitude) related to a full scene (100 Km x 100 Km) and all the required annotations. This product can be provided also on photographic print.

The ERS-x.SAR.PRI product will be generated with image compensation for antenna elevation gain pattern and range spreading loss and will be addressed to a large spectrum of users.

The ERS-x.SAR.PRI product is characterized by a set of parameters listed here; moreover, in order to check the spacecraft parameters during data generation and to test the quality of the data, a set of flags and parameters are computed and attached in product annotations. The convention for QA flags setting is that 0 value indicates nominal condition (no change in parameter or I-PAF QA thresholds not crossed).

The ERS1/2.SAR.PRI product is characterized by:

1. Azimuth output = 8200 pixels
2. Range output = 8000 pixels
3. Data representation = integer (Amplitude)
4. Bits per sample = 16
5. Calibration = internal plus image compensation
6. Output medium = CCT, EXABYTE, CD-ROM, photographic print
7. Output format = CEOS
8. Image coordinate system = ground range / zero Doppler
9. Range pixel spacing = 12.5 m
10. Azimuth pixel spacing = 12.5 m
11. Total processed azimuth bandwidth = 60 Hz
12. Number of temporal look = 3
13. Range spectral weighting function = Hamming window (coeff. 0.75)
14. Azimuth spectral weighting function = Hamming window (coeff. 0.75) centred
on estimated Doppler centroid frequency

The ERS1/2.SAR.PRI product contains in the annotations the following flags and parameters:

1. UTC time of the first line
2. The most precise orbit information available
3. Longitudes of the scene centre and four corners
4. Latitudes of the scene centre and four corners
5. PRF code change flag (0 or 1) 1
6. SWST code change flag (0 or 1)
7. Calibration system and receiver gain change flag (0 or 1)
8. Chirp replica quality flag (0 or 1)
9. Input data statistic flag (0 or 1)
10. OGRC/OBRC flag (flag = 0 for OGRC)
11. Number of PRF code changes
12. Number of SWST code changes
13. Number of calibration system and receiver gain changes
14. Number of missing lines
15. Number of duplicated lines
16. 3-db pulse width of replica ACF
17. PSLR of replica ACF
18. ISLR of replica ACF
19. Estimated mean of I input data
20. Estimated mean of Q input data
21. Estimated standard deviation of I input data
22. Estimated standard deviation of Q input data
23. I-Q channels gain imbalance

24. I-Q channels phase imbalance
25. PRF code
26. SWST code
27. Calibration system gain
28. Receiver gain
29. Internal calibration data time tag (UTC)
30. Number of valid calibration pulses
31. Number of valid noise pulses
32. Number of valid replica pulses
33. First sample in replica
34. Calibration pulse power
35. First valid replica pulse power
36. Noise signal power density
37. Range compression normalization factor
38. Doppler centroid confidence measure flag (0 or 1)
39. Doppler centroid value flag (0 or 1)
40. Doppler ambiguity confidence measure flag (0 or 1)
41. Output data mean flag (0 or 1)
42. Overall QA summary index (value 0-9)
43. Doppler Centroid confidence measure (processor specification)
44. Doppler Ambiguity confidence measure (processor specification)
45. Estimated Doppler centroid coefficients
46. Estimated Doppler FM rate coefficients

47. Estimated Doppler ambiguity number
48. Zero Doppler range time of first range pixel
49. Zero Doppler range time of centre range pixel
50. Zero Doppler range time of last range pixel
51. Zero Doppler azimuth time of first azimuth pixel
52. Zero Doppler azimuth time of centre azimuth pixel
53. Zero Doppler azimuth time of last azimuth pixel
54. Incidence angle at first range pixel
55. Incidence angle at centre range pixel
56. Incidence angle at last range pixel
57. Processor net multiplicative scaling factors
58. Normalization reference range R_0 Km (if available)
59. Antenna elevation gain pattern (if available)
60. Absolute calibration constant K (if available)
61. Upper bound K (+3 Std dev) (if available)
62. Lower bound K (-3 Std dev) (if available)
63. Processor Noise Scaling Factor (if available)
64. Date in which K generated (if available)
65. K version number $X.Y$ (if available)

Product Quality Requirements

The ERS1/2.SAR.PRI product satisfies the following quality performances:

1. Ground range resolution of IRF < 30 m
2. Azimuth resolution of IRF < 30 m
3. ISLR of IRF $< - 8$ dB
4. PSLR of IRF $< - 18$ dB
5. Point target range geometric misregistration 60 m
6. Point target azimuth geometric misregistration 60 m
7. Processor point target linearity > 0.95 over the linear dynamic range
8. Processor point target linear dynamic range = 30 dB
9. Processor gain = fixed at all times

VITA

Candidate's full name: John Neville Fleming Baeza

Place and date of birth: Valparaíso, Chile
August, 08, 1971

Permanent address: Errázuriz 254, Playa Ancha
Valparaíso, Chile

Schools attended: Liceo Eduardo de la Barra,
Valparaíso, Chile
1985-1988

Naval Academy "Arturo Prat"
Chilean Navy
Bachelor in Naval and Maritime Sciences
1989-1992

Universities attended: Naval Polytechnic Academy, Chilean Navy

- Bachelor in Naval and Maritime Sciences with major in Hydrography and Oceanography
1996-1998
- Hydrographic Engineering Course Certified with Category "A" from the International Hydrographic Organization
1997-1998

University of New Brunswick,
Fredericton, N.B., Canada. Department of Geodesy and Geomatics Engineering
Master of Science in Engineering
Candidate
2002-2004

PUBLICATIONS

Fleming, J., 2nd Lieutenant, Chilean Navy (1998). "Aplicación de un Modelo de Dispersión para Accidentes de Contaminación a lo largo de la Costa de Chile". ("Application of a Dispersion Model for Contamination Hazards along the Chilean Coast") B.Sc. thesis, Naval Polytechnic Academy, Chilean Navy.